Universita' degli Studi di Padova

Environmental Engineering

Department of civil, environmental and architectural Engineering - DICEA

Flow and pressure behaviour in a Pulse Duplicator loop: experimental analysis

Student: Valentina Bido

Supervisor: Francesca Maria Susin

Assistant supervisor: Luigi Di Micco

TABLE OF CONTENTS

CHAPTER 1
INTRODUCTION

1.1 The He.R laboratory

Once upon a time there was in Padua a woman named Francesca Maria Susin. She had a dream. She wanted to give her contribution to the research for the development of new technologies useful to help people with cardiac pathologies. She started to work to achieve her goal and she succeeded, founding the laboratory of cardiac vascular fluid dynamics He.R – Healing Research at the University of Padua.

The idea was that of sharing the knowledge of both engineers and doctors, in order to find out new technical solutions to offer always better treatments to heal cardiac disease. To do that, it is important to understand how exactly the prosthesis work, and which are the effect they generate on the organism. Assuming the cardio circulatory system as a hydraulic system constituted by a series of pipes of different diameters (representing the blood vessels) and by a pump (the heart), the HE.R Staff could start the research by the creation of a Pulse Duplicator.

A Pulse Duplicator is a mechanical device which enables to test cardiovascular components simulating the systemic circulation. It exist already some versions of the machinery but they decided to design a hand-made version. The advantages of fashioning a new device from scratch are most of all economic, and in the second place they regard the possibility to create it with the characteristic of the modularity; it means that each component of it can be isolated and modified from a geometric or a functional point of view in order to be suitable for different tests. That's why, even if the first device was ready to run in November 2014 (designed and dimensioned by Ing. Riccardo Toninato and Luigi di Micco), it is still being modified day by day depending on the relative study they are focus in.

1.2 Goal of the thesis

With my thesis I carry on the previous He.R's staff research work on the Pulse Duplicator, with the aim of improving its efficiency and getting more information on its potential and its limits too.
In particular my work is focused on the analysis of the working of the flow meter. Its installation had already been arranged, but just in this moment it could be possible to introduce it and test it.
Instead in the second part of the thesis I will report the experimental study on the behavior of the pressures in the device, both in conditions of constant and pulsatile flow.

The work is organized in five chapters, starting, as we will see in the next paragraph, from the description of the instrument and its components (*chapter 1*).
In the *chapter 2* I will show how, just with an easy modification on the configuration of the device, it is possible to create a closed system with a constant flow useful for our tests regarding the functioning of the flow meter and its sensitivity.
A similar conformation of the pulse duplicator is kept for the analysis of the pressures trend carried out on the section of the device preceding the aortic valve (*chapter 3*), comparing the behaviors we got with what it was theoretically expected.
Hence we achieved in testing the pulse duplicator on its original setting analyzing the pressures at pulsatile flow (*chapter 4*), and concluding my elaborate with the final considerations about the results we obtained and the future developments the pulse duplicator will experience.

1.3 The Pulse Duplicator

So, the Pulse duplicator is a hydraulic device at pulsatile flow with pressure pipes in variable motion condition. It is formed by several modules linked together; each of them can be isolated and modified according to need.
Here you are the photos of the device in its original configuration, which will be later partially changed.

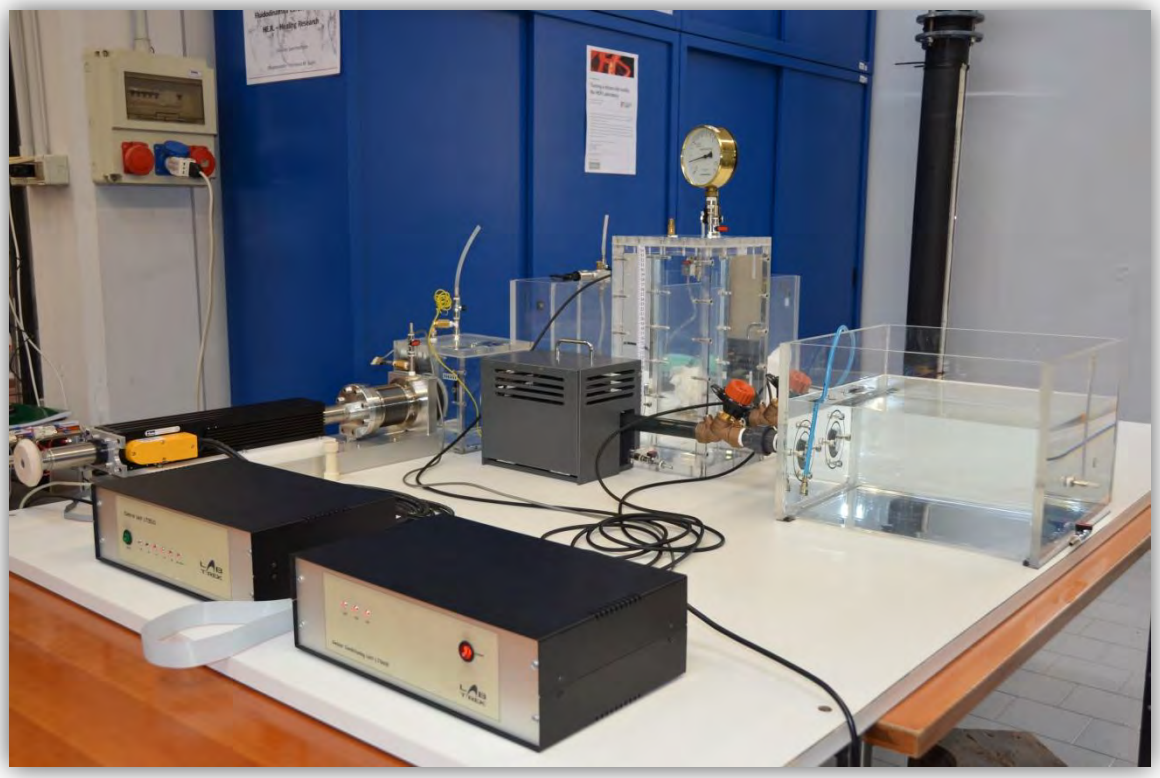

Figure 1.1: *Pulse duplicator, frontal view*

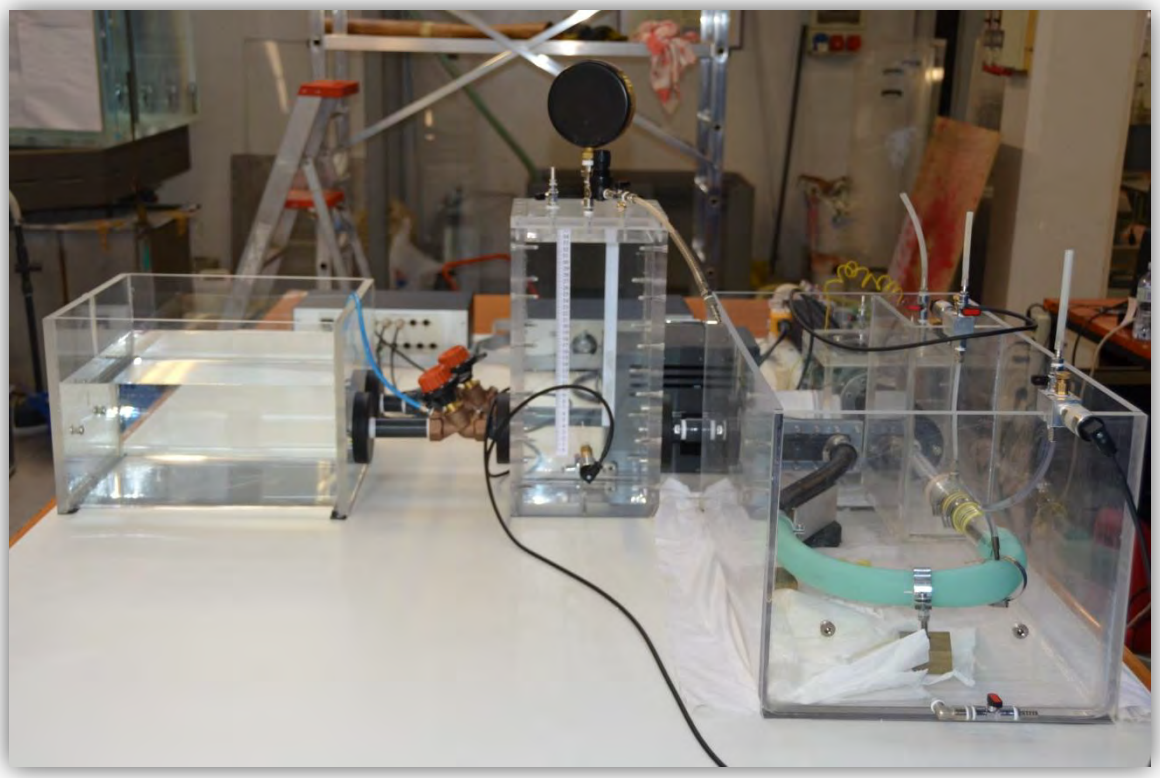

Figure 1.2: *Pulse duplicator, rear view*

The device is composed by several parts comprising four transparent tanks representing the aortic, ventricular, atrial and compliance chambers respectively, plus the electromagnetic motor, the PVC pipes, the local resistances and the heater.

The position and the connections between all the components can be easily seen in the following block scheme:

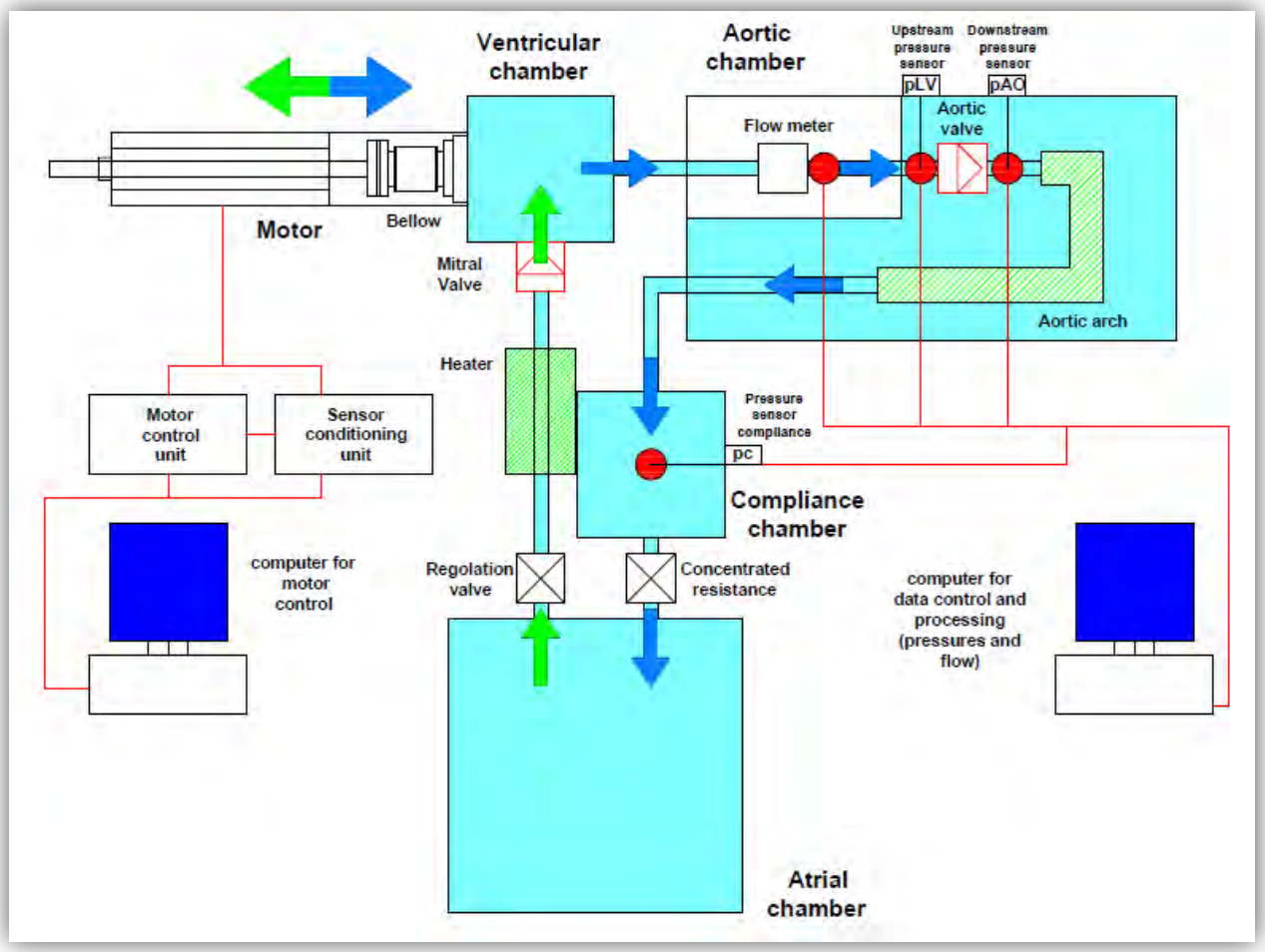

Figure 1.3: *Block scheme of the Pulse Duplicator*

In the next paragraphs I will present every single part of the device with its main characteristics.

1.3.1 The Pump

The electromagnetic linear engine with bellow represents an artificial ventricle that reproduces the pulsatile heart flow. The model chosen for its characteristics of high thermal efficiency (and consequent no need of adding cooling devices), lack of gears (subject to wear), maintenance ease and possibility to achieve great continuous peak force, is the PARKER PRA 3810S. It is connected to the control unit by two cables, one for its alimentation which is able to create a magnetic field, and the other for the transmission of the position signal. The motor fulfill the fundamental function of pumping the volume of fluid we want to be flowing in into the system. Practically when the motor moves forward, the bellow contracts and throw the flow out. The translational movement follows the curve of displacement that we impose to the engine through the computer, reproducing the real volumetric variations of blood flow during a complete cardiac cycle (systole and diastole). The forward shift is physiologically the period of ventricular ejection (systole's phase), while when it moves backwards it represents the diastole phase.

The motor can perform a number of beat per minute from 10 to 150, the area of the bellow is equal to 34.21 cm^2, and the amplitude between them is of 2.9 cm, giving therefore a maximum volume of fluid injected of 100 ml.

In order to establish the quantity of volume involved, and more in general to run the device and save the results, we use a software developed and implemented by the team He.R: LabView. By this program we can control the motor and manage the output data. Initially we set the values of the parameters connected to the mode of operation of the motor; these are: the displacement curve; the heart rate, defining the number of the beats in the unit of time, typically in a minute (bpm), and the stroke volume, representing the volume of fluid expelled in a pulsation (ml). The latter can be determined simply deciding the amplitude of the displacement the motor has to fulfill.

In our experiments we decided to set the heart rate equal to 67, which corresponds to the mean physiologic value for a man, and the amplitude of the motor as 1.9, even if the device let us the possibility to choose different settings too.

Figure 1.4: *Electromagnetic motor*

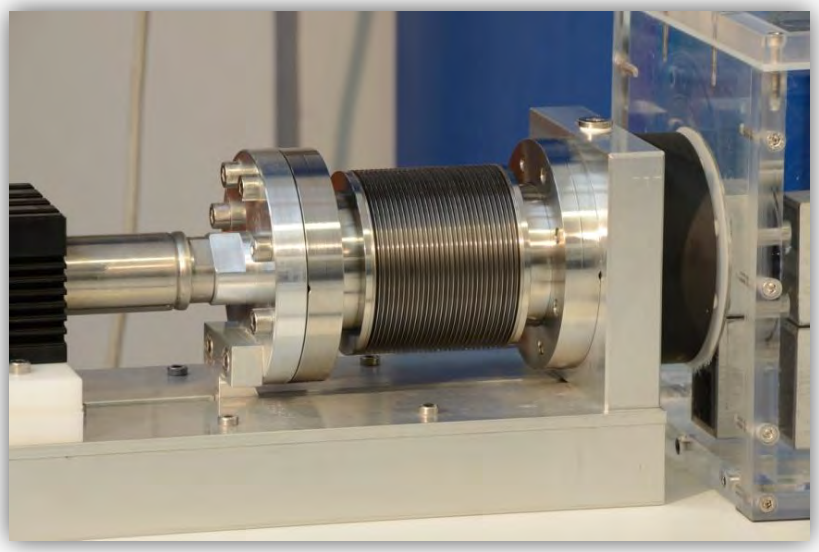

Figure 1.5: *Bellow*

1.3.2 Ventricular Chamber

The bellow of the motor is directly connected to the ventricular chamber, a transparent Plexiglas tank always filled with pressurized water and whose percentage of air is easily controlled by a vent valve. The walls of the chamber have a great thickness (15 mm), ensuring a good

mechanical resistance with respect to the pressure stresses that occur in this section. The tank presents two branches, connecting itself either with the aortic or with the mitral chamber; the flow follows one way or the other one depending on the position taken by the motor at the moment. In particular, when the motor pushes the flow from the ventricular towards the aortic chamber, the aortic valve located in this section opens because of the pressure difference, and it is exactly what it occurs in the systole phase in the human body. On the contrary in the diastole phase, represented by the retraction of the motor, this valve is closed, while the mitral valve situated in the second connection opens, letting the flow coming from the mitral tank to the ventricular one. Between these two chambers, in effect, we find a cylindrical component, built of Teflon, in the cavity of which it is inserted the valve; I can see the photo in figure 1.7 .

To sum up, we can say that this chamber is the crux of the device, from where the flow can take one direction or the opposite one, depending on time.

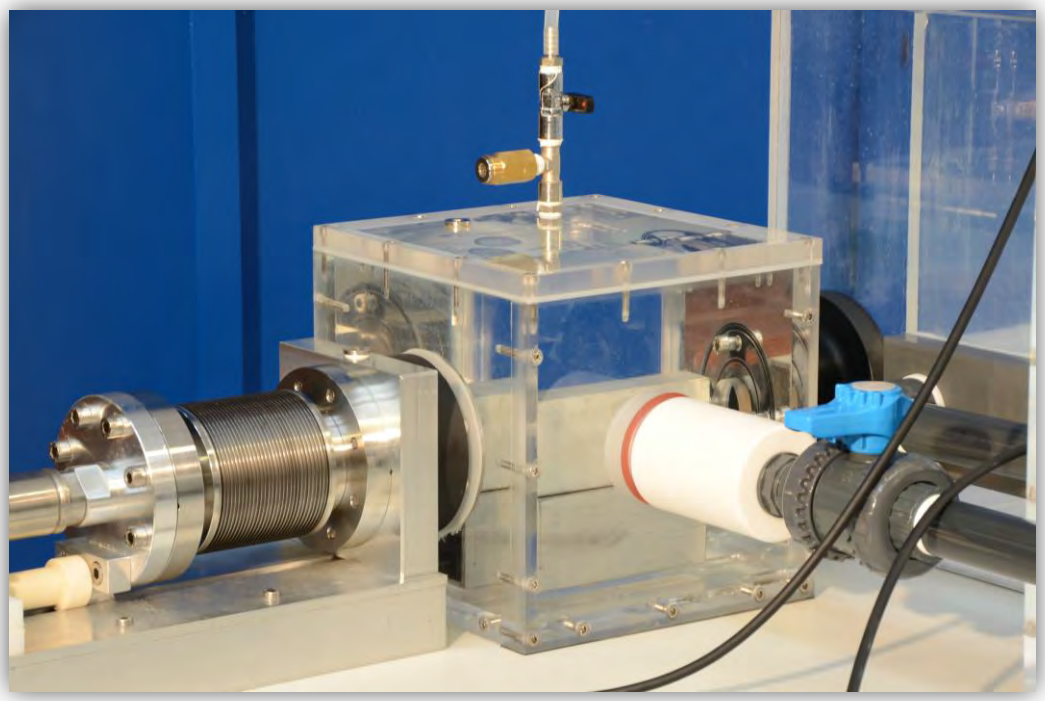

Figure 1.6: *Ventricular chamber*

Figure 1.7: *Connection of the mitral valve with the ventricular chamber*

1.4 Aortic Chamber

The aortic chamber represents the key part of the pulse duplicator, as regards the objectives of our research. This Plexiglas tank contains several components which are all very interesting for us. First of all we find in a watertight chamber the flow meter, whose description will be dealt with directly in the next chapter, entirely dedicated to it. The flow meter is connected by a tube to the rest of the aortic arch. We selected a deformable tube which could be easily bended without the risk of narrowing. In the middle of it we find another component, the “valve holder”. It is formed by a straight section of a Plexiglas pipe, and it hosts the aortic valve, 23 mm of diameter, as it is shown on the figure 1.9.

Before and after the valve, we installed some pressure sensors, in order to check how the pressures change in that stretch, as I will see in chapters 3 and 4.

This section of the device was designed in order to put a perfect tube able to reproduce the morphology and the mechanical characteristics of the physiological aortic arch.

Figure 1.8: *Aortic chamber*

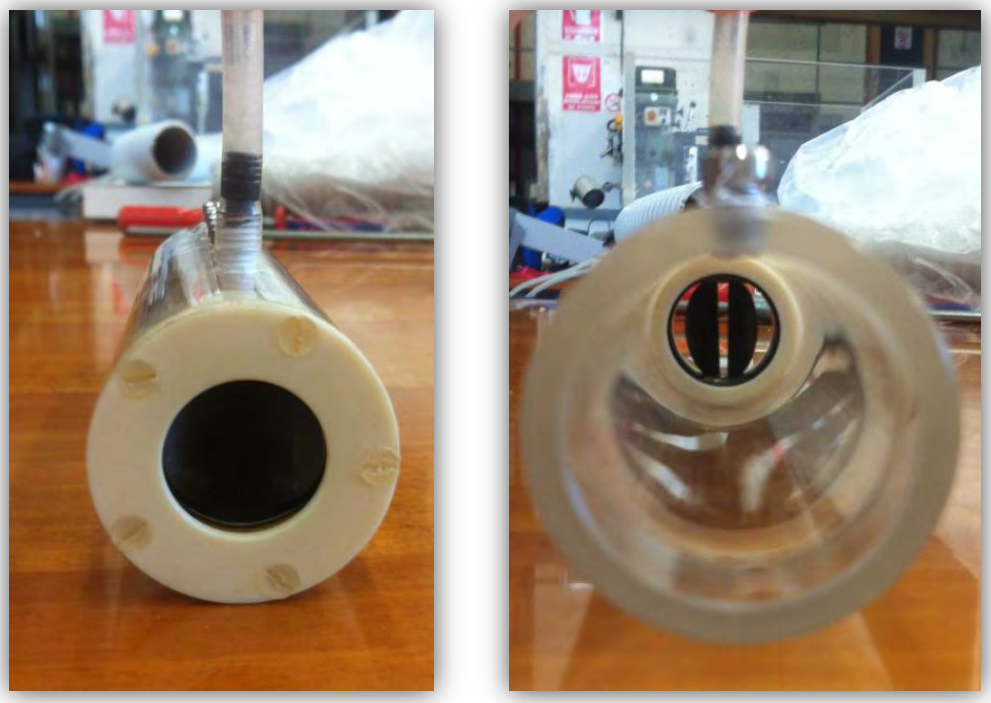

Figure 1.9: *Aortic valve, frontal and rear view*

1.5 Compliance chamber

The final part of the aortic arch is attached to the compliance, a Plexiglas transparent chamber with some additional elements, a nozzle for injecting compressed air inside, and a manometer to check it. This tank, together with the gate valve present at its output, has the aim to simulate the main characteristics of human systemic circulation, such as the elasticity of the arteries of greater diameter and the resistance offered by the peripheral vessels. The elasticity is very important because these arteries physiologically withstand the not inconsiderable radial deformations due to the ventricular pressure: in this way in the capillaries there is a quite constant flow with respect to the initial pulsatile motion generated by the heart. So the function of the compliance is that of exploiting the compressibility of air under pressure to absorb the pressure wave generated by the motion of the piston, and returning a more regular flow. In addition to this, even the second effect that we find in the human body, the resistance offered to the blood flow by the extremely high network of veins, it is important to be taken into account. That's why we try to replicate the same result in our device by inserting a specific gate valve whose regulation affects the flow and generates concentrated losses that we can control and modify almost in real time.

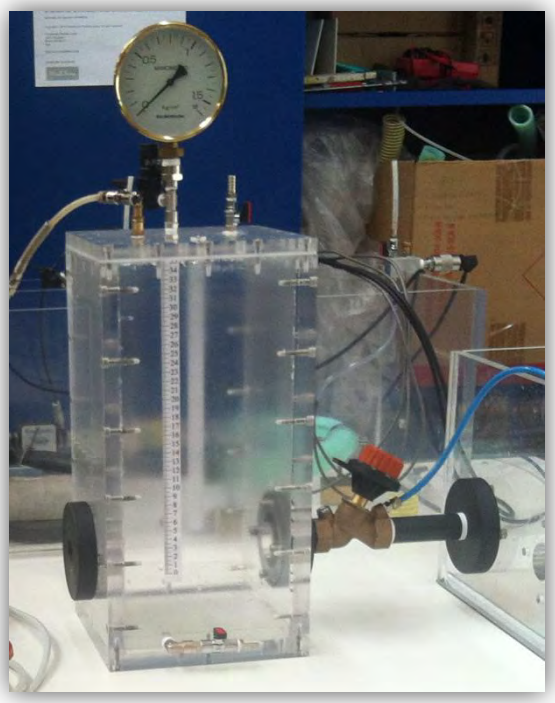

Figure 1.10: *Compliance chamber*

1.6 Atrial tank

The gate valve outside of the compliance chamber, it is directly linked with the atrial tank, a free surface basin made in Plexiglas. This stilling chamber has the function of damping the pulsatility of the motion, since the flow rate entering inside does not change the height of the free surface, having been dimensioned the entire tank for this purpose. The name 'atrial tank' is in analogy with the left atrium of the heart that carries blood to the left ventricle. From this element the device continues through a second gate valve (figure 1.11) that simulates the localized dissipation of energy again and from there we get back to the ventricular chamber.

Figure 1.11: *Gate valve*

Figure 1.12: *Atrial tank*

1.7 Heater

Along the tube connecting the atrial with the ventricular chamber, we find a heater. By passing through this metal heater, the fluid temperature rises to a value which we define according to our needs. Basically we deal with a resistance wrapped to the tube metal which supports a maximum power of 2000 W; starting from the mains supply (around 220 V) there is a thermostat that regulates the ignition resistance. When the temperature probe attached to it indicates that the fluid has reached the temperature that we choose, the resistance power is removed. The objective of this component is to bring the total fluid mass of the pulse duplicator at a temperature of 37 degrees in order to replicate the temperature at which the blood flows physiologically. Starting from the room temperature, the heater takes approximately 90 minutes to bring up the fluid degrees at about 37.

Figure 1.13: *Heater*

1.8 Control and Sensor Conditioning Unit

The control unit LT0510 made by LabTrek srl represents the main component for the control of the entire pulse duplicator. It manages the operation of the electric motor, it is connected to the unit of conditioning from which it receives the signals and, finally, it communicates with the computer. This device is made internally by three major electronic components:

-the drive of the electric motor that allows the movement of the motor on the basis of the information received from the computer on board, varying the voltages supplied as input to the motor. The driver receives a variable voltage representative of the law of displacement that we want to be imposed to the piston, and it converts it into the sequence of pulses that move the actuator;

-the board computer, Rabbit BL 2120, that acts as an intermediary between the computer and the drive of the motor through the use of the software LabView;

- the power supply circuit;

The sensor conditioning unit LS0609 made by LabTrek srl acquires, amplifies, filters and conditions the signals coming from the sensors located along the hydraulic circuit, so as to make them suitable for the subsequent processing performed by the computer. The hardware module is essentially constituted by two electronic components: the supply and filtering circuit, and the amplification board of the signals.

Figure 1.14: *Control and Sensor Conditioning Unit*

The description of the main characteristics of the components of the pulse duplicator is concluded. Further technical information and designed procedures can be found in the work thesis both of *Silvia Bellio* (1) and *Luigi Di Micco* (2).

CHAPTER 2
THE FLOWMETER

In this chapter I will describe in the details the measurement instrument that we use to monitor the flow rate flowing in the loop; after the illustration of all the components of the flow meter, I will depict the new configuration of the pulse duplicator used to test the efficiency of the above-mentioned device. The results of the experiment will be finally report with its sensitivity analysis.

2.1 The flow meter

The flow meter is an ultrasonic device which measures the flow rate of a fluid moving. The instrument is a *Transonic Systems Inc*. composed by two parts:

- The tubing flow module TS410, which measures volume flow in most non-aerated liquids. In particular it can be suitable for various fluids such as blood, saline water, cell culture, physiological buffers, blood analogs such as glycerin/water solutions, and even diesel fuel, with high resolution and low zero offset;

- the In-line ME-19PXN flowsensor, characterized by the highest sensitivity for low flow applications. It utilizes a scheme of ultrasonic illumination that makes it possible to manufacture a flow-through sensor with a smooth, cylindrical interior without compromising measurement accuracy; the four transducer sensor design offers precise and accurate flow measurement for low or high flow rates, steady state or pulsatile flows. Flow resolution is scaled to sensor size, and flow is measured accurately across the sensor's full dynamic range with little effect from turbulence. The sensor's smooth round flow channel is easy to clean and does not trap air bubbles that can degrade ultrasonic performance.

As I said this sensor we can have many fluids flowing inside, but it needs to be calibrated, and in our case the sensor results working properly with the saline solution. But this is not the only parameter that needs to be arranged; in effect, since temperature alter the transit time of the ultrasound signal and affect the acoustic properties of the tubing, we calibrate the sensor specifically for this parameter too. In particular, in this situation is either equal to 20°C, corresponding to the room temperature, or to 37°C, which is the physiologic body temperature, and the company told us the operational fluid temperature should be within $\pm 2°C$ of the specified calibration temperature. The sensor is supplied with a certificate of calibration for specified use valid for one year.

It is important to underline that the external case cannot be in touch with the water, so it was inserted in the watertight tank in between the ventricular basin and the aortic valve;

Here below I report the photos of the components followed by the data sheet:

Figure 2.1: Transonic tubing module TS410 (on the left), and inline ME19PXN flow sensor (on the right)

SENSOR SIZE	TUBING SPECIFICATIONS				INLINE FLOWSENSOR CALIBRATION RANGES[1]			
	TUBING ID		BARB OD		LOW FLOW (1/4 SCALE)[2]		STANDARD FLOW (FULL SCALE)	
	in	mm	in	mm	LOWER LINEAR LIMIT[3,4]	MAX MEASUREMENT RANGE[5]	LOWER LINEAR LIMIT	MAX MEASUREMENT RANGE[5]
1PXN	3/64	1.2	Flexible tubing		5 ml/min	-25 to +25 ml/min	10 ml/min	-100 to +100 ml/min
2PXN	1/16	1.6			10 ml/min	-50 to +50 ml/min	20 ml/min	-200 to +200 ml/min
3PXN	3/32	2.4			25 ml/min	-125 to +125 ml/min	50 ml/min	-500 to +500 ml/min
4PXN	1/8	3.2	0.16	4.0	50 ml/min	-250 to +250 ml/min	100 ml/min	-1 to +1 L/min
5PXN	3/16	4.8	0.23	5.8	100 ml/min	-500 to +500 ml/min	200 ml/min	-2 to +2 L/min
6PXN	1/4	6.4	0.3	7.6	250 ml/min	-1.25 to +1.25 L/min	500 ml/min	-5 to +5 L/min
10PXN	3/8	9.5	0.44	11.1	500 ml/min	-2.5 to +2.5 L/min	1 L/min	-10 to +10 L/min
13PXN	1/2	12.7	0.58	14.7	1 L/min	-5 to +5 L/min	2 L/min	-20 to +20 L/min
16PXN	5/8	15.9	0.72	18.3	2.5 L/min	-12.5 to +12.5 L/min	5 L/min	-50 to +50 L/min[6]
19PXN	3/4	19.1	0.86	21.9	2.5 L/min	-12.5 to +12.5 L/min	5 L/min	-50 to +50 L/min[6]
25PXN	1	25.4	1.14	29.0	5 L/min	-25 to +25 L/min	10 L/min	-100 to +100 L/min[6]

Figure 2.2: Data sheet of the flow sensor

SENSOR SIZE	BIDIRECTIONAL FLOW OUTPUTS				SYSTEM ACCURACY SPECIFICATIONS[1]			PHYSICAL SPECIFICATIONS[4]				ULTRASOUND FREQUENCY
	RESOLUTION	LOW FLOW (¼ SCALE)	STANDARD FLOW SCALE	MAX FLOW (STD SCALE)	MAX ZERO OFFSET[2]	ABSOLUTE ACCURACY	LINEARITY[3]	TOTAL LENGTH W/ TUBE ENDS		CASE LENGTH W/O TUBE ENDS		
	at 10 Hz in ml/min	1V output in ml/min	1V output in ml/min	5V output in L/min	ml/min	% of reading	%	in	mm	in	mm	MHz
1PXN	± 0.02	5	20	100	± 0.4	± 8	± 2	3.9	100	0.3	8	9.6
2PXN	± 0.02	10	40	200	± 0.6	± 4	± 2	3.9	100	0.5	12	9.6
3PXN	± 0.05	25	100	500	± 1	± 4	± 2	3.9	100	0.6	14	7.2
4PXN	± 0.1	50	200	1 L	± 2	± 4	± 2	1.0	25	0.6	16	4.8
5PXN	± 0.2	100	400	2 L	± 4	± 4	± 2	1.2	32	0.8	20	3.6
6PXN	± 0.5	250	1 L	5 L	± 10	± 4	± 2	1.6	41	1.0	26	2.4
10PXN	± 1	500	2 L	10 L	± 20	± 4	± 2	2.0	51	1.3	33	1.8
13PXN	± 2	1 L	4 L	20 L	± 40	± 4	± 2	2.7	69	1.8	45	1.2
16PXN	± 5	2.5 L	10 L	50 L	± 70	± 4	± 2	3.3	83	2.1	52	0.9
19PXN	± 5	2.5 L	10 L	50 L	± 100	± 4	± 2	4.0	101	2.5	64	0.9
25PXN	± 10	5 L	20 L	100 L	± 200	± 4	± 2	5.0	128	3.1	80	0.6

1. Stated system accuracy specifications apply to PXN Flowsensors with TS410 Flow Modules
2. Zero offset can be eliminated by Zero Adjustment prior to measurement
3. Within specified calibration range.
4. Standard cable length is 1.85 meters.

Figure 2.3: Second data sheet of the flow meter;

2.2 The configuration of the pulse duplicator for the costant flow

The original configuration of the pulse duplicator has a pump which allows having a pulsatile flow. However for this experiment we needed a constant flow, in order to be able to control the exact quantity of water flowing through the instrument; that's why we had to modify the setting of the device, passing from the standard block scheme reported in figure 1.3 to the new one, shown below.

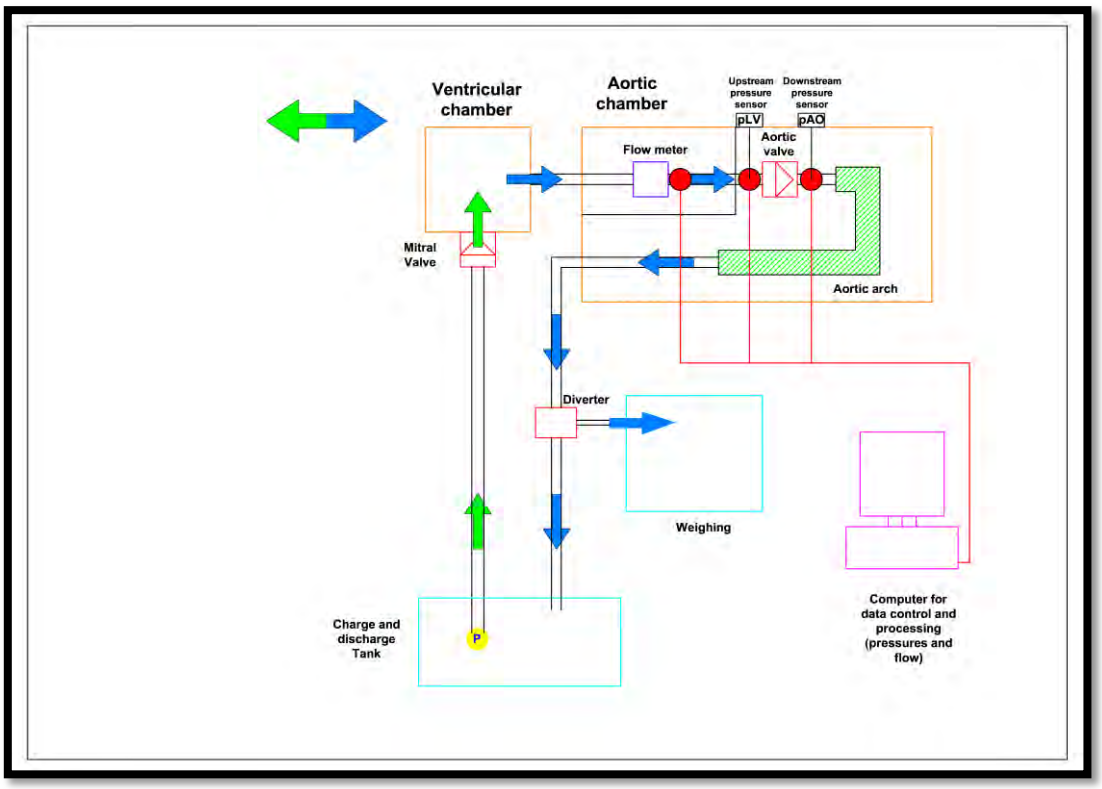

Figure 2.4: Block scheme of the new configuration

Basically we kept out the motor, the heater and the compliance chamber, and we added a pump able to maintain the water continuously flowing through the device. The pump was put in a container (figure 2.5), from which the water goes directly towards the ventricular chamber.

Figure 2.5: water tank with the pump

From this tank, the water is collected and it can follow two paths. This possibility to change direction is possible thanks to another component that we added for this experiment, a diverter. During the flow meter test, in fact, we needed not only a constant flow, but also the possibility to make the system open in some moments, as I will explain.

So, from the container where the pump is, the water is extracted and goes directly towards the aortic chamber flowing in the closed system, or, changing the position of the valve of the diverter, it is possible to change again the configuration obtaining an open system. In this case the water overflows in another tank.

Figure 2.6: closed loop in constant flow

2.3 Density calculation and flow meter test

The goal of the experiment is that of testing the flow meter and having an idea of the percentage of error that we can commit using it.

Substantially the test consists in comparing the flow rate recorded by the flow meter and the one obtained calculating mathematically its value.

The recorded flow rate is obtained by the input file coming from the flow meter and processed by the computer through the program LabView. Hence the value we took as 'recorded flow rate' comes from the mean of all the values recorded in the time interval.

As regards the calculated flow rate, the procedure is quite easy but little bit longer. Immediately after the utilization of the flow meter we changed the configuration of the system into an open one, just by turning the valve of the diverter (figure 2.7),

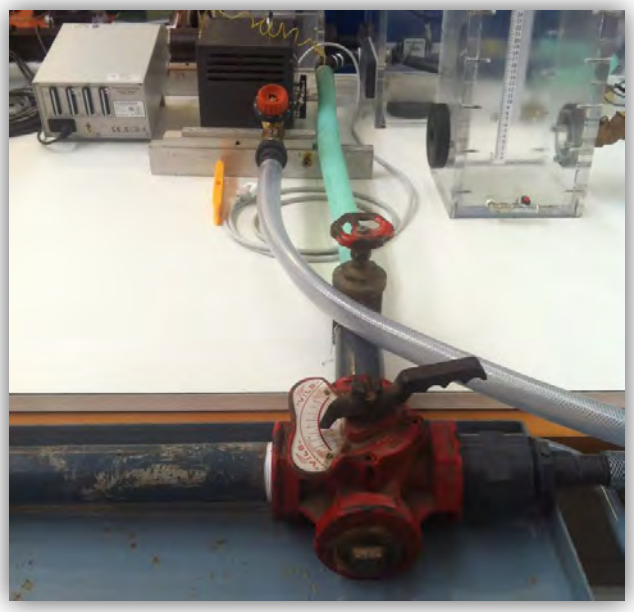

Figure 2.7: diverter

and letting the water flowing outside in a holding tank. The time employed to fill it was clocked, and then the container was weighted. Knowing the tare of the container we could obtained its net weight, and knowing the density of the solution, we can immediately calculate the volume of the tank. Therefore a data indispensable for our calculation is the density, which is not known a priori, since the fluid we use in the device is not simple water but a saline solution. Thus we needed to find out its value.

We proceeded with taking a sample of it in a measuring cup and weighing it taking into account the tare of the container; then, knowing the volume occupied by the liquid, we could obtain its density. We repeated the proof several times to obtain a quite precise number of its density. I resume all the calculation in the following charts:

TEST 1	WEIGHT	P [g]	P [Kg]				ϱ [Kg/m³] = 1100.96
		393.86	0.39386				
	VOLUME	d [cm]	A [cmq]	h [cm]	V [cmq]	V [mq]	
		6.65	34.73227	10.3	357.7424	0.000358	

Figure 2.8: Density calculation, test 1

TEST 2	WEIGHT	P [g]	P [Kg]				ϱ [Kg/m³] = 1070.063
		791.63	0.79163				
	VOLUME	d [cm]	A [cmq]	h [cm]	V [cmq]	V [mq]	
		6.65	34.73227	21.3	739.7974	0.00074	

Figure 2.9: Density calculation, test 2

TEST 3	WEIGHT	P [g]	P [Kg]				ϱ [Kg/m³] = 1021.777
		984.81	0.98481				
	VOLUME	d [cm]	A [cmq]	h [cm]	V [cmq]	V [mq]	
		6.65	34.73227	27.75	963.8205	0.000964	

Figure 2.10: Density calculation, test 3

TEST 4	WEIGHT	P [g]	P [Kg]				ϱ [Kg/m³] = 1015.17
		1096.56	1.09656				
	VOLUME	d [cm]	A [cmq]	h [cm]	V [cmq]	V [mq]	
		6.65	34.73227	31.1	1080.174	0.00108	

Figure 2.11: Density calculation, test 4

From all the numbers of density we obtained in each test we took the mean value, equal to:

$$\bar{\rho} = \frac{\rho_1 + \rho_2 + \rho_3 + \rho_4}{4} = 1052\ Kg/m^3$$

At this point just by dividing the net weight of the solution for the density, we could obtain the volume of the tank. The latter, divided by the filling time, gave us the calculated flow rate.

Here below I report the values I measured, from which I could extend my considerations over the efficiency of the instrument, comparing (figure 2.12) the recorded flow rate with the calculate one.

We repeated the test at different ranges of flow rate.

Recorded flow rate [l/min]	T [°C]	Filling time [s]	Gross weight [kg]	Tare [kg]	Net weight [kg]	Density [Kg/m3]	Volume [l]	Calculated flow rate [l/min]
7.1094	19.6	222	30.9	3.1	27.8	1052	26.4259	7.1421
13.8456	20.5	118	31.4	3.1	28.3	1052	26.9011	13.6785
22.0181	20.8	88	36.7	3.1	33.6	1052	31.9392	21.7767
32.9281	21.1	68	40.4	3.1	37.3	1052	35.4563	31.2849
43.3561	21.6	54	42.2	3.1	39.1	1052	37.1673	41.2970

Table 2.1: calculation of the flow rate

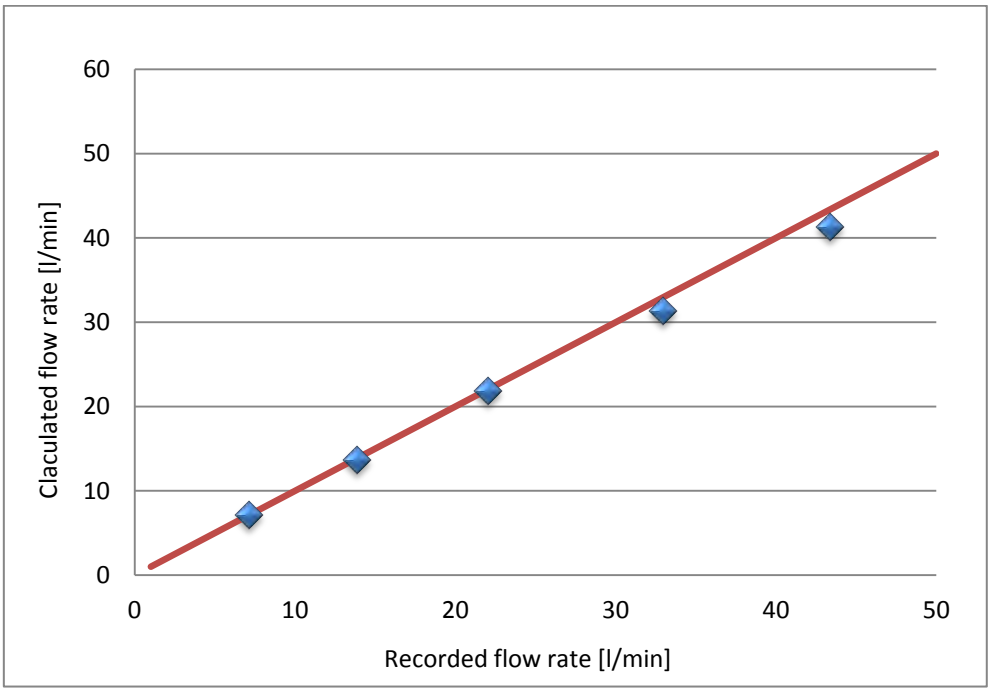

Figure 2.12: Recorded versus calculated flow rate

I could verify that the error between the flux measured by the flow meter and the real one grows progressively increasing the flow rate.

In fact, as you can see in the following table, for low flow rates the two values almost coincide, while when we start to have around 30 litres per minute, the error becomes about 5 per cent (acceptable anyway).

Recorded flow rate [l/min]	Calculated flow rate [l/min]	Error (%)
7.1094	7.1421	-0.4610
13.8456	13.6785	1.2069
22.0181	21.7767	1.0965
32.9281	31.2849	4.9902
43.3561	41.2970	4.7493

Table 2.2: differences between the recorded and calculated flow rates

One of the reason for which we could have this difference is related to the characteristics of the flow meter itself, calibrated to properly work with a temperature either of 20°C or 37°C. In our tests we started with a quite exact value but we could not avoid reaching the temperature of fast 22°C, due to the effect of the pump working which heated the water up.

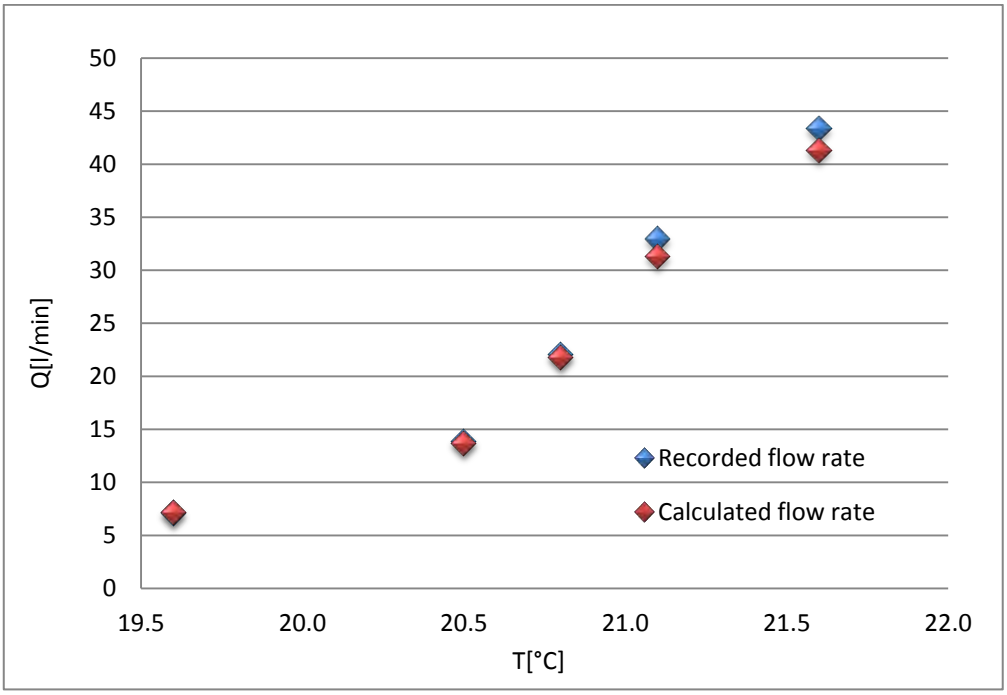

Figure 2.13: Recorded and calculated flow rate, function of the temperature;

2.4 Sensitivity Analysis and evaluation of the errors

Obviously we have to consider that, carrying out the measurements, we may have made some mistakes too, and we take it into account in the next graphs. They concern our ability to take the exact periods in which the water is discharged that is the time employed to fill the tank, which in our opinion could vary of more or less 1 second, and the weight of the tank filled, which depends on the sensitivity of our scale, equal to +/- 200 grams; all the 8 combinations are shown below.

- The first case is that in which the filling time remains constant and we suppose to add 0.2 kilograms to the weight of the tank.

CONSTANT TIME, **WEIGHT +0.2Kg**							
Recorded flowrate [l/min]	T [°C]	Filling time [s]	Net weight [kg]	Density [Kg/m3]	Volume [l]	Calculated flow rate [l/min]	Error (%)
7.1094	19.6	222	28.0	1052	26.6160	7.1935	-1.1837
13.8456	20.5	118	28.5	1052	27.0913	13.7752	0.5087
22.0181	20.8	88	33.8	1052	32.1293	21.9063	0.5078
32.9281	21.1	68	37.5	1052	35.6464	31.4527	4.4808
43.3561	21.6	54	39.3	1052	37.3574	41.5082	4.2621

Table 2.3: calculation of the flow rate, changing the weight of the tank of +200 grams

It seems that the flow meter works perfectly with the temperature of 20°C indeed, while a lower or higher value tends to create some differences, even if they result slightly smaller than the standard case;

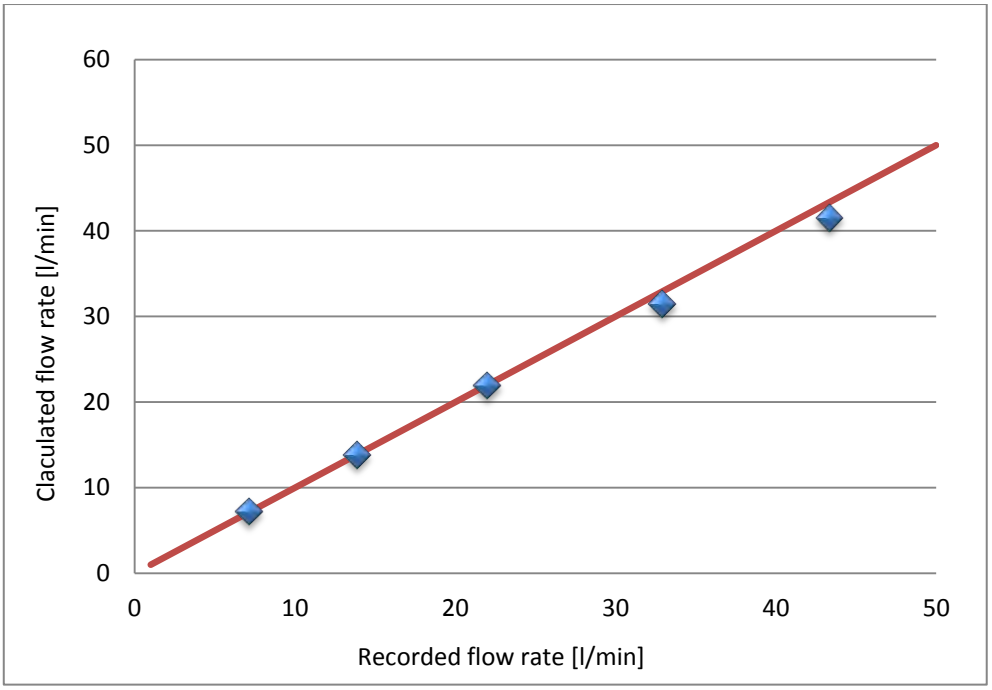

Figure 2.14: Recorded versus calculated flow rate, weight +200g

- The second one is that in which we suppose to remove 0.2 Kilograms to the weight of the tank, while the filling time remains the same.

CONSTANT TIME, **WEIGHT -0.2Kg**							
Recorded flowrate [l/min]	T [°C]	Filling time [s]	Net weight [kg]	Density [Kg/m3]	Volume [l]	Calculated flow rate [l/min]	Error (%)
7.1094	19.6	222	27.6	1052	26.2357	7.0907	0.2618
13.8456	20.5	118	28.1	1052	26.7110	13.5819	1.9051
22.0181	20.8	88	33.4	1052	31.7490	21.6471	1.6852
32.9281	21.1	68	37.1	1052	35.2662	31.1172	5.4997
43.3561	21.6	54	38.9	1052	36.9772	41.0858	5.2366

Table 2.4: calculation of the flow rate, changing the weight of the tank of -200 grams

This time it exceeds lightly the threshold of 5 per cent which is the number we do not want to surpass; so we notice that considering a smaller weight influences the measurement more than the previous case.

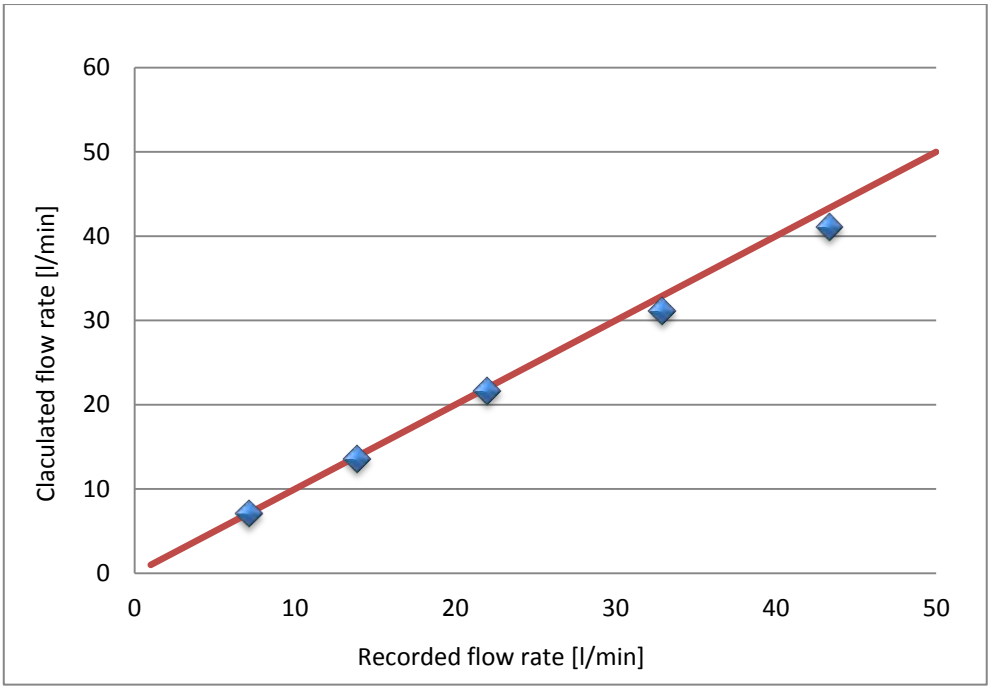

Figure 2.15: Recorded versus calculated flow rate, weight -200 grams

- The third case is that in which we suppose, keeping the weight as constant, that the tank took 1 second more to be filled.

CONSTANT WEIGHT, **FILLING TIME +1s**							
Recorded flowrate [l/min]	T [°C]	Filling time [s]	Net weight [kg]	Density [Kg/m3]	Volume [l]	Calculated flow rate [l/min]	Error (%)
7.1094	19.6	223	27.8	1052	26.4259	7.1101	-0.0105
13.8456	20.5	119	28.3	1052	26.9011	13.5636	2.0371
22.0181	20.8	89	33.6	1052	31.9392	21.5320	2.2078
32.9281	21.1	69	37.3	1052	35.4563	30.8315	6.3672
43.3561	21.6	55	39.1	1052	37.1673	40.5461	6.4812

Table 2.5: calculation of the flow rate, changing the filling time of +1 second

Considering a longer time to discharge the water from the circuit, it rather influences the results in a negative way, leading the differences between the recorded and calculated flow rates to reach fast the 6.5 %;

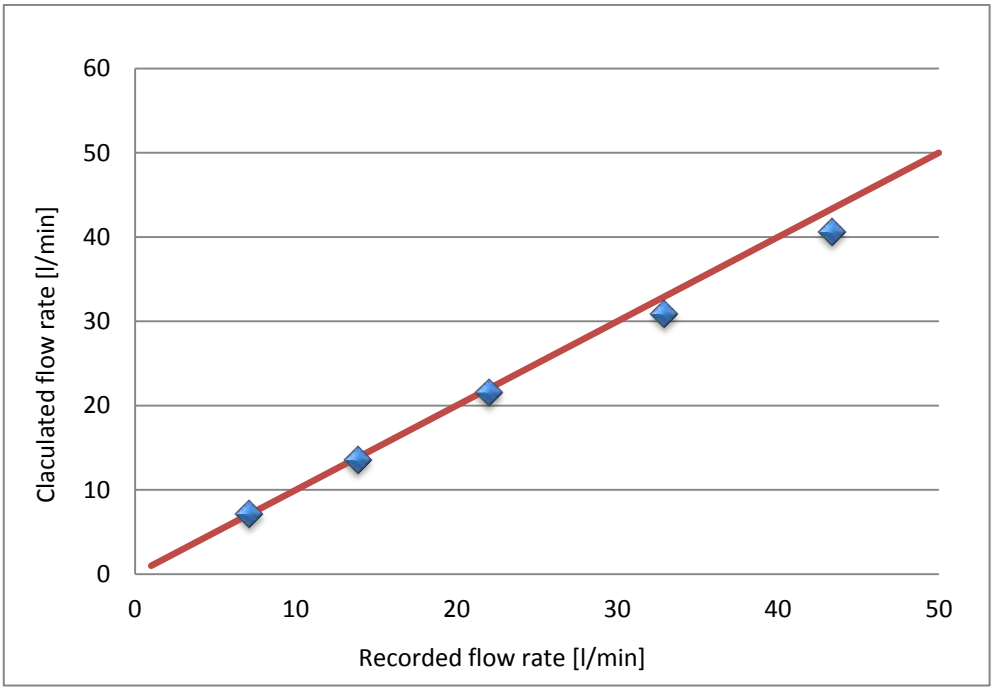

Figure 2.16: Recorded versus calculated flow rate, filling time +1second

- The fourth case is that in which we suppose, still keeping the weight as constant , that the tank took 1 second less to be filled.

CONSTANT WEIGHT, **FILLING TIME -1s**							
Recorded flowrate [l/min]	T [°C]	Filling time [s]	Net weight [kg]	Density [Kg/m3]	Volume [l]	Calculated flow rate [l/min]	Error (%)
7.1094	19.6	221	27.8	1052	26.4259	7.1744	-0.9155
13.8456	20.5	117	28.3	1052	26.9011	13.7955	0.3625
22.0181	20.8	87	33.6	1052	31.9392	22.0270	-0.0403
32.9281	21.1	67	37.3	1052	35.4563	31.7519	3.5722
43.3561	21.6	53	39.1	1052	37.1673	42.0762	2.9522

Table 2.6: calculation of the flow rate, changing the filling time of -1 second

In contrast with the previous situation, here the errors decrease resulting fast null for flow rates lower than 30 litres per minute;

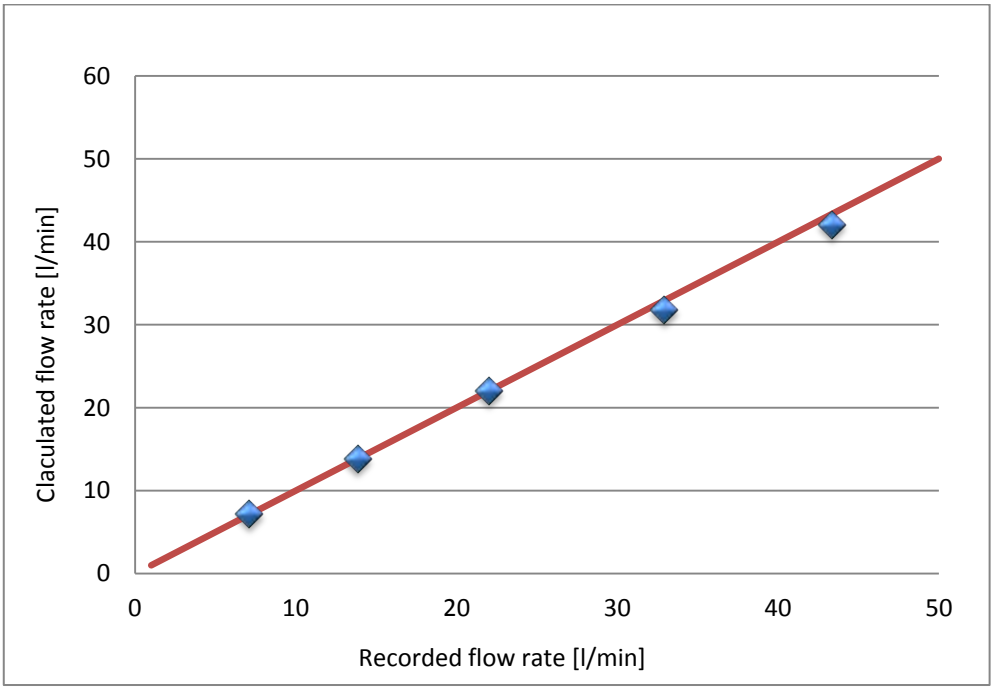

Figure 2.17: Recorded versus calculated flow rate, filling time -1second

- In this situation we start to combine the effects due to the change of both the filling time and of the weight, increased of one second and 200 grams, respectively.

WEIGHT +0.2Kg, FILLING TIME +1s							
Recorded flowrate [l/min]	T [°C]	Filling time [s]	Net weight [kg]	Density [Kg/m3]	Volume [l]	Calculated flow rate [l/min]	Error (%)
7.1094	19.6	223	28.0	1052	26.6160	7.1612	-0.7300
13.8456	20.5	119	28.5	1052	27.0913	13.6595	1.3448
22.0181	20.8	89	33.8	1052	32.1293	21.6602	1.6257
32.9281	21.1	69	37.5	1052	35.6464	30.9969	5.8651
43.3561	21.6	55	39.3	1052	37.3574	40.7535	6.0028

Table 2.7: calculation of the flow rate, changing the filling time of +1 second and the weight of +200 grams

This case shows the different import the two modifications have. We combined an heavier weight, which before showed to help the gap between recorded and calculated flow rates to decrease, with a longer filling time which on the contrary had the opposite effect, and which results being the most influent.

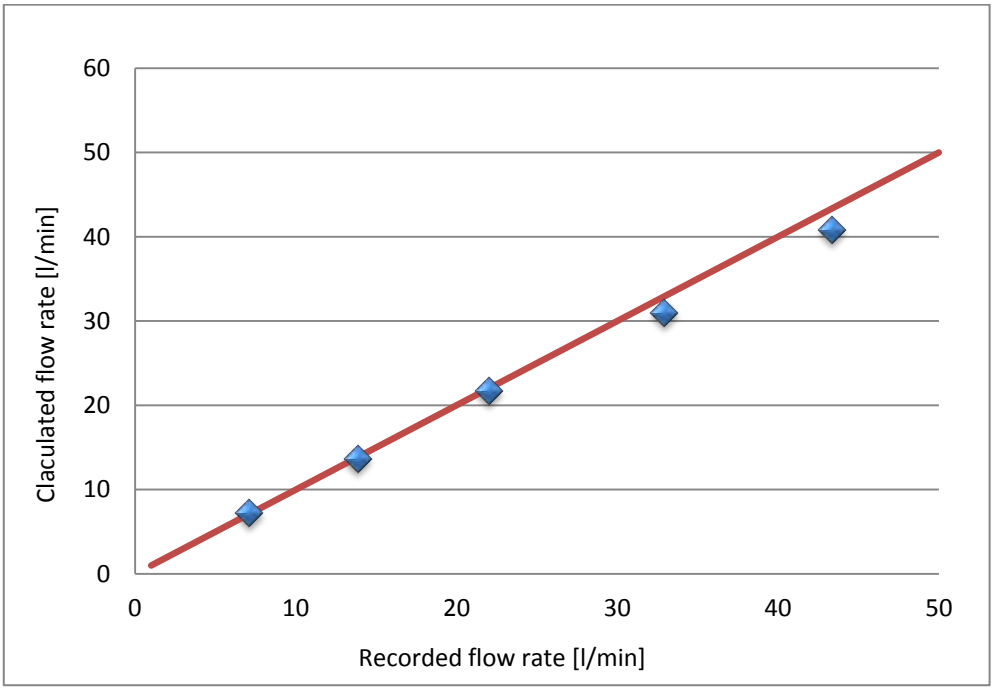

Figure 2.18: Recorded versus calculated flow rate (weight +200g, filling time +1second)

- Keeping the weight equal to the previous case, we remove here one second to the basic filling time.

WEIGHT +0.2kg, FILLING TIME -1s							
Recorded flowrate [l/min]	T [°C]	Filling time [s]	Net weight [kg]	Density [Kg/m3]	Volume [l]	Calculated flow rate [l/min]	Error (%)
7.1094	19.6	221	28.0	1052	26.6160	7.2261	-1.6416
13.8456	20.5	117	28.5	1052	27.0913	13.8930	-0.3417
22.0181	20.8	87	33.8	1052	32.1293	22.1581	-0.6358
32.9281	21.1	67	37.5	1052	35.6464	31.9221	3.0551
43.3561	21.6	53	39.3	1052	37.3574	42.2914	2.4558

Table 2.8: calculation of the flow rate, changing the filling time of -1 second and the weight of +200 grams

As we expected, here is it the best situation. Summing the variations we found out being the most positive, we reach in achieving the lowest distance between the two values of the flow rates, the recorded and the calculated one, with a maximum error of 3%, more than acceptable.

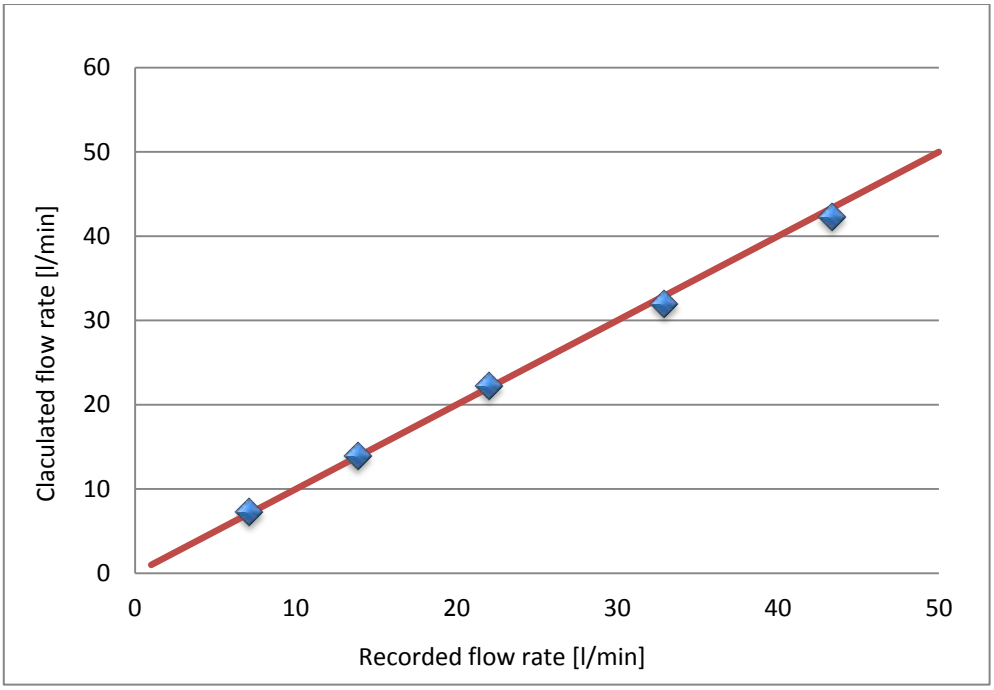

Figure 2.19: Recorded versus calculated flow rate, weight +200g filling time -1second

- In the last but one case we combine a lighter tank filled in a longer time

WEIGHT -0.2kg, FILLING TIME +1s							
Recorded flowrate [l/min]	T [°C]	Filling time [s]	Net weight [kg]	Density [Kg/m3]	Volume [l]	Calculated flow rate [l/min]	Error (%)
7.1094	19.6	223	27.6	1052	26.2357	7.0589	0.7090
13.8456	20.5	119	28.1	1052	26.7110	13.4677	2.7294
22.0181	20.8	89	33.4	1052	31.7490	21.4039	2.7899
32.9281	21.1	69	37.1	1052	35.2662	30.6662	6.8692
43.3561	21.6	55	38.9	1052	36.9772	40.3387	6.9595

Table 2.9: calculation of the flow rate, changing the filling time of +1 second and the weight of -200 grams

This is the worst situation, achieving the biggest distance between the values of the two flow rates, giving an error of fast 7%

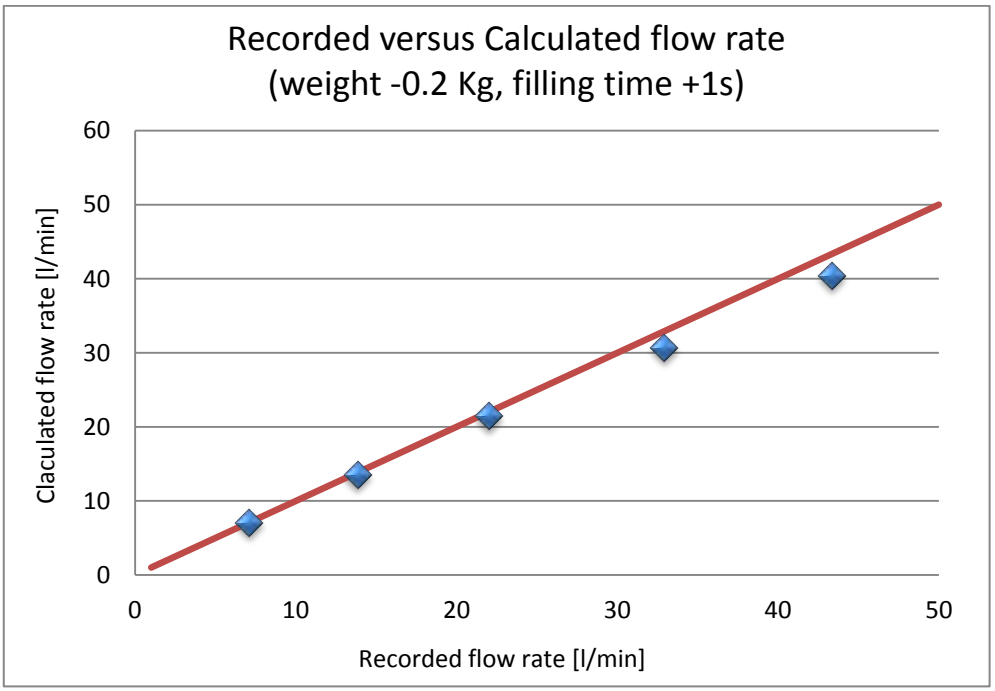

Figure 2.20: Recorded versus calculated flow rate, weight -200g filling time +1second

- The last situation regards the combination between having weighed a lighter tank filled in a smaller time.

WEIGHT -0.2kg, FILLING TIME -1s							
Recorded flowrate [l/min]	T [°C]	Filling time [s]	Net weight [kg]	Density [Kg/m3]	Volume [l]	Calculated flow rate [l/min]	Error (%)
7.1094	19.6	221	27.6	1052	26.2357	7.1228	-0.1895
13.8456	20.5	117	28.1	1052	26.7110	13.6980	1.0666
22.0181	20.8	87	33.4	1052	31.7490	21.8959	0.5552
32.9281	21.1	67	37.1	1052	35.2662	31.5816	4.0892
43.3561	21.6	53	38.9	1052	36.9772	41.8610	3.4486

Table 2.10: calculation of the flow rate, changing the filling time of -1 second and the weight of -200 grams

Even if having a lighter tank influence negatively in the calculation to get the value of the real flow rate, imaging having discharge the water in a faster time avoid in reaching a gap too high between the two values, staying below the limit of 5% of error;

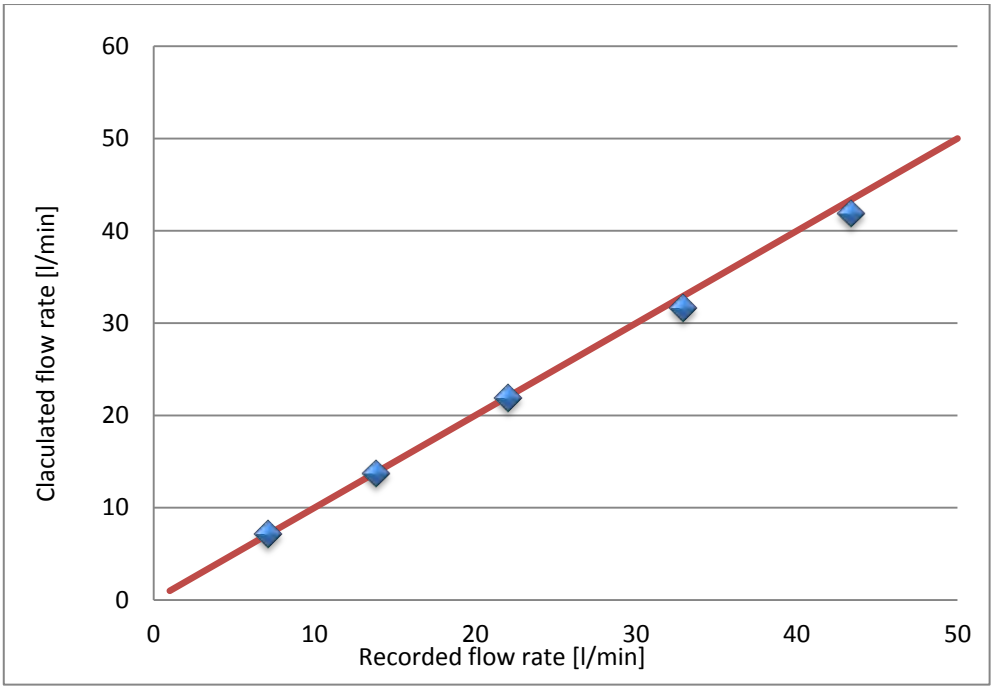

Figure 2.21: Recorded versus calculated flow rate, weight -200g filling time -1second

2.5 Results

To sum up here there are the total results comparing the values of the test from which we started up and the modifications giving the lowest and highest errors, respectively.

Recorded flowrate [l/min]	Calculated flow rate [l/min]	Error (%)
BASIC TEST		
7.1094	7.1421	-0.4610
13.8456	13.6785	1.2069
22.0181	21.7767	1.0965
32.9281	31.2849	4.9902
43.3561	41.2970	4.7493
WEIGHT +0.2kg, FILLING TIME -1s		
7.1094	7.2261	-1.6416
13.8456	13.8930	-0.3417
22.0181	22.1581	-0.6358
32.9281	31.9221	3.0551
43.3561	42.2914	2.4558
WEIGHT -0.2kg, FILLING TIME +1s		
7.1094	7.0589	0.7090
13.8456	13.4677	2.7294
22.0181	21.4039	2.7899
32.9281	30.6662	6.8692
43.3561	40.3387	6.9595

Table 2.11: resuming tests

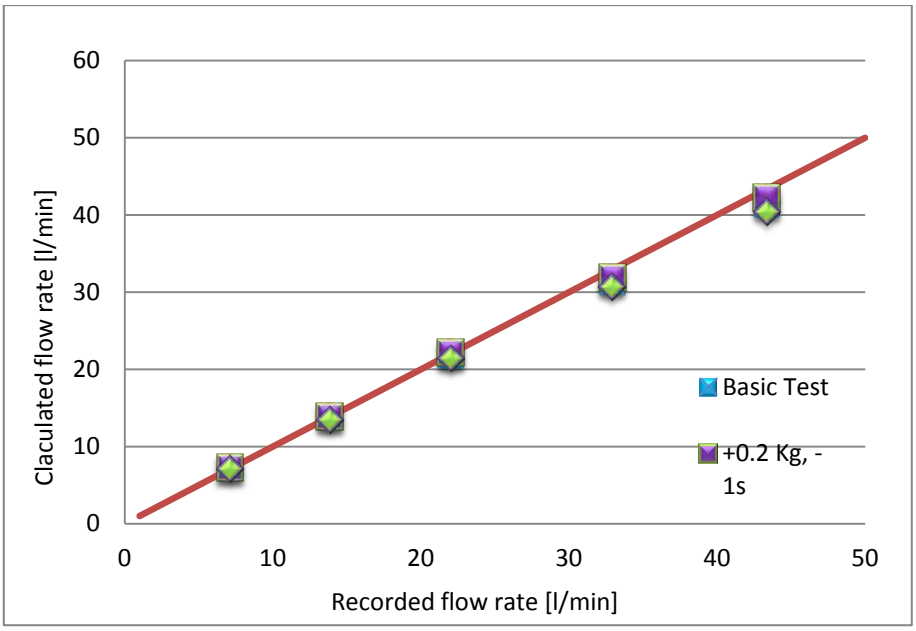

Figure 2.22: Recorded versus calculated flow rate comparing the tests

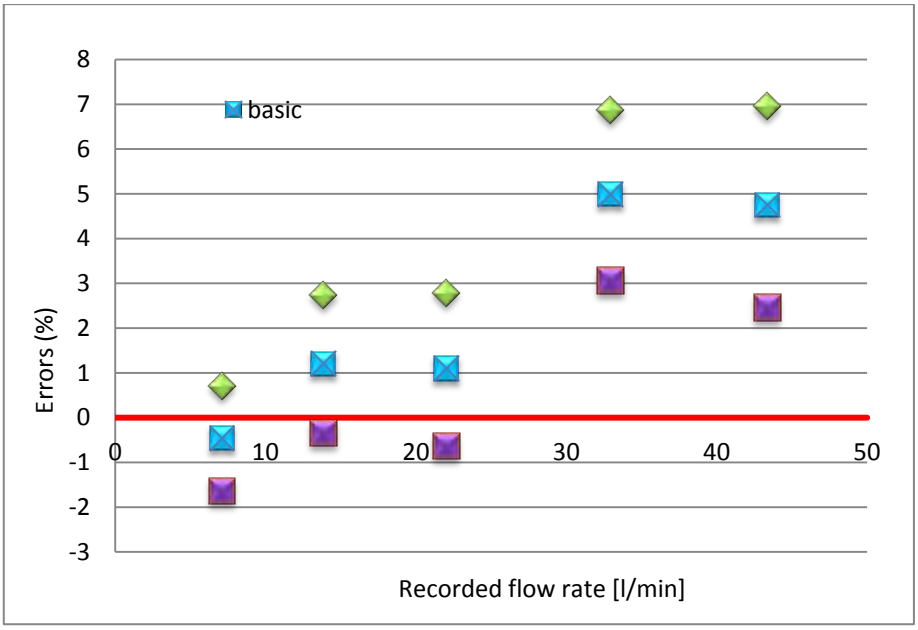

Figure 2.23: Recorded flow rate function of the errors comparing the tests

In the worst situation the error is near 7% but we think that this case is not realistic because we paid attention in taking the measurements and it is really difficult that we committed this combination of mistakes together. So, taking everything into account I can say that my test to proof the efficiency of the flow meter was satisfactory, and I can consider the values the instrument records as corresponding to the reality.

CHAPTER 3
PRESSURE TESTS – CONSTANT FLOW

In this chapter we are interested in investigating the trend of pressure in the section of the device situated upstream respect to the aortic valve. After the explanation of the experiment and the description of the instruments used for it, I will report the theoretical lines of the problem, to which I will refer in order to judge the results I obtained from the test.

3.1 Description of the experiment

For the following experiment we kept the same configuration of the device prepared for the previous tests on the flow meter. This means that, even in this situation, we will not use the engine because we need to have a constant flow. Our goal is to study how the pressures change at different distances along the section preceding the aortic valve.

In figure 3.1 I report the scheme of the area interested with the relative positions of the probes:

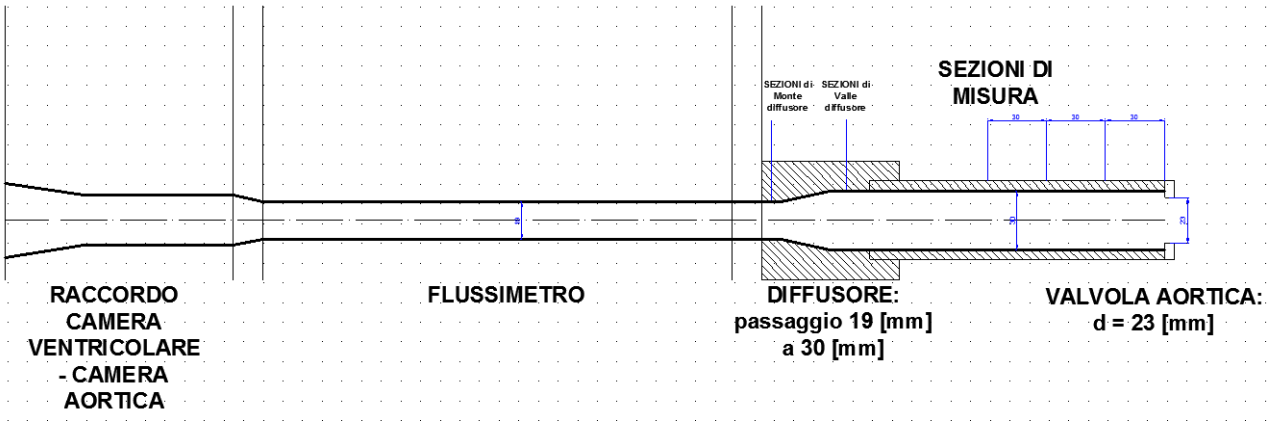

Figure 3.1: Section of the pulse duplicator interested by the pressure tests at constant flow

The fact of analyzing the trend of pressures in this part, at constant flow, is a fundamental field to study mainly for two causes.

First of all the normative EN 5840 outlines some points that need to be follow for the verification of hydrodynamic performance of a pulse duplicator (3). In fact, in order to ensure that the device meets the design intent and the minimum performance requirements, it is important to proceed with the tests in steady forward state, in addition and before of the pulsatile flow conditions.

But, beyond this more formal motivation, it is for us really a key subject to be investigated. The reason can be easily understood if we think about what we explained in the last chapter talking about the flow meter. The inline flowsensor that was chosen to fit at best our device has a size of 19 mm, hence it was inserted in a tube of that width. On the contrary the part of the pipe forming the aortic arch, and where the valve is inserted in, has a diameter of 30 mm corresponding to the mean dimension of the aorta. Consequently, we had to create a junction between the two tubes, which will probably cause some dissipation and thus it will inevitably influence the behavior of the pressures. Precisely through this test we want to quantify the disturbance created by this problem to understand to what extent it affects the operation of the pulse duplicator.

To conduct this experiment we need some pressure sensors that I am going to present in the next section.

3.2 Pressure transducers and transmittance

There are some instruments whose sensitivity is fundamental to obtain significant data: these are the pressure sensors. In particular for this work we used three PCB Piezotronics sensors from the series 1500, in particular the models 1760, 1761 and 1762, which are measuring instruments characterized by high performance and reliability. In effect, it is just thanks to them that it can be possible to measure the pressures in the aortic tract in real time; these data are thus provided first to the conditioning unit and then to the computer, which is able to read the signals by means of the Software LabView.

Here below you can have a look at the data sheet of one sensor, farther than seeing its photo.

Test Sensor:			Test Equipment:	
Model Number:	1502B02EZ10PSIG		Calibration Method:	AT-403-2
Serial Number:	1761		Pressure Source[4]:	DHI PPC2+ S/N 348
Manufacturer:	PCB Piezotronics Inc.		Test Sensor Readout:	HP S/N 101
Description:	Pressure Sensor			
			Ambient Temp.	71 °F [22 °C]
Pressure Range[5]:	0 to 10 psi	[0 to 69.0 kPa]	Relative Humidity:	56%
Mode[5]:	Gauge		Atmospheric Pressure:	14.38 PSI [99.15 kPa]
Test Sensor Output[5]:	0 to 10 V		Pressure Medium:	N2
Calibration Data:				
Sensitivity:	0.9987 V/psi	[0.1448 V/kPa]	Linearity[1]:	0.07% FS
Zero Output:	-0.005 V		Hysteresis:	0.15% FS
Zero Output Error:	-0.1% FS		Accuracy[6]:	0.17% FS
Full Scale Output:	9.9895 V			
Full Scale Output Error:	-0.1% FS			

Figure 3.2: Specifications of one Piezometrics sensor, provided by the manufacturer;

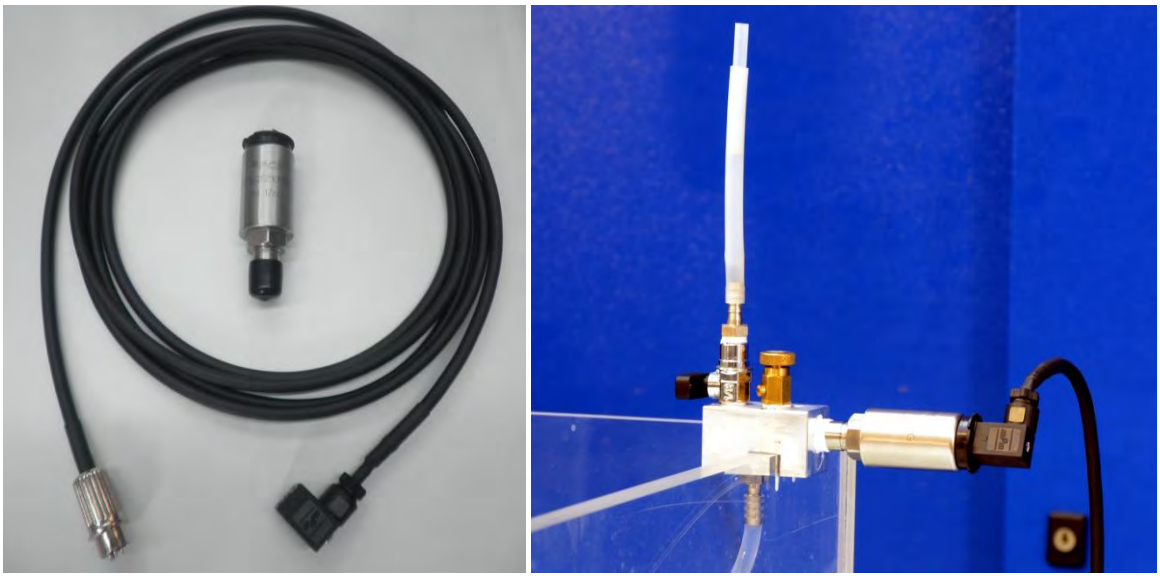

Figure 3.3: Piezotronics sensor with its transmission cable (to the left) and pressure transducer installed in the device;

For their utilization we need to have the calibration line of each sensors, which gives us the conversion and the relationship between the voltages measured and the height in mmHg to which the Volts corresponds in terms of pressure.

Here you are one of the calibration lines, provided by PCB Piezotronics factory:

Reference Pressure		Test Sensor Output
(psi Gauge)	(kPa)	(V)
0.000	0.0000	0.019
2.000	13.790	2.019
4.000	27.580	4.017
6.000	41.370	6.013
8.000	55.160	8.007
10.000	68.950	9.999
10.000	68.950	9.999
8.000	55.160	8.012
6.000	41.370	6.021
4.000	27.580	4.025
2.000	13.790	2.026
0.000	-0.0007	0.023

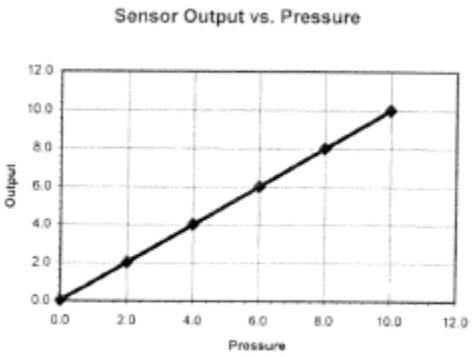

Figure 3.4: Calibration curve of one piezotronics sensor, provided by the company;

As I can see from the table this instrument is able of detecting a voltage varying linearly between 0 and 10 V, equivalent to a capacity of full scale equal to 10 psi, corresponding to 68.95 kPa and to 571.17 mmHg.

The factory provides these data, but this is not enough. Indeed, precisely because we are talking about very precise tools, the same turn out to be also very delicate. You should pay attention to handle them, in particular during the installation and when you change their positions in case of need. Neglecting to always check the conditions at which they can work, or using them inappropriately can quite easily lend them to go out of calibration, which results immediately into an incorrect measurement.

That's why we preferred to verify the values we had been giving by the PCB Piezotronics company to add in the block scheme of LabView. In order to totally avoid this problem, we paid attention in repeating the calibration tests quite often, each time that we displaced some 'structural element' of the device or when we did not use them for a long time, at least.

The procedure for this experiment is quite easy. We did not even need to work with the mercury, water was enough for us, at the end it was just sufficient to convert the centimeter of water into millimeter of mercury, according to this relation:

$$1\ cm\ H_2O = 0.735559121015\ mm\ Hg \qquad (3.1)$$

To sum up, we used a column about 4 meters high, inside which we applied a metric scale for the detection of the measurement. The lower extremity of the cylindrical tube was connected via a three-way conduit, necessary for the entry of water (from a tube connected to the aqueduct), for its release, and for the attachment to the pressure sensors which were directly connected by the transmitter cables to the conditioning unit to get the measure in volts of the height of the water. At this point it was sufficient to open the tap to bring up the water in the column, and after taking note of the measure in centimeters, it was detected the voltage for each of the sensors. The operation was repeated at different heights to obtain the calibration curve.

Figure 3.6: column for the calibration

Figure 3.5: attachment of the pressure sensors

Figure 3.7: Particular of the connection between the column, the sensors and the conditioning unit;

It's a matter of a series of static measurements necessary to compare the measurement of the sensor and the data read via the piezometer.

Below I report one of the several tests carried out: the table shows the liquids levels taken into account and the relative values measured in volts; the measurements taken allow determining the conversion line between Volt and mmHg, which is then implemented in the program LabView developed.

Height read [cmH2O]	h - cm	h - mmHg	Sensor 1 [V]	Sensor 2 [V]	Sensor 3 [V]
33.0	32.6	23.979	-2.288	-1.250	-2.174
64.4	64.0	47.076	-0.352	0.663	-0.322
91.6	91.2	67.083	1.345	2.336	1.315
120.0	119.6	87.973	3.168	4.110	3.051
161.9	161.5	118.793	5.728	6.630	5.521
199.7	199.3	146.560	8.060	8.920	7.780
247.2	246.8	181.536	10.990	11.790	10.610
210.7	210.3	154.688	8.740	9.590	8.450
182.2	181.8	133.725	6.980	7.870	6.760
152.1	151.7	111.584	5.121	6.053	4.965
126.4	126.0	92.680	3.525	4.486	3.431
97.7	97.3	71.570	1.720	2.723	1.711
78.3	77.9	57.300	0.509	1.534	0.558
52.8	52.4	38.543	-1.084	-0.034	-0.977
30.1	29.7	21.846	-2.489	-1.420	-2.330

Table 3.1: Data of the calibration test of the three Piezotronics sensors

In the graphs below I found out the calibration curve for each sensor:

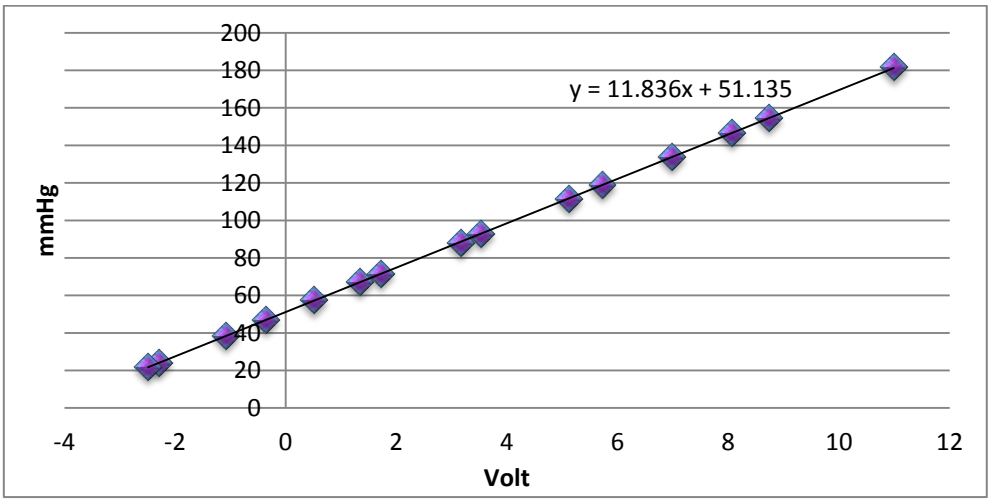

Figure 3.8: Sensor 1 output versus pressure, with the calibration line resulting;

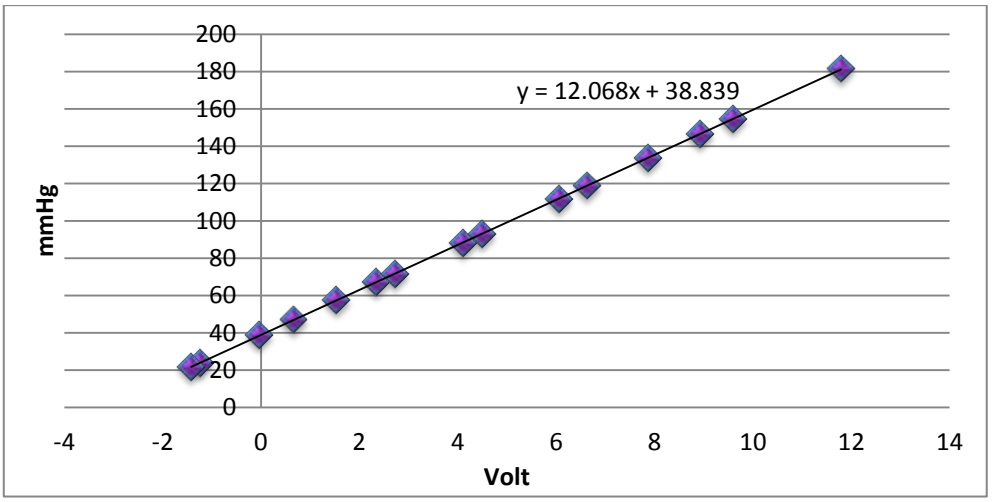

Figure 3.9: Sensor 2 output versus pressure, with the calibration line resulting;

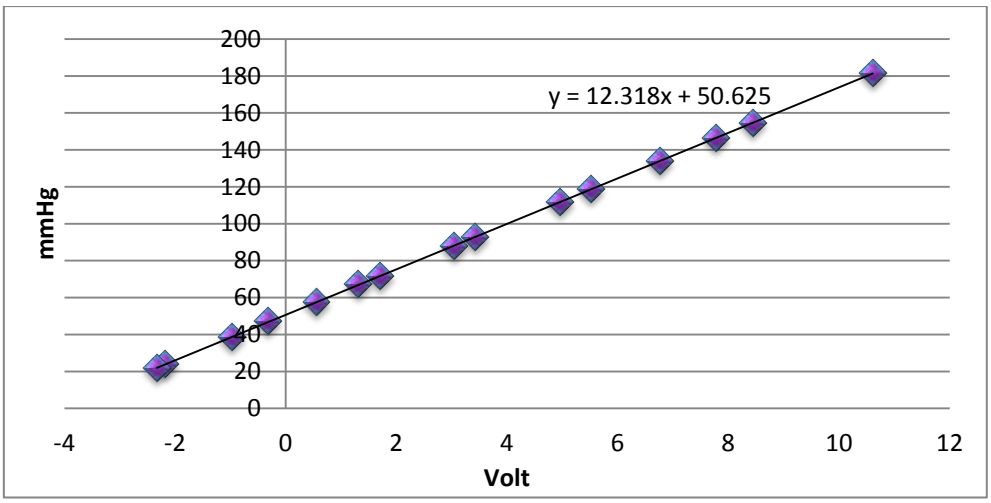

Figure 3.10: Sensor 3 output versus pressure, with the calibration line resulting;

Once the calibration procedure is completed, I can proceed with the installation of the sensors in the device and with their utilization.

3.3 Theoretical Overview

Going back to our experiment, in this chapter we want to study the pressure trend in the aortic chamber resulting from a change in a cross-sectional area. In particular in the configuration of our device we have an enlargement of the pipe, whose diameter of 19 mm becomes equal to 30 mm.

Of course we already expect the pressures to behave in a certain way, due to the knowledge of hydrodynamics that we have; in this paragraph in fact I report the theory that underlies the problem and on which we rely.

Generally speaking, one of the most important statement in fluid dynamics belong to Bernoulli, who stated that for an ideal flow of a non-conducting fluid, an increase in the speed of the fluid occurs simultaneously with a decrease in pressure or a decrease in the fluid's potential energy.

The basis form of Bernoulli's principle is valid for incompressible flows (their density is constant) and it can be derived from the principle of conservation of energy which states that, in a steady flow, the sum of all forms of energy in a fluid along a streamline is the same at all points on that streamline.

As a result, the common form of Bernoulli's equation for an incompressible flow is:

$$\frac{p}{\gamma} + h + \frac{v^2}{2g} = constant \qquad (3.2)$$

Therefore, between two points of the trajectory we have:

$$\frac{p_2 - p_1}{\gamma} + (h_2 - h_1) + \frac{v_2^2 - v_1^2}{2g} = 0 \qquad (3.3)$$

where:

- → h is the potential energy of a unit weight of fluid with respect to the reference plane represented by the elevation of the point above a reference plane;
- → $\frac{v^2}{2g}$ is the kinetic energy of the mass corresponding to the unit weight (kinetic height);
- → $\frac{p}{\gamma}$ is the piezometric height, that is the work that must fulfill the unit of weight of the fluid, i.e. the energy that the pressure forces can provide;

Moreover I can say the constant of the equation 3.2 represents the sum of the three forms of mechanical energy: the kinetic energy, potential energy and internal energy remains constant. Thus an increase in the speed of the fluid, implying an increase in both its dynamic pressure and

kinetic energy, occurs with a simultaneous decrease in the sum of its static pressure, potential energy and internal energy.

This total energy is called Specific Energy E of the fluid:

$$E = \frac{p}{\gamma} + h + \frac{v^2}{2g} = constant \qquad (3.4)$$

This is the theory that underlies the problem, of course in our case we must pay attention to the conditions in which we work, which differs from the basic problem and involves the concept of the modifications of the equation due to the geometry that we have.

Specifically in reality we cannot consider the formula of Bernoulli as correct if we do not take into account the fact that there are some energy losses along the flow path. Through the pipe there are in fact continuous losses of energy due to the friction of the water along the wall, which in our case we consider negligible. In addition to these, however, there are some localized losses due to the change in the geometry of the section, and in this case particularly to the enlargement of the tube, which is important to consider for a correct evaluation of the influence that this configuration has on our analysis.

When the water flow through a sudden expansion in a piping system, as you can see in figure 3.11, there are some mechanical energy losses of the fluid.

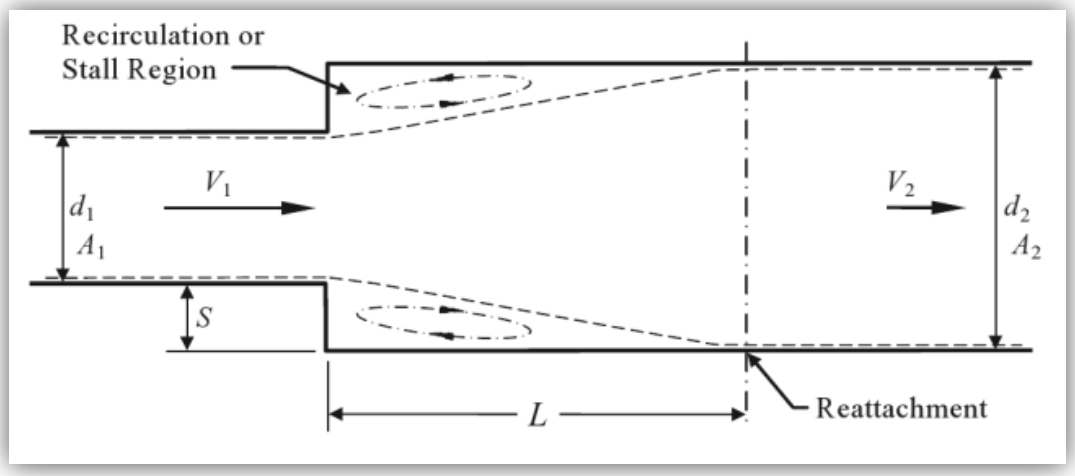

Figure 3.11: change in geometry, sudden expansion

In order to consider these effects we refer to the theory of Borda – Carnot, whose equation gives the decrease in the constant of the Bernoulli equation.
In particular for an incompressible flow the equation becomes:

$$\frac{p_2-p_1}{\gamma} + (h_2 - h_1) + \frac{v_2^2-v_1^2}{2g} = \Delta E \qquad (3.5)$$

that is

$$E_2 = E_1 + \Delta E \qquad (3.6)$$

where *ΔE* is the fluid's mechanical energy loss, quantified by Borda as (4):

$$\Delta E = \frac{v_1^2}{2g} \cdot \left[\left(\frac{A_1}{A_2}\right) - 1\right]^2 \qquad (3.7)$$

Besides of the sudden expansion described by Borda, another geometry can depict even better the configuration of our device by considering the transition from a smaller flow passage to a larger one as gradual. This can be possible by the use of a diffuser (figure 3.12), whose primary purpose is to recover fluid static pressure with minimal loss of total pressure while reducing the flow velocity.

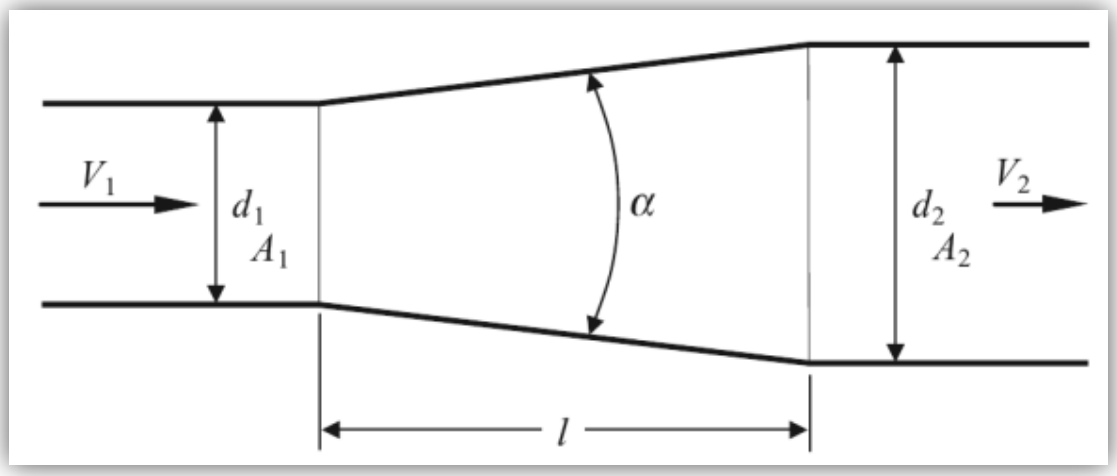

Figure 3.12: Example of a diffuser

The increase in the cross-sectional area of the diffuser causes a drop in the average flow velocity, and a portion of the kinetic energy of the flow is converted into the potential energy of pressure. An efficient diffuser is one that converts the highest possible percentage of kinetic energy into pressure energy within a given limitation on diffuser length or divergence angle α. (2)
The coefficient of dissipation of a diffuser depends, in addition to the opening angle α, even on the ratio of the enlargement $\frac{A_2}{A_1}$, on the shape of the profile, on the distribution of the velocities, and on the Reynolds' number of the current.
The loss of energy in the diffuser can theoretically be assessed as the sum of two contributes: one due to the tangential friction, ΔE_a and the other due to the separation of the current, ΔE_s, that is:

$$\Delta E_t = \Delta E_a + \Delta E_s = (\zeta_a + \zeta_s) \cdot \frac{v_1^2}{2g} = \zeta \cdot \frac{v_1^2}{2g} \qquad (3.8)$$

The first coefficient can be calculated by the formula:

$$\zeta_a = \frac{f}{8sin\alpha}\left[1 - \left(\frac{d_1}{d_2}\right)^4\right] \qquad (3.9)$$

where f is the number of resistance which, for a smooth tube and a number of Reynolds $\mathbb{R}e \leq 10^5$, it can be calculated by the formula of H. Blasius:

$$f = \frac{0.3164}{\mathbb{R}e^{0.25}} \qquad (3.10)$$

Going back to the equation (3.8), the second coefficient, ζ_s, can be evaluated by the experimental data of A. Gibson integrated by I.E. Idel'cik through the following diagram:

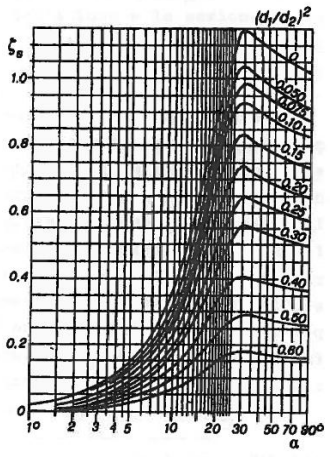

Figure 3.13: Diagram for the calculation of ζ_s, given α and $(d_1/d_2)^2$

Now we have all the information that we need to calculate the influence of the geometry of our device on the flow of pressures; in the next paragraph I am going to apply the theory to the reality of our experiment.

3.4 Experimental Analysis

Finally in this paragraph I present the heart of the experiment, which consists in measuring the pressures at different distances in order to verify what is the effect of the diffuser; in particularly we want to study their behavior to check if, even with the energy dissipation given by the geometry, the veins reattach. This happens if the pressure trend shows us that in the final part the pressures keep a constant value. The test will be repeated for different ranges of flow rate, in particular for 25, 35 and 50 liters per minute;

As regards the points chosen to install the sensors, we called:

- pressure 8 (corresponding to the sensor number 8), the one measured in a point of the pipe immediately outside of the flowmeter, characterized by a diameter of 19 mm. For us it will be the first point, that we set at distance 0;
- pressure 7, the first sensor located in the point of the device where the geometry changes increasing the diameter to 30 mm; it is situated at a distance of 45 m from the first;
- pressure 3, at a distance of 115 mm;
- pressure2, at a distance of 145 mm;
- pressure 1, at a distance of 175 mm;

In the next pages I will report the results.

❖ TEST 1, Q = 25 l/min

Test with Q = 25 l/min		
Position	Distance [mm]	Pressure [mmHg]
1	175	19.48740386
2	145	19.08177307
3	115	19.09361535
7	45	16.39095274
8	0	13.39416061

Table 3.2: Results of test 1

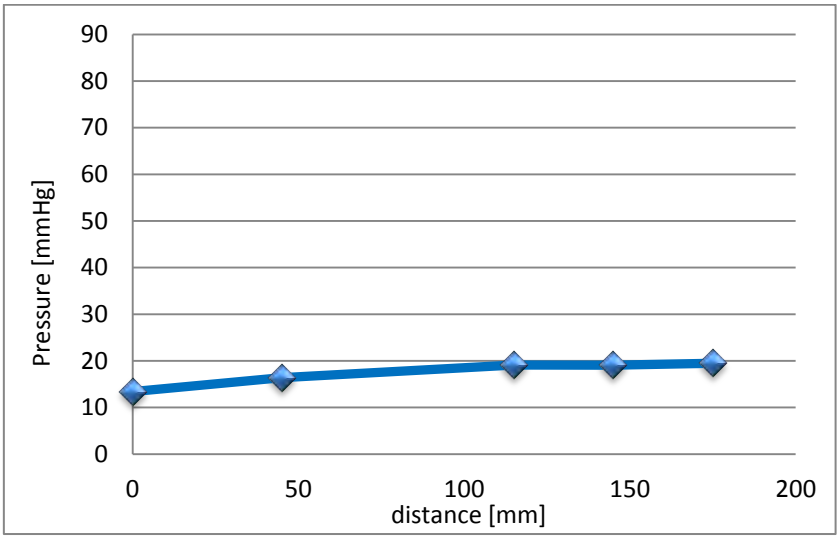

Figure 3.14: Pressures versus distance, Q=25 l/min

❖ TEST 2, Q = 35 l/min

Test with Q = 35 l/min		
Position	Distance [mm]	Pressure [mmHg]
1	175	43.93911969
2	145	43.63812982
3	115	43.91934536
7	45	38.46009929
8	0	32.1946911

Table 3.3: Results of test 2

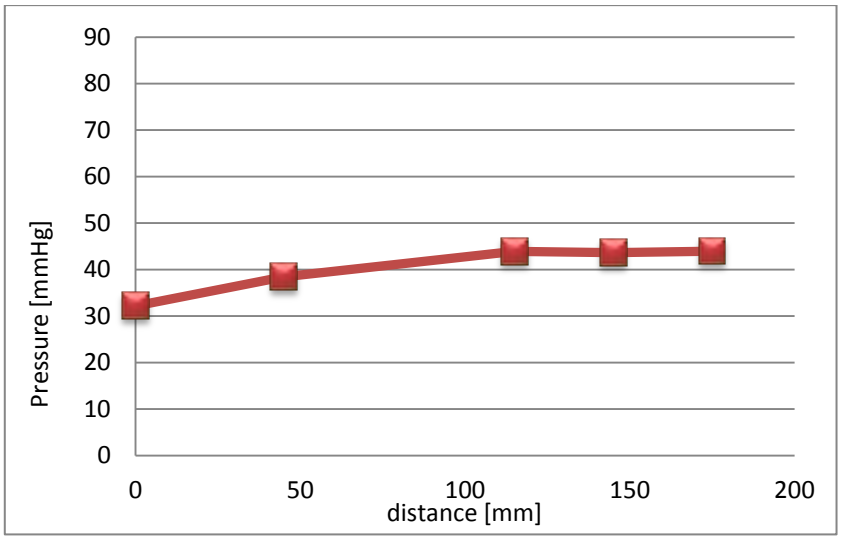

Figure 3.15: Pressures versus distance, Q=35 l/min

- TEST 3, Q = 50 l/min

Test with Q = 50 l/min		
Position	Distance [mm]	Pressure [mmHg]
1	175	88.17877321
2	145	88.27641783
3	115	87.96787642
7	45	80.28428873
8	0	66.92349874

Table 3.4: Results of test 3

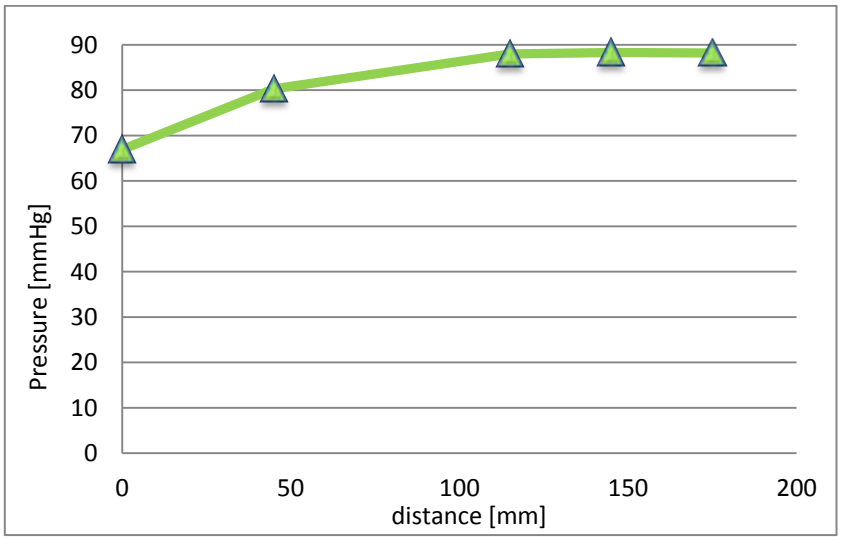

Figure 3.16: Pressures versus distance, Q=50 l/min

To sum up, I report the results in the same diagram, in order to compare the values:

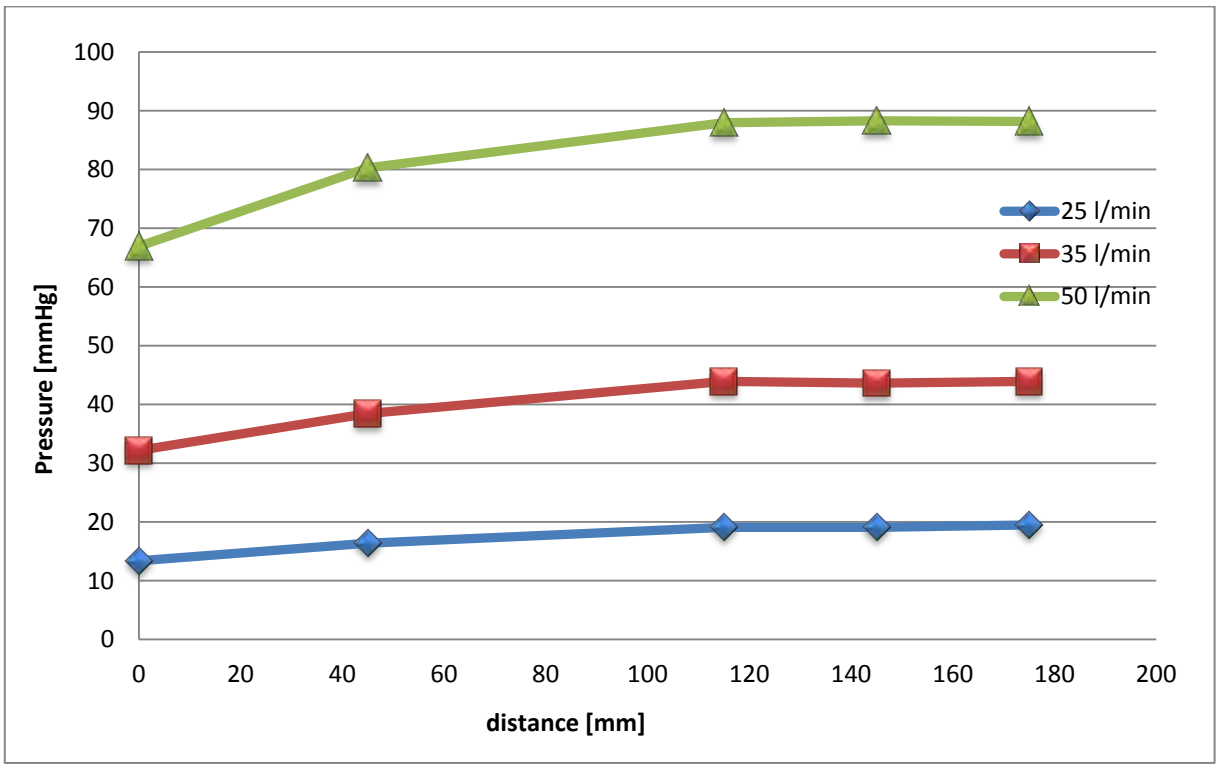

Figure 3.17: Pressures versus distances, at different flow rates

Taking everything into account, we verified that effectively the veins reattach, in particular it happens from the third position.

3.5 Theoretical Experimental Analysis

Taking everything into account we are finally ready to apply the theoretical knowledge to our case study in order to see if the results that we find out from our test agree with what we were expected studying the theoretical solution. In particular we will start from the geometrical data of our device to be able to calculate all the coefficients we need and find out the results in terms of energy and pressure. I will repeat this study for all the three flow rates that we took as exemplifying flow conditions, which are approximately 25, 35, and 50 liters per minute. I say 'approximately' because these are the values we started with, but in order to use the quite exact value we extract the data from the flow meter and we took the average value;

For each flow rate all the calculations are summarized in a table followed by the diagrams showing the results:

- **Flow rate = 24.7 liters per minute**

GEOMETRY OF THE SECTIONS 1 and 2		
Diameter	$d_1[m]$	0.01900
	$d_2[m]$	0.03000
Radius	$r_1[m]$	0.00950
	$r_2[m]$	0.01500
Area	$A_1[m^2] = \pi \cdot r_1^2$	0.00028
	$A_2[m^2] = \pi \cdot r_2^2$	0.00071
Flow rate	$Q[m^3/s]$	
Velocity	$v_1[m/s] = \frac{A_1}{Q}$	1.45185
	$v_2[m/s] = \frac{A_2}{Q}$	0.58235

Table 3.5: Geometry of the sections 1 and 2

SPECIFIC ENERGY and PRESSURE, section 1						
Acceleration of gravity	g [m/s²]	9.806				
Kinetic energy	$\frac{v_1^2}{2g}[m]$	0.1075	$\frac{v_1^2}{2g}[mmH_2O]$	107.479	$\frac{v_1^2}{2g}[mmHg]$	7.906
	$\frac{v_2^2}{2g}[m]$	0.0173	$\frac{v_2^2}{2g}[mmH_2O]$	17.292	$\frac{v_2^2}{2g}[mmHg]$	1.272
Density	$\rho(H_2O)\ [Kg/m^3]$	1052				
Specific weight	$\gamma(H_2O)\ [N/m^3]$	10315.9				
Measured Pressure	$P_1[N/m^2]$	1784.528	$P_1[mmH_2O]$	182.095	$P_1[mmHg]$	13.394
Piezometric Height	$\frac{P_1}{\gamma}[m]$	0.173	$\frac{P_1}{\gamma}[mmH_2O]$	172.988	$\frac{P_1}{\gamma}[mmHg]$	12.724
Specific Energy $E_1 = h + \frac{p}{\gamma} + \frac{v_1^2}{2g}$ $(h = const = 0)$	$E_1[m]$	0.2805	$E_1[mmH_2O]$	280.467	$E_1[mmHg]$	20.630

Table 3.6: Calculations in terms of energy and pressure for the section 1

THEORY OF BORDA						
THEORETICAL PRESSURE in section 2						
Theoretical pressure	$P_2[N/m^2]$	2317.216	$P_2[mmH_2O]$	236.290	$P_2[mmHg]$	17.381
Theoretical piezometric pressure	$\frac{P_2}{\gamma}[m]$	0.225	$\frac{P_2}{\gamma}[mmH_2O]$	224.625	$\frac{P_2}{\gamma}[mmHg]$	16.523
THEORETICAL ENERGY in section 2						
Energy Loss $\Delta E = \frac{v_1^2}{2g} \cdot \left[\left(\frac{A_1}{A_2} - 1\right)\right]^2$	$\Delta E[m]$	0.039	$\Delta E[mmH_2O]$	38.549	$\Delta E[mmHg]$	2.836
Specific Energy $E_2 = E_1 - \Delta E$	$E_2[m]$	0.242	$E_2[mmH_2O]$	241.918	$E_2[mmHg]$	17.795

Table 3.7: Calculation of the theoretical values of energy and pressure in section 2, according to the theory of Borda

THE THEORY OF THE DIFFUSER						
THEORETICAL PRESSURE in section 2						
Theoretical pressure	$P_2[N/m^2]$	2533.575	$P_2[mmH_2O]$	258.353	$P_2[mmHg]$	19.004
Theoretical Piezometric Height	$\frac{P_2}{\gamma}[m]$	0.246	$\frac{P_2}{\gamma}[mmH_2O]$	245.599	$\frac{P_2}{\gamma}[mmHg]$	18.065
THEORETICAL ENERGY in section 2						
Divergence angle	α [°C]	11	α [rad]	0.192		
Diameters Ratio	$\left(\frac{d_1}{d_2}\right)^2[m]$	0.401				
Coefficient of separation	ζs (from figure)	0.150				
Friction coefficient (H. Blasius)	$\zeta_a = \frac{f}{8sin\alpha}\left[1 - \left(\frac{d_1}{d_2}\right)^4\right]$	0.014				
Number of Resistance	$f = \frac{0.3164}{\mathbb{R}e^{0.25}}$	0.025				
Number of Reynolds	$\mathbb{R}e = \frac{\rho v d}{\mu} = \frac{v d}{\nu}$	27312.111				
Kinematic viscosity	$\nu[m^2/s]$	10^{-6}				
Energy Loss $\Delta E_t = \Delta E_a + \Delta E_s = (\zeta_a + \zeta_a) \cdot \frac{v_1^2}{2g}$	$\Delta E_t[m]$	0.018	$\Delta E_t[mmH_2O]$	17.576	$\Delta E_t[mmHg]$	1.293
Specific Energy $E_2 = E_1 - \Delta E$	$E_2[m]$	0.263	$E_2[mmH_2O]$	262.891	$E_2[mmHg]$	19.337

Table 3.8: Calculation of the theoretical values of energy and pressure in section 2, according to the theory of the diffuser

So, starting from the initial value of Pressure P_1 measured in section 1 (in the previous paragraph we called it pressure 8), and from the calculations inherent the geometry of the pipe, we could obtain the results attended in terms of Pressure and Energy both considering to use the equations of Borda (fig. 3.18), and the one characterizing a diffuser (fig. 3.19).

You can see them in the following graphs:

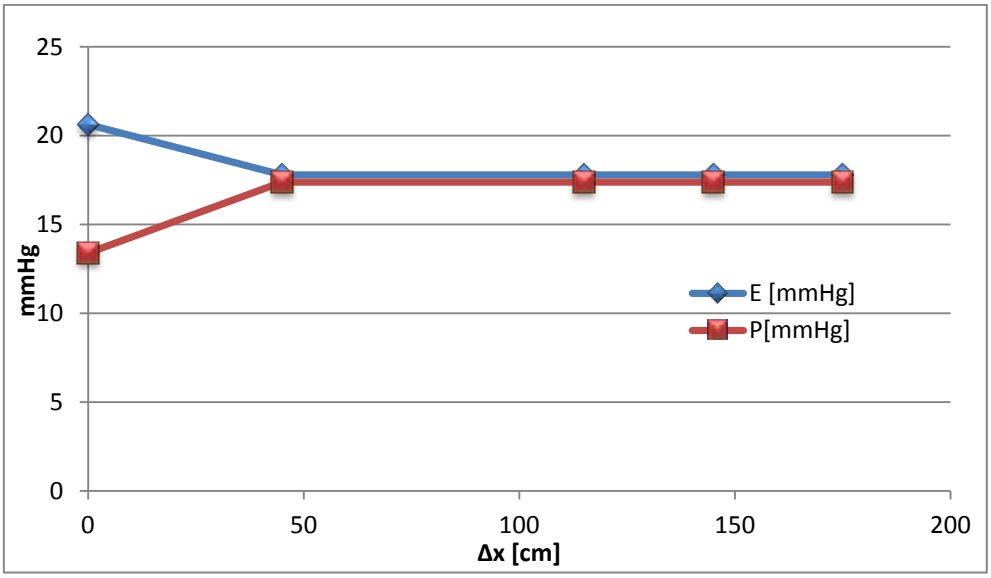

Figure 3.18: Variation of Energy and Pressure from section 1 to section 2, considering Borda;

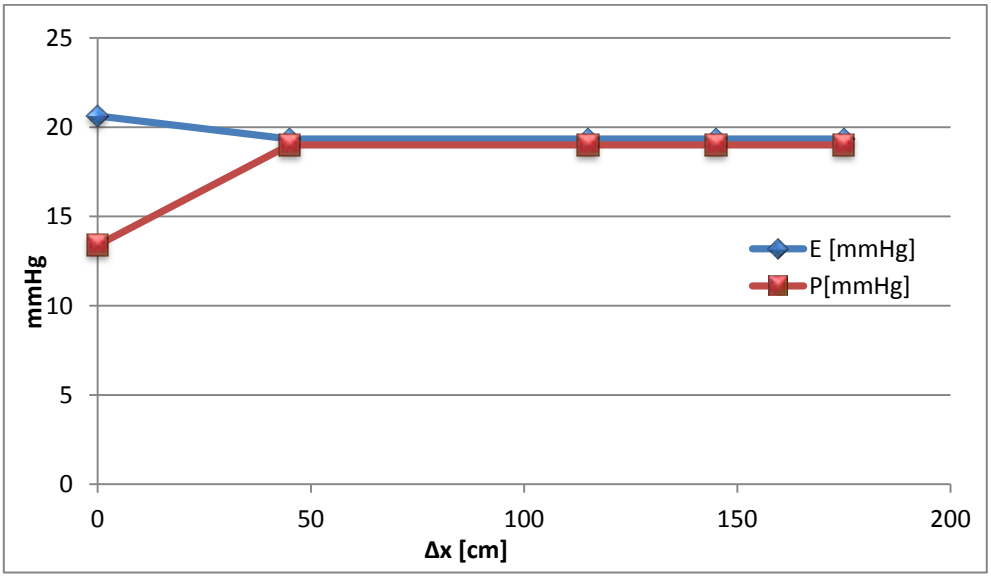

Figure 3.19: Variation of Energy and Pressure from section 1 to section 2, considering the diffuser;

Of course we must underline that the values calculated by the equations represent what, from a theoretical point of view, it would happen passing from the section 1 (of 19 mm) to the section 2 (of 30 mm). I considered this situation as coinciding with the first sensor situated at the beginning of the 30 mm diameter, but I am not sure about it, that's why I am going to compare these theoretical results with the real one.

Therefore in order to verify if the real pressure trend measured in my experiment is coherent with the result obtained from the theoretical analysis, I compare both the solutions summarizing the resulting values (table 3.9) which are then reported in the graph (figure 3.20).

Position	Distance [mm]	Pressure Test [mmHg]	Theoretical Pressure Borda [mmHg]	Theoretical Pressure Diffuser [mmHg]
8	0	13.39416061	13.39416061	13.39416061
7	45	16.39095274	17.38130666	19.00420257
3	115	19.09361535	17.38130666	19.00420257
2	145	19.08177307	17.38130666	19.00420257
1	175	19.48740386	17.38130666	19.00420257

Table 3.9: Comparison between the real and theoretical pressures

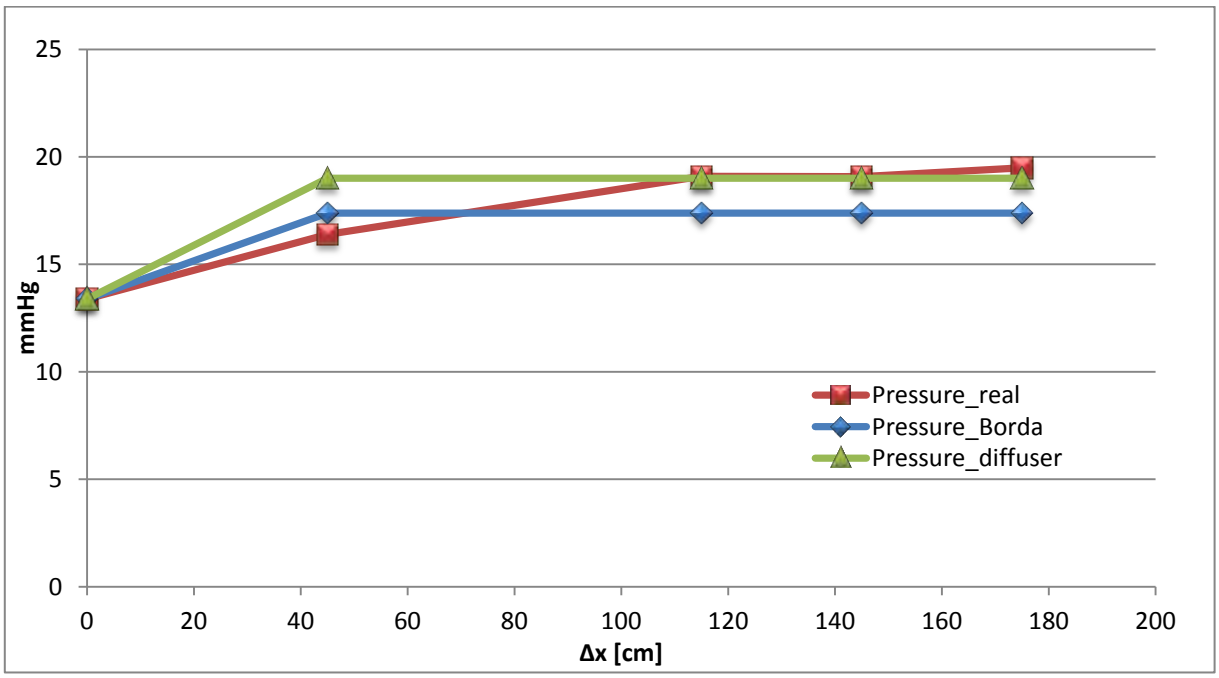

Figure 3.20: Pressures trend from section 1 to section 2, comparison between the theoretical and real values

- **Flow rate = 35.7 liters per minute**

GEOMETRY OF THE SECTIONS 1 and 2		
Diameter	$d_1[m]$	0.019
	$d_2[m]$	0.03
Radius	$r_1[m]$	0.0095
	$r_2[m]$	0.015
Area	$A_1[m^2] = \pi \cdot r_1^2$	0.00028
	$A_2[m^2] = \pi \cdot r_2^2$	0.00071
Flow rate	$Q[m^3/s]$	0.00059512
Velocity	$v_1[m/s] = \frac{A_1}{Q}$	2.099
	$v_2[m/s] = \frac{A_2}{Q}$	0.842

Table 3.10: Geometry of the sections 1 and 2

SPECIFIC ENERGY and PRESSURE, section 1						
Acceleration of gravity	g [m/s²]	9.806				
Kinetic energy	$\frac{v_1^2}{2g}[m]$	0.225	$\frac{v_1^2}{2g}[mmH_2O]$	224.643	$\frac{v_1^2}{2g}[mmHg]$	16.524
	$\frac{v_2^2}{2g}[m]$	0.036	$\frac{v_2^2}{2g}[mmH_2O]$	36.143	$\frac{v_2^2}{2g}[mmHg]$	2.659
Density	$\rho(H_2O)\ [Kg/m^3]$	1052				
Specific weight	$\gamma(H_2O)\ [N/m^3]$	10315.9				
Measured Pressure	$P_1[N/m^2]$	4289.357	$P_1[mmH_2O]$	437.690	$P_1[mmHg]$	32.195
Piezometric Height	$\frac{P_1}{\gamma}[m]$	0.416	$\frac{P_1}{\gamma}[mmH_2O]$	415.800	$\frac{P_1}{\gamma}[mmHg]$	30.585
Specific Energy $E_1 = h + \frac{p}{\gamma} + \frac{v_1^2}{2g}$ $(h = const = 0)$	$E_1[m]$	0.640	$E_1[mmH_2O]$	640.443	$E_1[mmHg]$	47.108

Table 3.11: Calculations in terms of energy and pressure for the section 1

THEORY OF BORDA						
THEORETICAL PRESSURE in section 2						
Theoretical pressure	$P_2[N/m^2]$	5402.731	$P_2[mmH_2O]$	550.925	$P_2[mmHg]$	40.526
Theoretical piezometric pressure	$\frac{P_2}{\gamma}[m]$	0.524	$\frac{P_2}{\gamma}[mmH_2O]$	523.728	$\frac{P_2}{\gamma}[mmHg]$	38.523
THEORETICAL ENERGY in section 2						
Energy Loss $\Delta E = \frac{v_1^2}{2g} \cdot \left[\left(\frac{A_1}{A_2} - 1\right)\right]^2$	$\Delta E[m]$	0.081	$\Delta E[mmH_2O]$	80.572	$\Delta E[mmHg]$	5.927
Specific Energy $E_2 = E_1 - \Delta E$	$E_2[m]$	0.560	$E_2[mmH_2O]$	559.871	$E_2[mmHg]$	41.182

Table 3.12: Calculation of the theoretical values of energy and pressure in section 2, according to the theory of Borda

THE THEORY OF THE DIFFUSER						
THEORETICAL PRESSURE in section 2						
Theoretical pressure	$P_2[N/m^2]$	5857.704	$P_2[mmH_2O]$	597.320	$P_2[mmHg]$	43.938
Theoretical Piezometric Height	$\frac{P_2}{\gamma}[m]$	0.568	$\frac{P_2}{\gamma}[mmH_2O]$	567.832	$\frac{P_2}{\gamma}[mmHg]$	41.767
THEORETICAL ENERGY in section 2						
Divergence angle	α [°C]	11	α [rad]	0.192		
Diameters Ratio	$\left(\frac{d_1}{d_2}\right)^2[m]$	0.401				
Coefficient of separation	ζs (from figure)	0.15				
Friction coefficient (H. Blasius)	$\zeta_a = \frac{f}{8sin\alpha}\left[1 - \left(\frac{d_1}{d_2}\right)^4\right]$	0.012				
Number of Resistance	$f = \frac{0.3164}{\mathbb{R}e^{0.25}}$	0.022				
Number of Reynolds	$\mathbb{R}e = \frac{\rho v d}{\mu} = \frac{v d}{\nu}$	39485.659				
Kinematic viscosity	$\nu[m^2/s]$	10^{-6}				
Energy Loss $\Delta E_t = \Delta E_a + \Delta E_s = (\zeta_a + \zeta_a) \cdot \frac{v_1^2}{2g}$	$\Delta E_t[m]$	0.036	$\Delta E_t[mmH_2O]$	36.468	$\Delta E_t[mmHg]$	2.682
Specific Energy $E_2 = E_1 - \Delta E$	$E_2[m]$	0.604	$E_2[mmH_2O]$	603.975	$E_2[mmHg]$	44.426

Table 3.13: Calculation of the theoretical values of energy and pressure in section 2, according to the theory of the diffuser

As before, starting from the initial value of Pressure P_1 measured in section 1 (pressure 8), and from the calculations inherent the geometry of the pipe, we could obtain the results attended in terms of Pressure and Energy both considering to use the equations of Borda (fig. 3.21), and the one characterizing a diffuser (fig. 3.22).

You can see them in the following graphs:

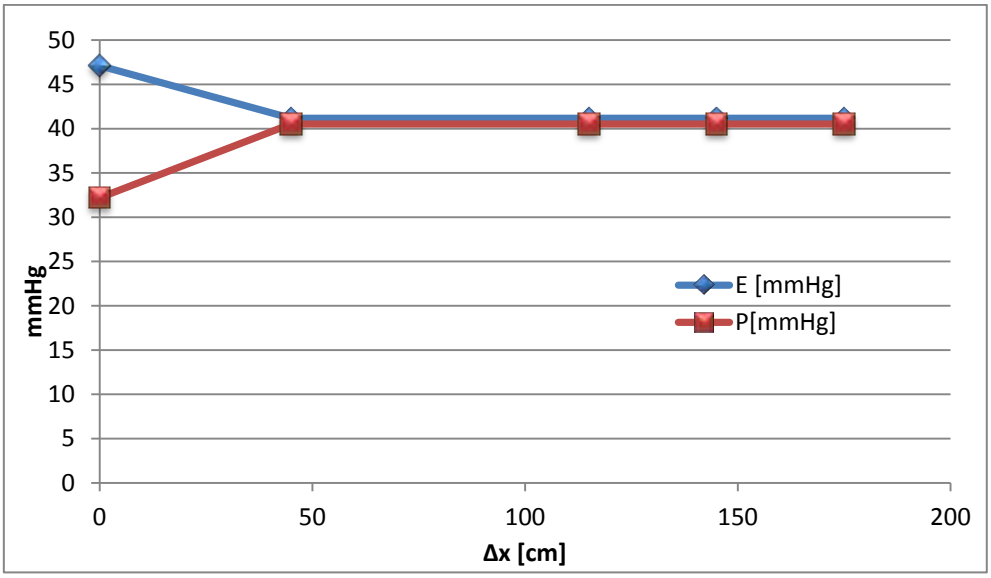

Figure 3.21: Variation of Energy and Pressure from section 1 to section 2, considering Borda;

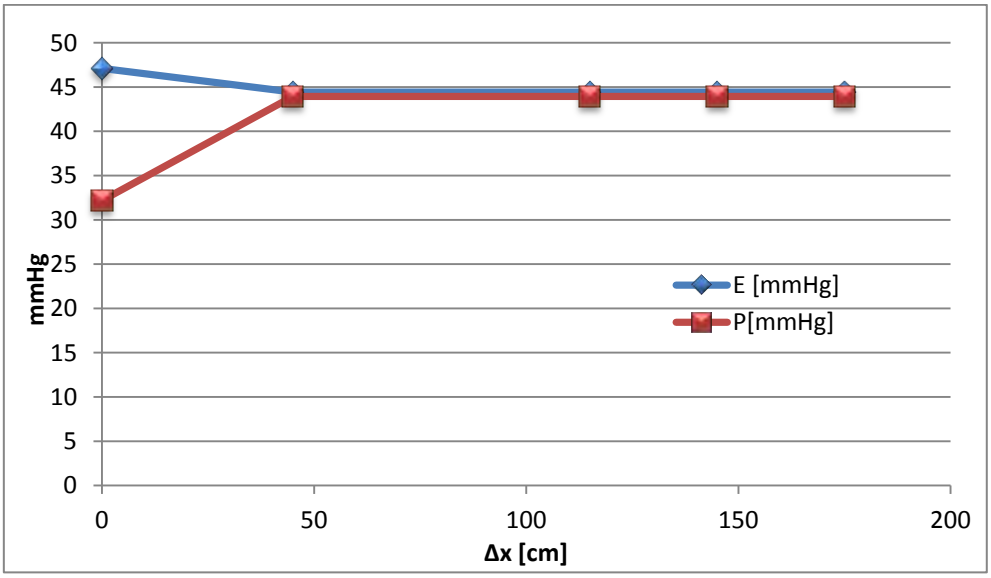

Figure 3.22: Variation of Energy and Pressure from section 1 to section 2, considering the diffuser;

Keeping as valid the consideration that I did in the previous case, again I compare the real pressure trend with the result obtained from the theoretical analysis to verify if they are still congruent. Have a look at the next table followed by the graph (figure 3.23).

Position	Distance [mm]	Pressure Test [mmHg]	Theoretical Pressure Borda [mmHg]	Theoretical Pressure diffuser [mmHg]
8	0	32.1946911	32.1946911	32.1946911
7	45	38.46009929	40.52557811	43.93830548
3	115	43.91934536	40.52557811	43.93830548
2	145	43.63812982	40.52557811	43.93830548
1	175	43.93911968	40.52557811	43.93830548

Table 3.14: Comparison between real and theoretical pressures

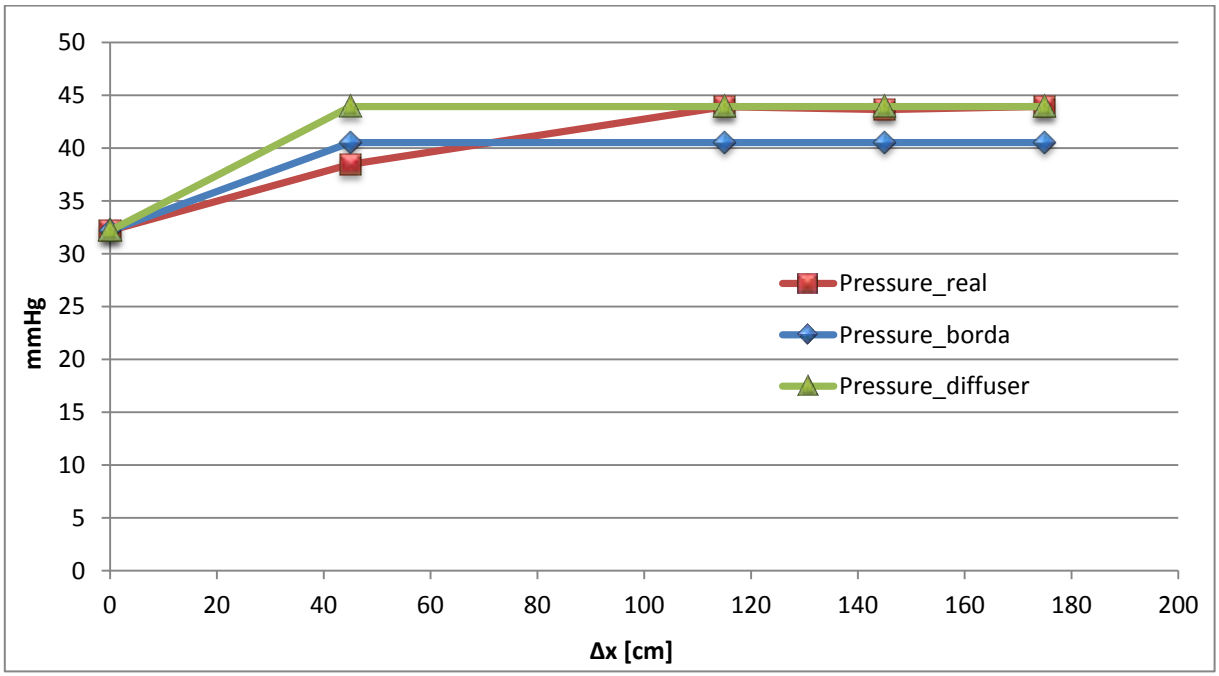

Figure 3.23: Pressures trend from section 1 to section 2, comparison between the theoretical and real values

- **Flow rate = 49.5 liters per minute**

GEOMETRY OF THE SECTIONS 1 and 2		
Diameter	$d_1[m]$ $d_2[m]$	0.019 0.03
Radius	$r_1[m]$ $r_2[m]$	0.00950 0.01500
Area	$A_1[m^2] = \pi \cdot r_1^2$ $A_2[m^2] = \pi \cdot r_2^2$	0.00028 0.00071
Flow rate	$Q[m^3/s]$	0.00083
Velocity	$v_1[m/s] = \frac{A_1}{Q}$ $v_2[m/s] = \frac{A_2}{Q}$	2.91051 1.16744

Table 3.15: Geometry of the sections 1 and 2

SPECIFIC ENERGY and PRESSURE, section 1						
Acceleration of gravity	g [m/s²]	9.806				
Kinetic energy	$\frac{v_1^2}{2g}[m]$	0.432	$\frac{v_1^2}{2g}[mmH_2O]$	431.933	$\frac{v_1^2}{2g}[mmHg]$	31.771
	$\frac{v_2^2}{2g}[m]$	0.069	$\frac{v_2^2}{2g}[mmH_2O]$	69.494	$\frac{v_2^2}{2g}[mmHg]$	5.112
Density	$\rho(H_2O)\ [Kg/m^3]$	1052				
Specific weight	$\gamma(H_2O)\ [N/m^3]$	10315.9				
Measured Pressure	$P_1[N/m^2]$	8916.340	$P_1[mmH_2O]$	909.831	$P_1[mmHg]$	66.923
Piezometric Height	$\frac{P_1}{\gamma}[m]$	0.864	$\frac{P_1}{\gamma}[mmH_2O]$	864.329	$\frac{P_1}{\gamma}[mmHg]$	63.577
Specific Energy $E_1 = h + \frac{p}{\gamma} + \frac{v_1^2}{2g}$ $(h = const = 0)$	$E_1[m]$	1.296	$E_1[mmH_2O]$	1296.262	$E_1[mmHg]$	95.348

Table 3.16: Calculations in terms of energy and pressure for the section 1

THEORY OF BORDA						
THEORETICAL PRESSURE in section 2						
Theoretical pressure	$P_2[N/m^2]$	11057.085	$P_2[mmH_2O]$	1127.509	$P_2[mmHg]$	82.939
Theoretical piezometric pressure	$\frac{P_2}{\gamma}[m]$	1.072	$\frac{P_2}{\gamma}[mmH_2O]$	1071.848	$\frac{P_2}{\gamma}[mmHg]$	78.841
THEORETICAL ENERGY in section 2						
Energy Loss $\Delta E = \frac{v_1^2}{2g} \cdot \left[\left(\frac{A_1}{A_2} - 1\right)\right]^2$	$\Delta E[m]$	0.155	$\Delta E[mmH_2O]$	154.920	$\Delta E[mmHg]$	11.395
Specific Energy $E_2 = E_1 - \Delta E$	$E_2[m]$	1.141	$E_2[mmH_2O]$	1141.341	$E_2[mmHg]$	83.952

Table 3.17: Calculation of the theoretical values of energy and pressure in section 2, according to the theory of Borda

THE THEORY OF THE DIFFUSER						
THEORETICAL PRESSURE in section 2						
Theoretical pressure	$P_2[N/m^2]$	11936.201	$P_2[mmH_2O]$	1217.154	$P_2[mmHg]$	89.533
Theoretical Piezometric Height	$\frac{P_2}{\gamma}[m]$	1.157	$\frac{P_2}{\gamma}[mmH_2O]$	1157.067	$\frac{P_2}{\gamma}[mmHg]$	85.109
THEORETICAL ENERGY in section 2						
Divergence angle	α [°C]	11	α [rad]	0.192		
Diameters Ratio	$\left(\frac{d_1}{d_2}\right)^2[m]$	0.401				
Coefficient of separation	ζs (from figure)	0.15				
Friction coefficient (H. Blasius)	$\zeta_a = \frac{f}{8sin\alpha}\left[1 - \left(\frac{d_1}{d_2}\right)^4\right]$	0.011				
Number of Resistance	$f = \frac{0.3164}{\mathbb{R}e^{0.25}}$	0.021				
Number of Reynolds	$\mathbb{R}e = \frac{\rho v d}{\mu} = \frac{v d}{\nu}$	54752.171				
Kinematic viscosity	$\nu[m^2/s]$	10^{-6}				
Energy Loss $\Delta E_t = \Delta E_a + \Delta E_s = (\zeta_a + \zeta_a) \cdot \frac{v_1^2}{2g}$	$\Delta E_t[m]$	0.070	$\Delta E_t[mmH_2O]$	69.701	$\Delta E_t[mmHg]$	5.127
Specific Energy $E_2 = E_1 - \Delta E$	$E_2[m]$	1.227	$E_2[mmH_2O]$	1226.561	$E_2[mmHg]$	90.221

Table 3.18: Calculation of the theoretical values of energy and pressure in section 2, according to the theory of the diffuser

Again, starting from the initial value of Pressure P_1 measured in section 1 (pLV), and from the calculations inherent the geometry of the pipe, we could obtain the results attended in terms of Pressure and Energy both considering to use the equations of Borda (fig. 3.22), and the one characterizing a diffuser (fig. 3.23).

You can see them in the following graphs:

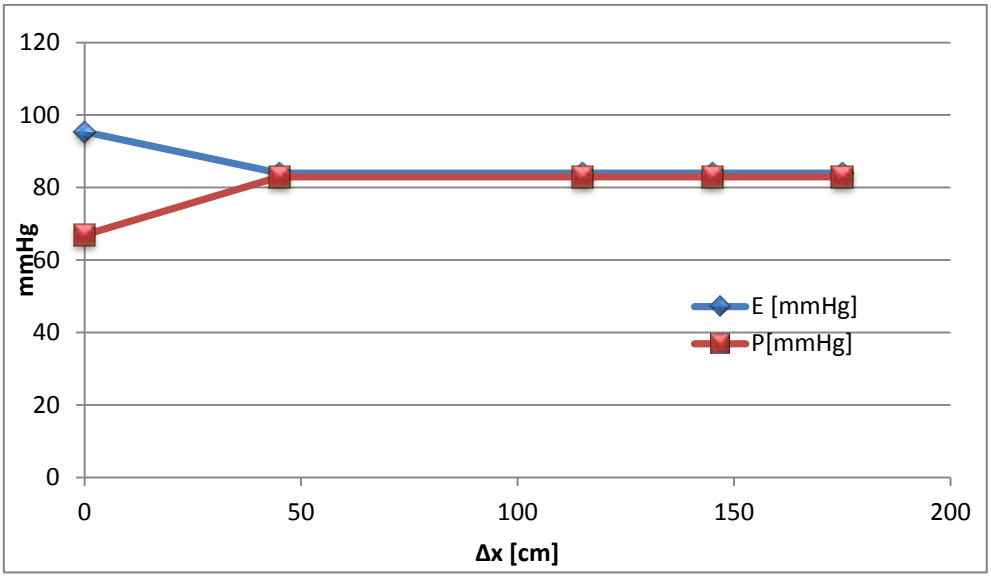

Figure 3.24: Variation of Energy and Pressure from section 1 to section 2, considering Borda;

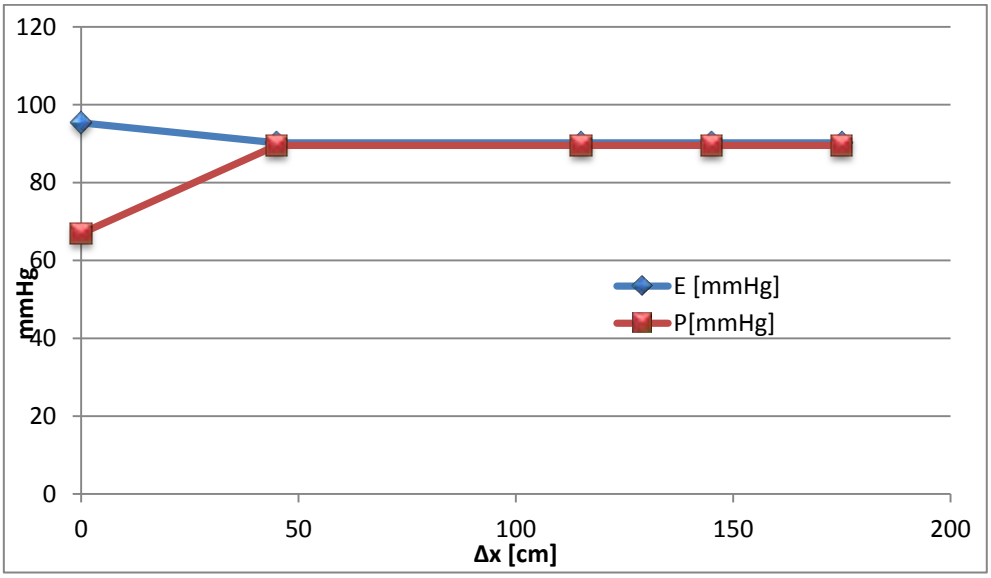

Figure 3.25: Variation of Energy and Pressure from section 1 to section 2, considering the diffuser;

Once again I compare the real pressure trend with the result obtained from the theoretical analysis to verify if they are still congruent. The results are reported in next table followed by the graph (figure 3.26).

Position	Distance [mm]	Pressure Test [mmHg]	Theoretical Pressure - Borda [mmHg]	Theoretical Pressure - diffuser [mmHg]
8	0	66.9235	66.92349874	66.92349874
7	45	80.28429	82.93856016	89.5327576
3	115	87.96788	82.93856016	89.5327576
2	145	88.27642	82.93856016	89.5327576
1	175	88.17877	82.93856016	89.5327576

Table 3.19: Comparison between real and theoretical pressures

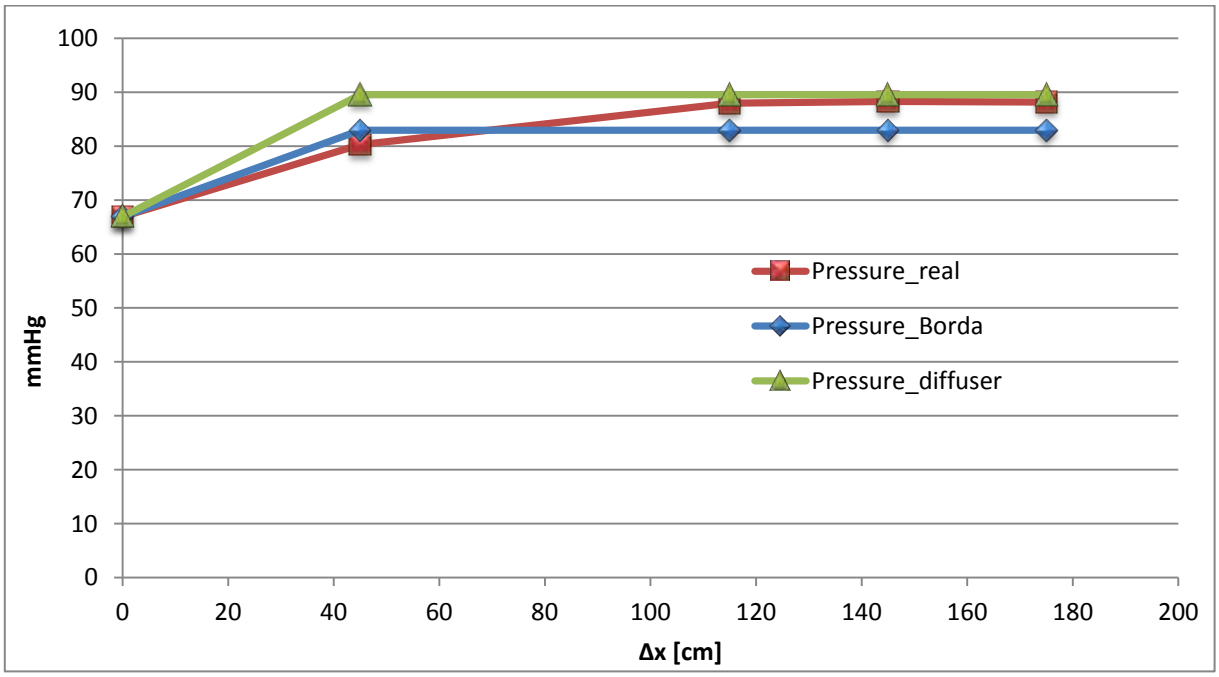

Figure 3.26: Pressures trend from section 1 to section 2, comparison between the theoretical and real values

Comparing for all the flow rates the pressure trend of the real values with that of the theoretical computation, I can assert that I effectively verify the assumption of considering the

theory of the diffuser as correct for my device. The data correspond to the fast exact behaviour I was attended for the pressures in the section 2, after the expansion of the pipe. The only difference is that in the reality the vein takes a little longer distance to reattach. I detect the reattachment of the vein in the position 3, situated at a distance of 115 mm from the first pressure sensor. I can suppose that maybe this phenomenon could be fulfilled even at a shorter distance, in a region between the position 7 and 3, but I cannot know it because it was not possible to take farther measurement in that area.

CHAPTER 4
PRESSURES – PULSATILE FLOW

As I already said, the pulse duplicator is designed to assess heart valve prosthesis performance under simulated cardiac conditions. The system replicates the function of the heart's ventricle which generates pulsatile flow through a heart valve in the model left Heart. The purpose of the device is thus to simulate the mechanical and hemodynamic functions of the left ventricle of the human heart to investigate the flow regimes through and around artificial heart valves. In this chapter I will analyze the behavior of pressures in this area, upstream and downstream of the aortic valve.

4.1 Introduction to the physiological system

In order to understand the importance of studying the trend of pressures around the aortic valve and to be able to compare the physiological reality with the functionality of the experimental model, I frame the human systemic circulation briefly.

The cardiovascular (or circulatory) system provides a transport mechanism for oxygen through the body as a fuel source for cellular respiration, and then the return transport of carbon dioxide, a by-product of cellular respiration, that the body expels as waste through breathing. It also provides for the transport of amino acids, nutrients, hormones, and the other components that make up blood. It is composed of the heart and blood vessels, including arteries, veins, and capillaries. Our bodies actually have two circulatory systems: the pulmonary circulation is a short loop from the heart to the lungs and back again, and the systemic circulation sends blood from the heart to all the other parts of our bodies and back again.

The heart is the key organ in the circulatory system. It provides the driving force as it acts as the hydraulic pump for the body constantly moving the blood in a continuous flow though the various

vessels. The heart has four chambers, each isolated by a set of four valves. In the upper hemisphere of the heart are the atria, and the lower hemisphere are the ventricles.

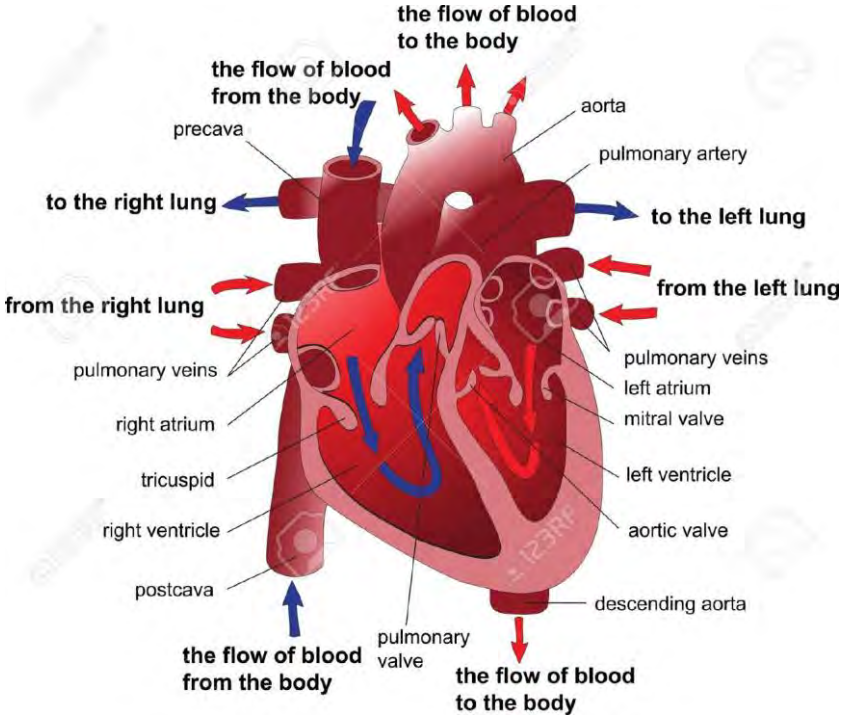

Figure 4.1: human heart and circulation

Oxygen-poor and carbon dioxide-rich blood flows into the right atrium from the body and is contained there momentarily until the opening of the tricuspid valve, which allows it to travel into the right ventricle (this process happens during diastole, one part of a complete cardiac cycle). During systole, the second part of the cardiac cycle, the heart muscles contract. The atrium contracts first, producing an additional blood flow from the right atrium to the right ventricle. Once the right ventricle fills completely the ventricle contracts allowing for a rush of blood up through the pulmonary valve and into the pulmonary artery where the blood will be transported to the lungs in order to allow the carbon dioxide to exit the blood and allow for an intake of oxygen. The structure of the heart with its valves allows for the heart to work while preventing backflow into the chambers due to low pressure drops when certain chambers are empty or filled. This process is repeated as oxygen rich blood returns to the left atrium from the lungs via the pulmonary veins. When the mitral valve opens, blood flows into the left ventricle. During the same

beat which previously allowed the right ventricle to contract (systole) the left ventricle contracts pushing the blood through the aortic valve and into the aorta. The aorta carries oxygen rich blood to the systemic circulation, which provides the entire body oxygen.

The heart usually beats from 60 to 100 times per minute, but can go much faster when necessary. For example when humans exercise the increase in the heart rate is a direct result of the cells needing oxygen at a faster rate and therefore the blood must deliver it at a higher flow rate through the body.

Blood pressure measured is recorded in millimeters (mm) of mercury (Hg). Average air pressure is 760 mm of Hg. Average blood pressure is 120 mmHg over 80 mmHg, with the first number representing systole, and the second measuring diastole. The numbers represent the relative pressure in the blood, which is above atmospheric pressure. This means that the actual pressure in the body is 760mm of Hg plus the systole or the diastole number.

Blood pressure is generated by the rhythmic pumping of the heart. Here, I focus on the action of the left side of the heart. Figure 4.2 shows the cardiac cycle. The length of time for the cardiac cycle is 0.8 seconds for a person with an average heartbeat of 72-74 beats per minutes. As blood flows into the heart from the lungs it enters the left atrium and is prevented from entering the left ventricle by the closed mitral valve. The mitral valve opens as the upper hemisphere of the heart contracts forcing the blood into the ventricle. Contraction of the muscle in the ventricle forces blood up through the aortic valve and into the aorta at high pressure. The pressure produces blood flow through the body. As the ventricle relaxes, the aortic valve closes, preventing backflow into the ventricle.

In the figure, the top picture follows the cardiac cycle starting in late diastole. The graph below the diagram emphasizes changes in pressure in different regions of the heart. The aortic pressure goes through a periodic increase and decrease in pressure, between diastole and systole, with its lowest (diastole) being about 40 mm of Hg less than the greatest (systole). Blood pressure measured by your doctor reflects the pressure changes in the aorta. (6)

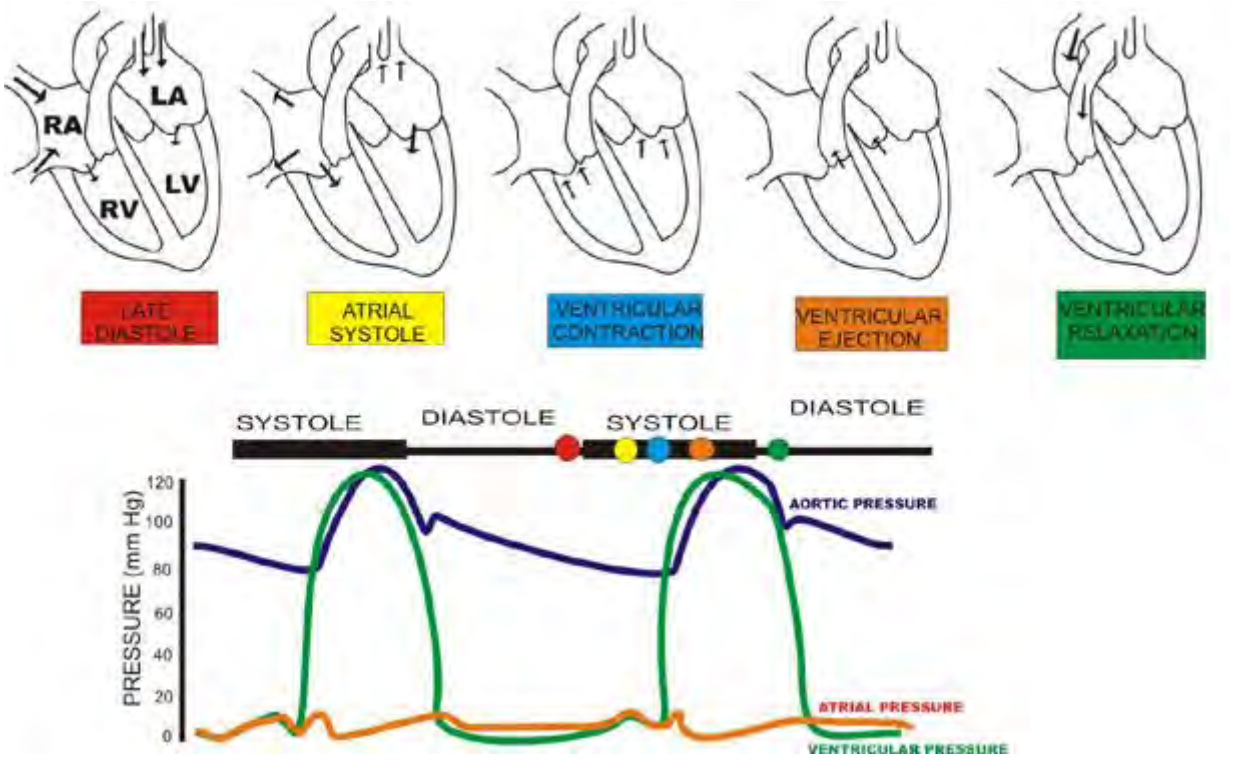

Figure 4.2: Cardiac circle

4.2 Analysis upstream of the aortic valve

In the following paragraphs we will analyse the pressures upstream of the valve; beyond this, I will focus on the effect of the ventricular pressures in some fundamental parameters for the verification of the hydrodynamics performance of the valves, referring directly to the guidelines given in the normative.

4.2.1 Experimental Analysis - Pressure Trend in physiological working conditions

In chapter 3 we investigated the behavior of the pressures at different distances from the aortic valve finding out that after the dissipation zone due to the geometry of the pipe, in the last three measurement points before the valve the flow resumes its layout occupying the whole area and showing a constant trend of pressures. That experiment was carried out at constant flow, while in

order to understand what does it happen in the reality around the aortic valve we need to reproduce the same conditions we find in the heart, that is operating with a pulsatile flow.
Thanks to the pulse duplicator we could thus measure the pressures at different distances before and immediately after the valve, evaluating the differences respect to the previous case.

I measure the pressures in three points, two upstream and one downstream of the aortic valve; first of all keeping the latter fixed, we analyze the pressures at 1 and 2 diameters before the valve. We choose these two points because, investigating the pressures trend in steady condition for the different flow rates, we verified that in that positions the vein reattached, that is, after the disturbances given by the geometry changing in diameter, the liquid section reoccupied the entire pipe diameter, as I can see in figures 3.11, 3.12, 3.13. Therefore we selected these points to test how the situation change having a pulsatile flow which represents the physiologic condition.

We decided to record the flow for different values in terms of peaks of flow rates corresponding to 20, 25, 30, and 35 liters per minute, each of them taken together with the respective pressures in the same three points at one and two diameters upstream (1D and 2D), and immediately downstream of the aortic valve. I reported all the results in the following graphs.

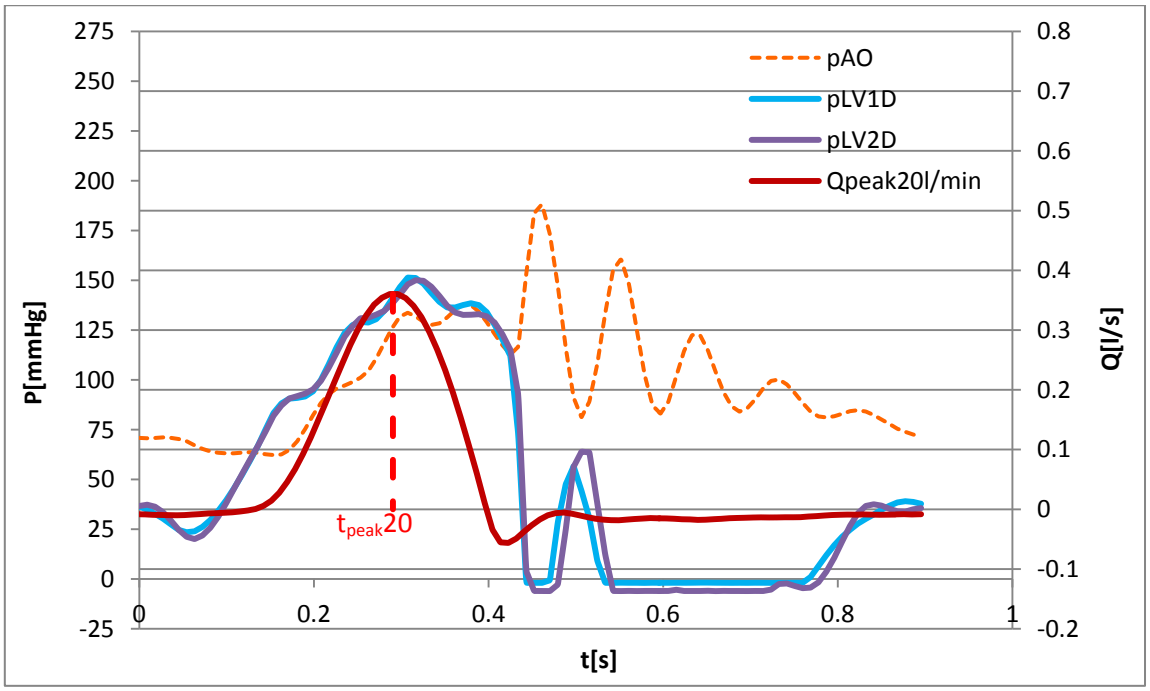

Figure 4.3: Flow of peak around 20 l/min, (0.33 l/s) with the pressures at 1D, 2D (pLV1D, pLV2D) upstream and the one downstream of the aortic valve (pAO)

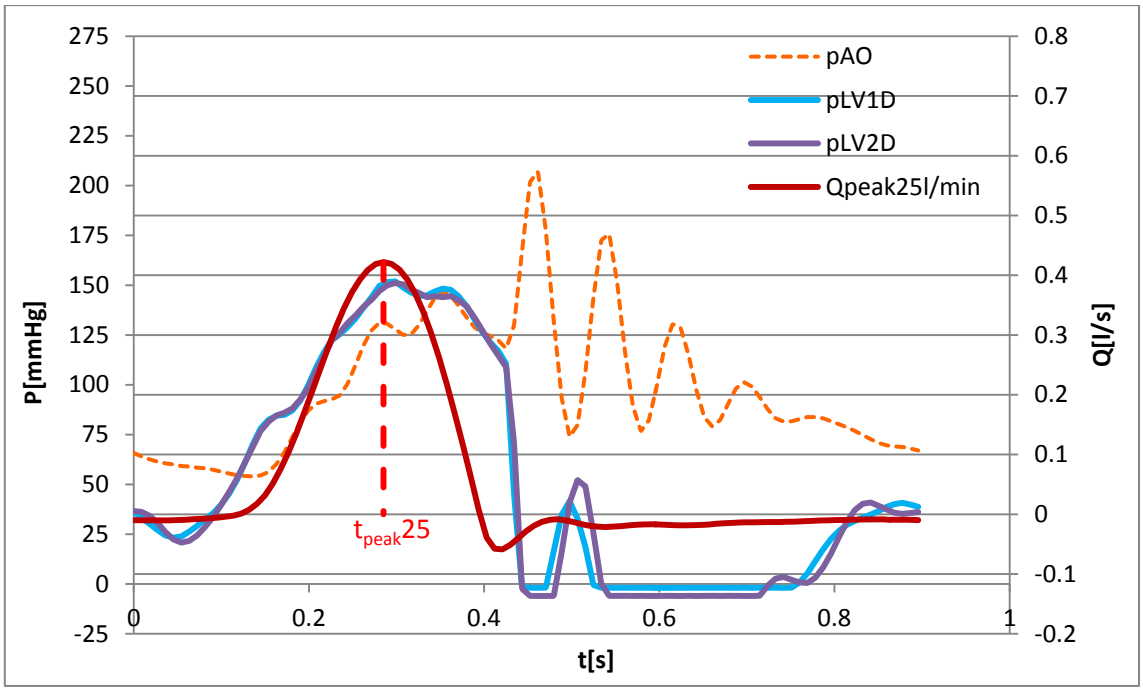

Figure 4.4: Flow of peak around 25 l/min, (0.41 l/s) with the pressures at 1D, 2D (pLV1D, pLV2D) upstream and the one downstream of the aortic valve (pAO)

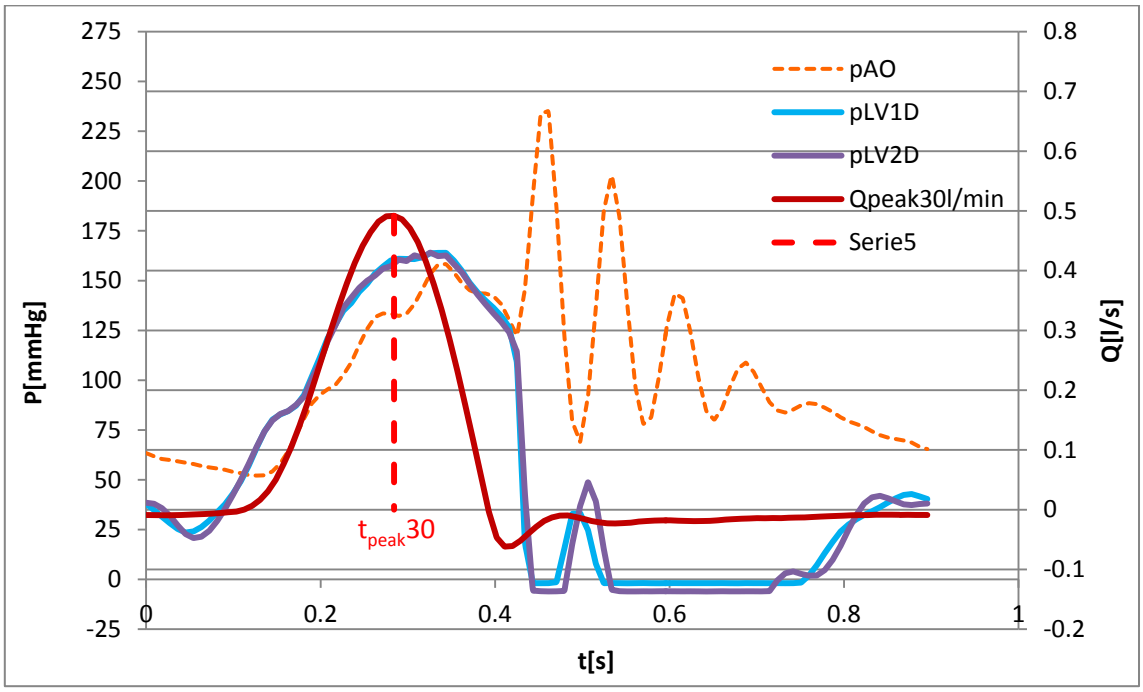

Figure 4.5: Flow of peak around 30 l/min, (0.5 l/s) with the pressures at 1D, 2D (pLV1D, pLV2D) upstream and the one downstream of the aortic valve (pAO)

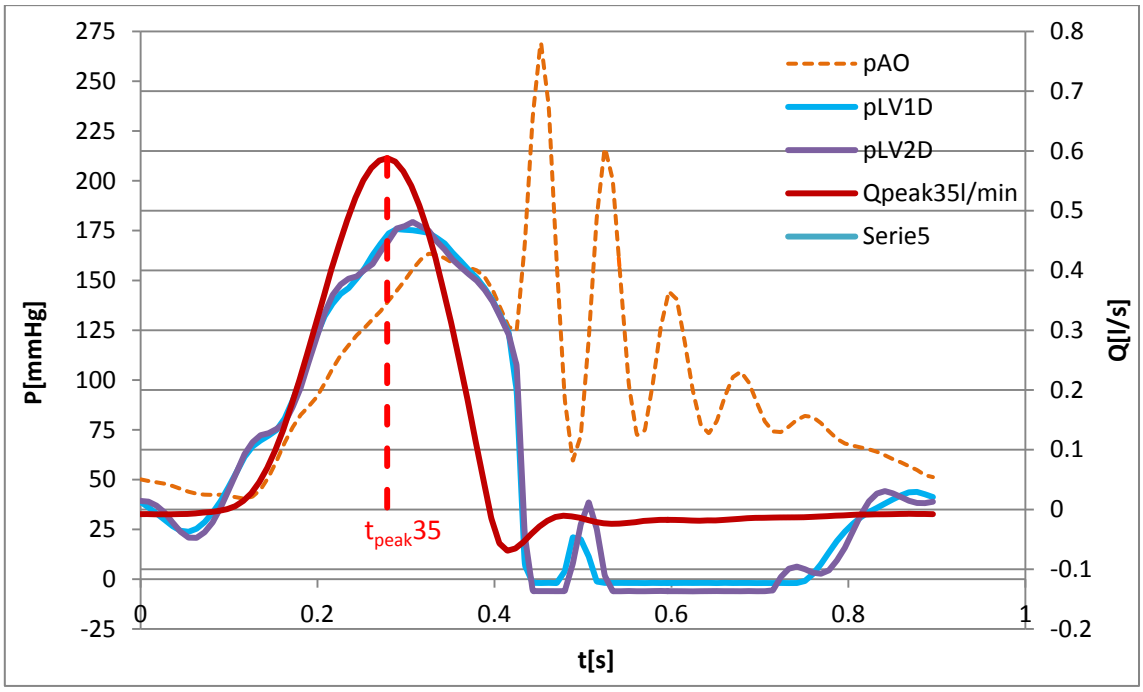

Figure 4.6: Flow of peak around 35 l/min, (0.58 l/s) with the pressures at 1D, 2D (pLV1D, pLV2D) upstream and the one downstream of the aortic valve (pAO)

So as you can see from the previous figures, we recorded four different flows with peaks of 20, 25, 30, and 35 liters per minute, and for each one we measured the pressures in the points of interest.

Let's see the differences between all the flows in figure 4.5:

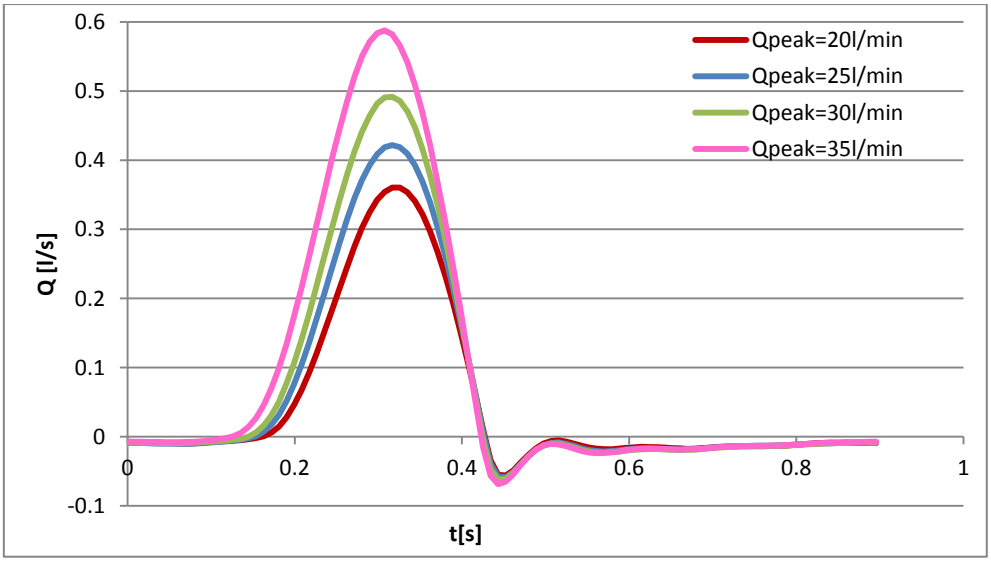

4.7: Pulsatile flows characterised by peaks of 20, 25, 30 and 35 l/min

The next step consists in analysing the effect of the acceleration of the flow on the pressures for the different sections and for the different flow rates recorded. Since the acceleration a is the derivative of the velocity v in time, we easily find that for a constant area A it is given by the derivative of the flow rate Q in time:

$$a = \frac{dv}{dt} \qquad (4.1)$$

$$Q = v \cdot A \qquad (4.2)$$

$$\frac{dQ}{dt} = \frac{d(v \cdot A)}{dt} = A \cdot \frac{dv}{dt} = A \cdot a \qquad (4.3)$$

Let's study the problem fixing from time to time the value of the flow rate we want in every flow, investigating the relationship between their derivatives and pressures.

❖ <u>Reference flow rate = 20 l/min</u>

I start fixing the flow rate equal to 20 l/min. It coincide with the peak value of the first flow I recorded, so that the respective derivative will be of course zero (yellow dot in figure 4.6):

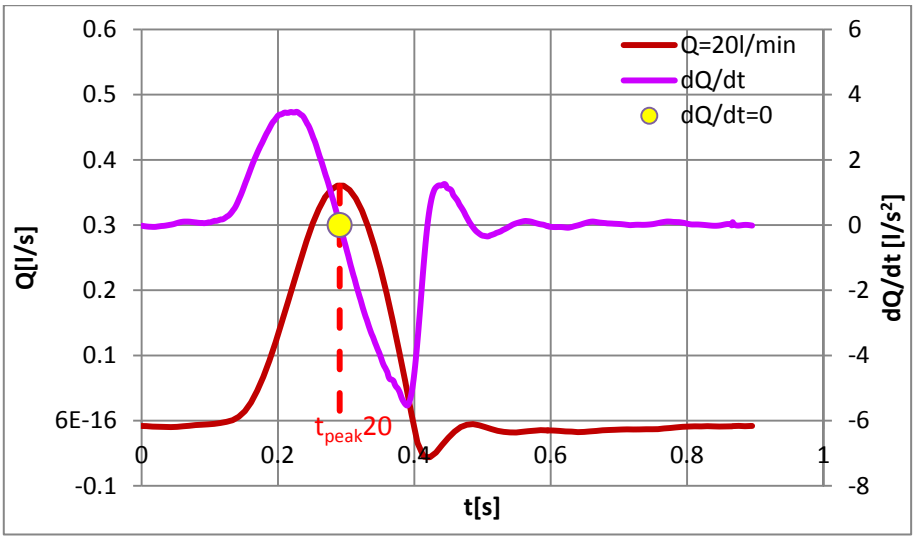

Figure 4.8: pulsatile flow with peak of 20 l/min (red line) with its derivative (purple line);

The value in the flow curve corresponding to the fixed one (always 20 l/min) is characterised by a time in the x-axis, called '$t_{peak}20$'. Hence I verify the relations between the accelerations and the pressures at that time highlighted also in figure 4.1. The same operation will be repeat for all the other curves, calculating for every one the derivatives and the pressures.

Going back to the flows I recorded, I find all the moments in which I have the value of 20 l/min,

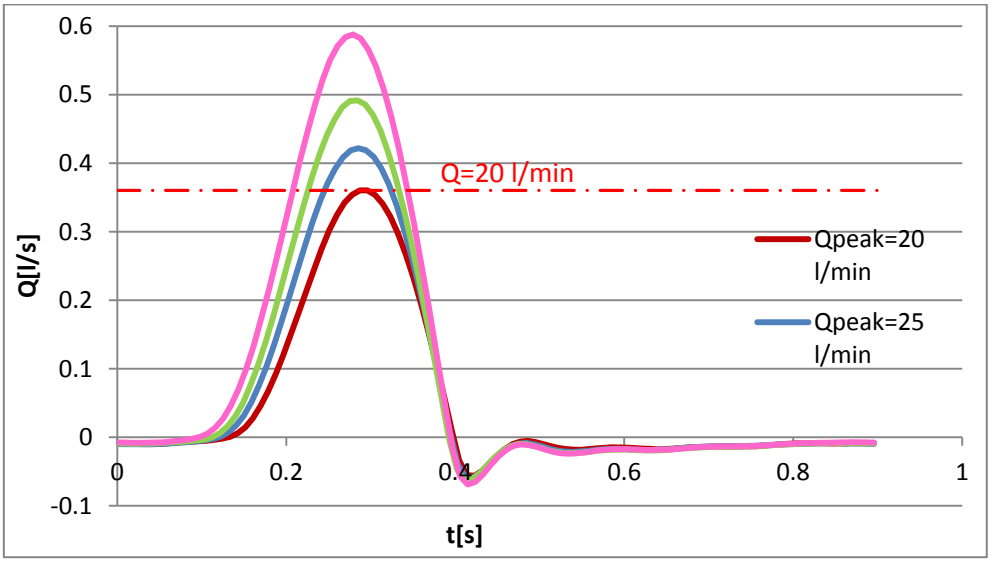

Figure 4.9: Pulsatile flow rate curves of peaks equal to 20, 25, 30 and 35 litres per minute crossed by the line Q=20l/min

and for each point crossed by the line equal to 20 l/min I report the relations of the respective acceleration with the pressure measured, for both the two points upstream of the aortic valve, at 1D and 2D from it (figures 4.8 and 4.9).

In practice, keeping the value of 20 l/min (0.36 l/s) as fixed, we take for every curve the correspondent values of pressures.

We caught indeed the pressure recorded at 7 time steps which are:

- the peak time, moment at which the Q=20 l/min peak curve records its higher value;
- the 2 times at which the flow rate is 0.36 l/s in the curve of 25 l/min peak;
- the 2 times at which the flow rate is 0.36 l/s in the curve of 30 l/min peak;
- the 2 times at which the flow rate is 0.36 l/s in the curve of 35 l/min peak

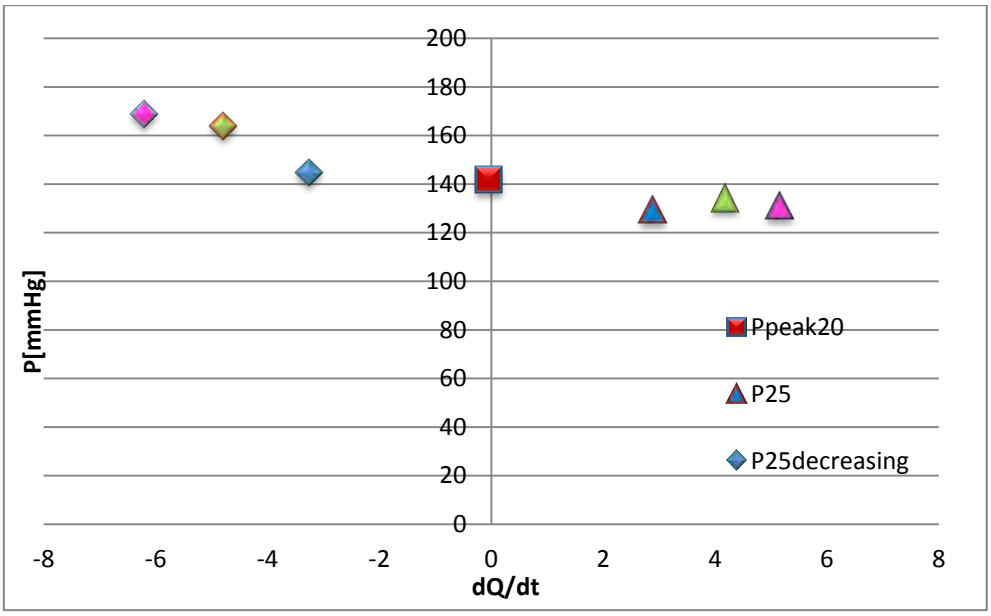

Figure 4.10: Pressures at 1 diameter (1D) upstream of the aortic valve, function of the acceleration of the flow, fixed Q=20l/min

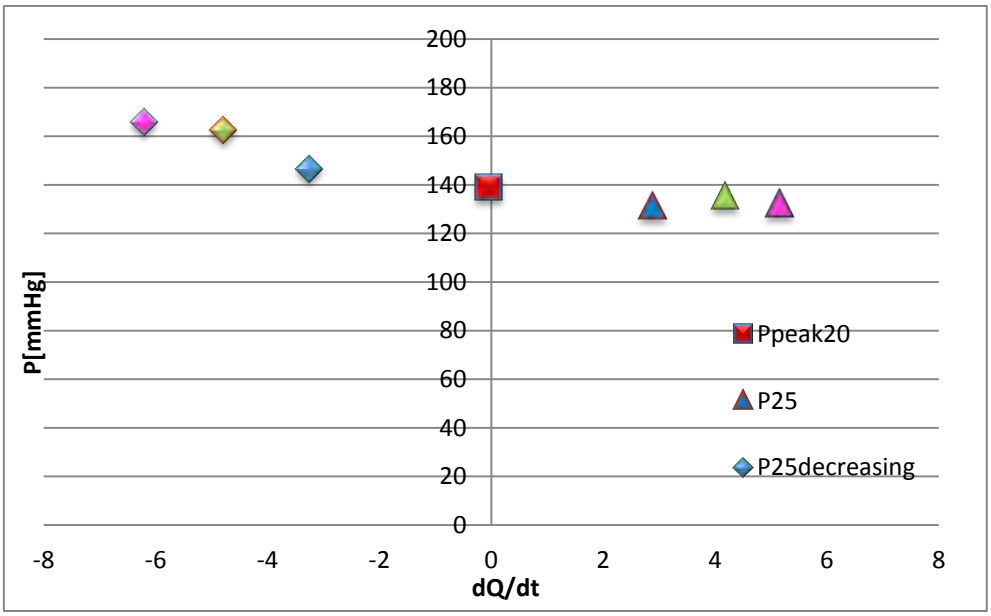

Figure 4.11: Pressures at 2 diameters (2D) upstream of the aortic valve, function of the acceleration of the flow, fixed Q=20l/min

❖ Reference flow rate = 25 l/min

In this case I repeat all the previous operations by fixing the flow rate equal to 25 l/min. Of course I will not consider the first flow recorded which never reaches this value, being its peak equal to 20 l/min. In this situation the value of 25 coincides with the peak value of the second flow I recorded, so that the respective derivative will be of course zero (yellow dot in figure 4.10):

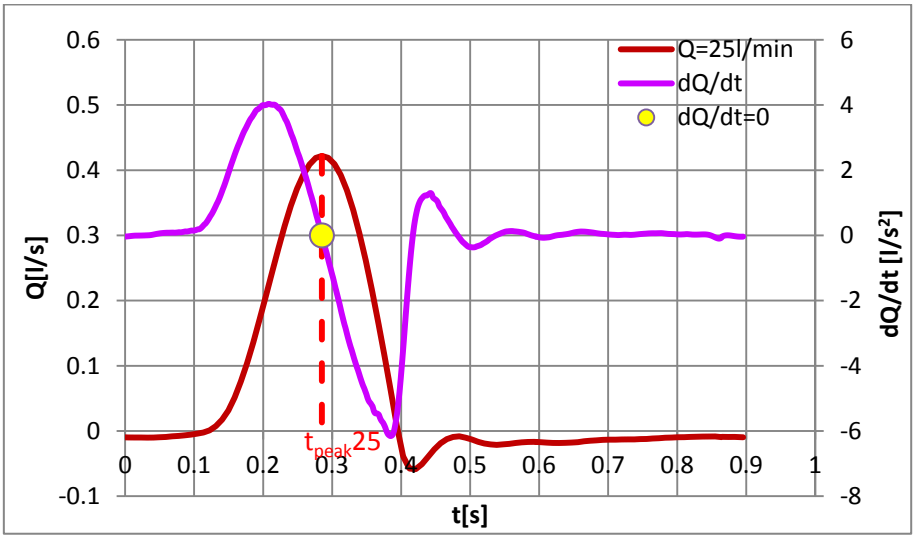

Figure 4.12: pulsatile flow with peak of 25 l/min (red line) with its derivative (purple line);

Even in this case I find out all the points in the curves characterised by a value of 25 l/min (that is 0.4 l/s):

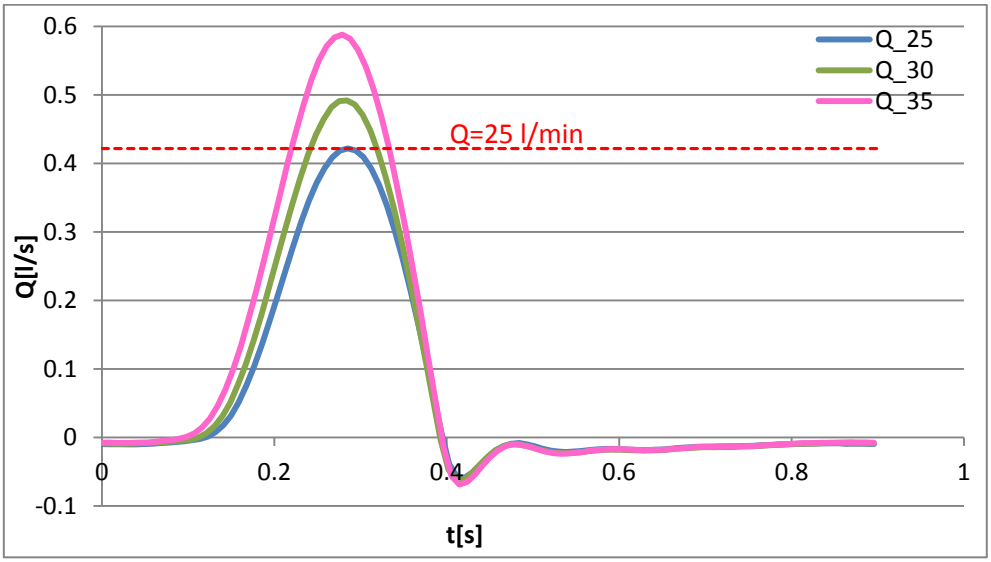

Figure 4.13: Pulsatile flow rate curves of peaks equal to 20, 25, 30 and 35 litres per minute crossed by the line Q=25l/min

and for each of these points I report the relations of the respective acceleration with the pressure measured at 1D and 2D from the valve (figures 4.12 and 4.13).

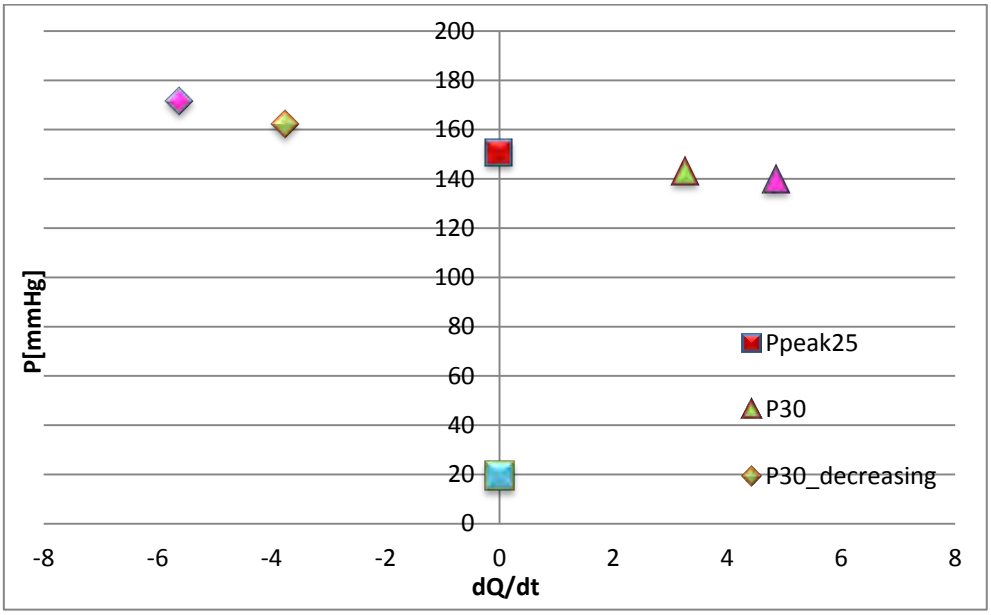

Figure 4.14: Pressures at one diameter (1D) upstream of the aortic valve, function of the acceleration of the flow, fixed Q=25l/min

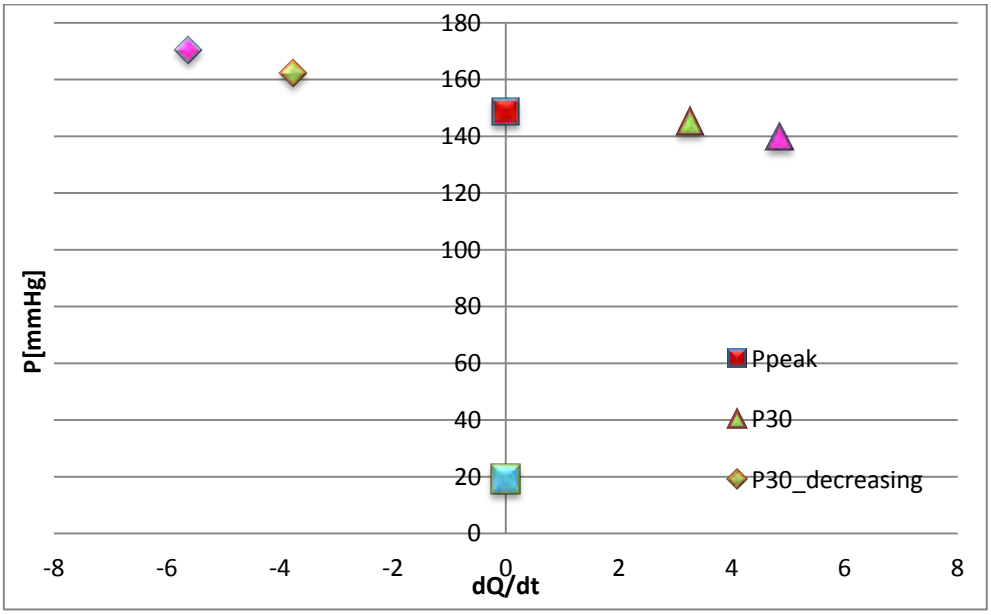

Figure 4.15: Pressures at 2 diameters (2D) upstream of the aortic valve, function of the acceleration of the flow, fixed Q=25l/min

❖ Reference flow rate = 15 l/min

Even if we don't have the peak flow equal to 15 l/min, we decided to fix this value and evaluate the derivatives and pressures to obtain additional data and be able to compare the results.

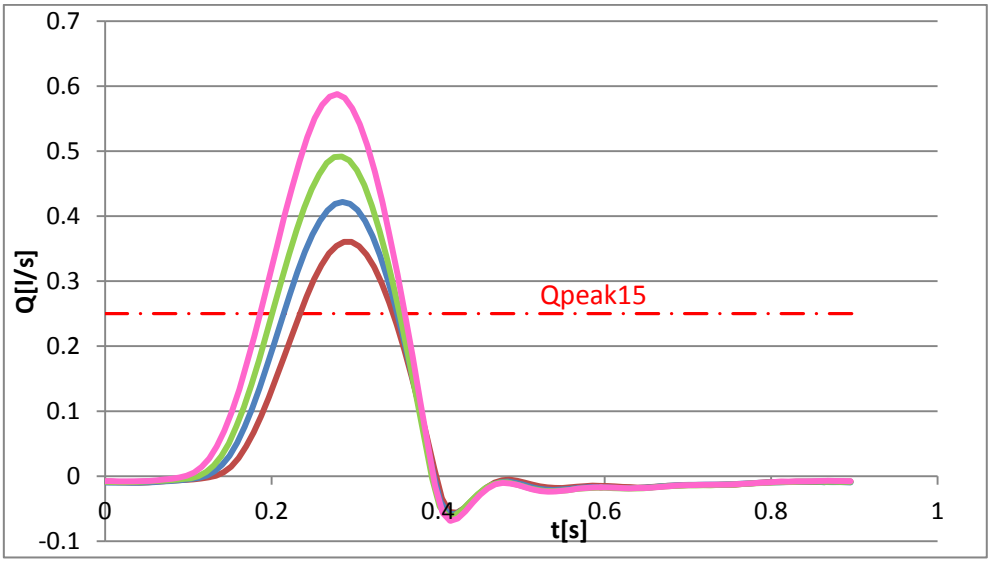

Figure 4.16: Pulsatile flow rate curves of peaks equal to 20, 25, 30 and 35 litres per minute crossed by the line Q=15l/min

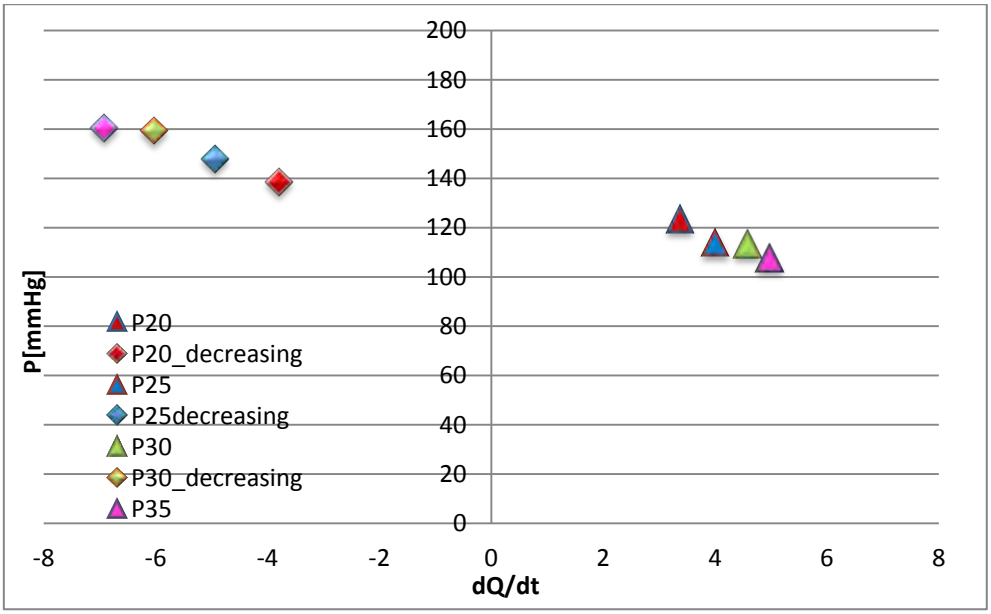

Figure 4.17: Pressures at 1 diameter (1D) upstream of the aortic valve, function of the acceleration of the flow, fixed Q=15l/min

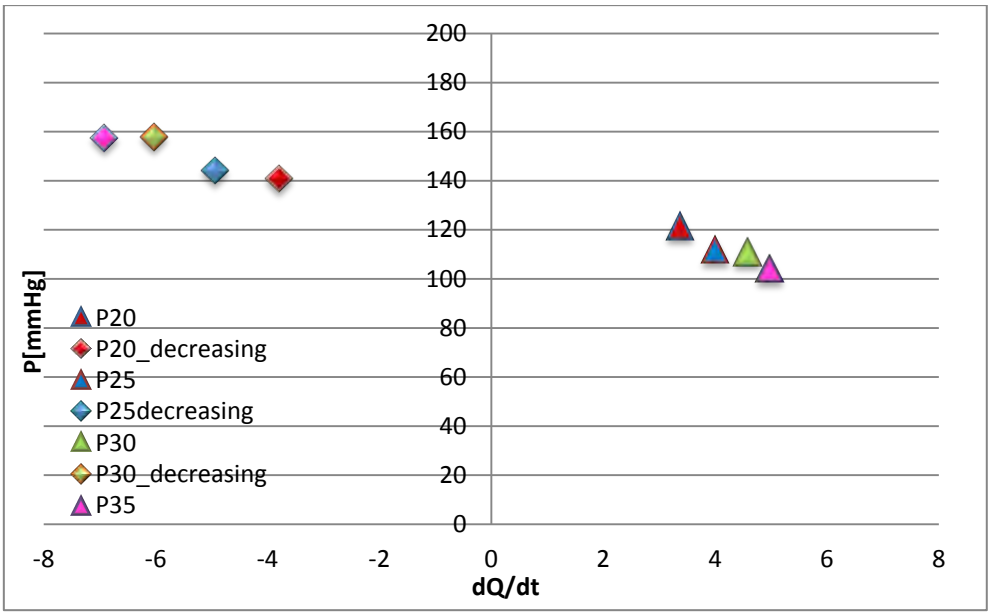

Figure 4.18: Pressures at 2 diameters (2D) upstream of the aortic valve, function of the acceleration of the flow, fixed Q=15l/min

❖ Final Results

In the following charts I gathered the data on the relationship between acceleration and pressure found for the three values of flow rates of 20, 25 and 15 litres per minute for both the two sections of 1D and 2D.

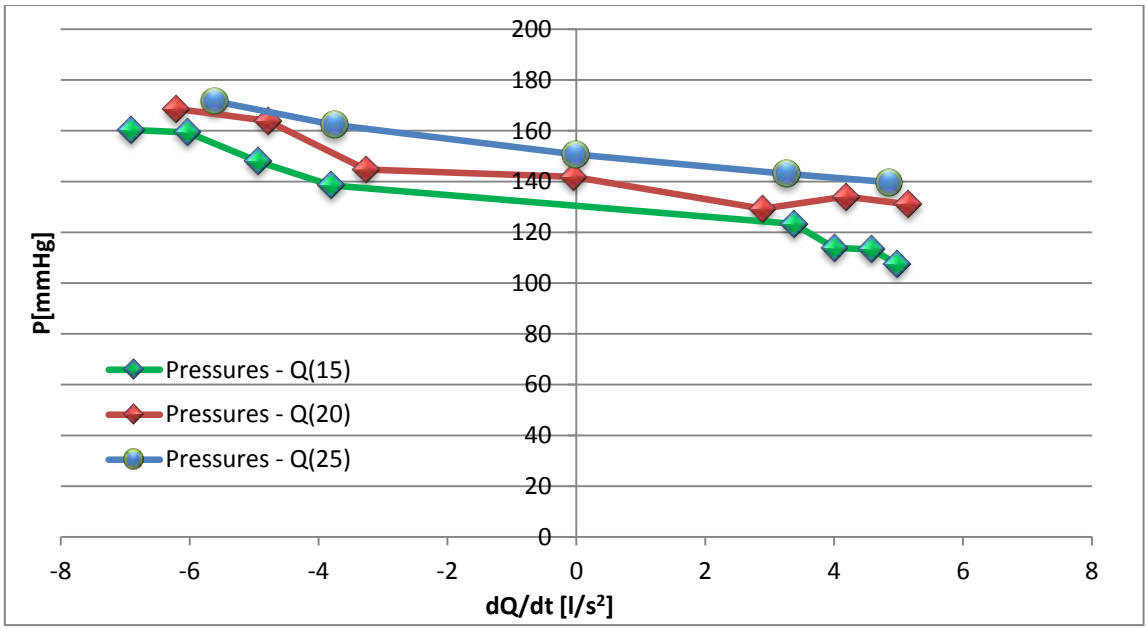

Figure 4.19: Pressure trend function of the acceleration of the flow in the section at 1D upstream of the valve for the three flow rates of 20, 25 and 15 litres per minute;

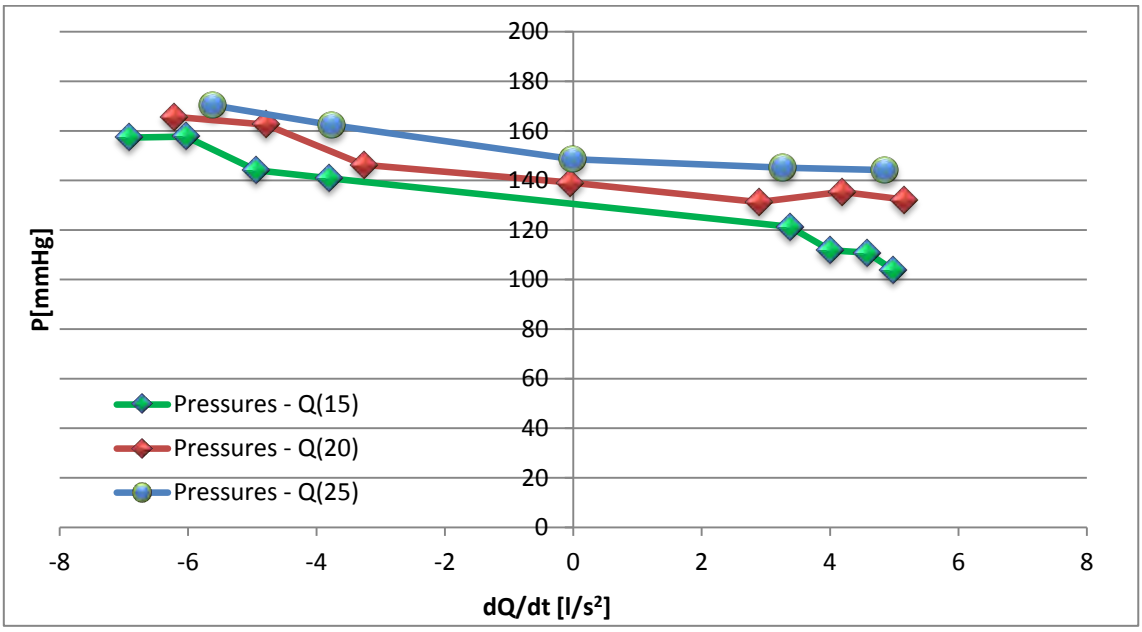

Figure 4.20: Pressure trend function of the acceleration of the flow in the section at 2D upstream of the valve for the three flow rates of 20, 25 and 15 litres per minute;

As I can see from the graphs, the pressures for the different flow rates follow the same trend, they decrease with the increase of the acceleration, while, keeping the acceleration as constant, they decrease for lower values of the flow rate;

4.2.2 Theoretical and experimental analysis – Hydrodynamics valve performance

Hydrodynamic testing shall be performed to provide information on the fluid mechanical performance of the heart valve substitute and provide indicators of valve performance. The in vitro test results shall meet or exceed the minimum performance requirements provided in table 2 of the normative (figure 4.3) , which are given in function of valve size and position, corresponding to the following pulsatile-flow conditions: beat rate = 70 cycles/min, simulated cardiac output = 5,0 l/min, mean aortic pressure = 100 mmHg, and systolic duration = 35%.

Table 2 — Minimum performance requirements

Position	Aortic							Mitral			
Valve size (TAD, mm)	19	21	23	25	27	29	31	25	27	29	31
A_{EO} (cm^2)	⩾ 0,70	⩾ 0,85	⩾ 1,00	⩾ 1,20	⩾ 1,40	⩾ 1,60	⩾ 1,80	⩾ 1,20	⩾ 1,40	⩾ 1,60	⩾ 1,80
Regurgitant Fraction (%)	⩽ 10	⩽ 10	⩽ 10	⩽ 15	⩽ 15	⩽ 20	⩽ 20	⩽ 15	⩽ 15	⩽ 20	⩽ 20
NOTE See Yoganathan and Travis [26] and Marquez et al.[16].											

$$A_{EO} = \frac{q_{v\,RMS}}{51{,}6 \times \sqrt{\frac{\Delta p}{\rho}}}$$

where

A_{EO} is the effective orifice area in square centimetres;

$q_{v\,RMS}$ is the root mean square forward flow in millilitres per second;

Δp is the mean pressure difference (measured over the positive pressure period of the forward flow phase) in millimetres of mercury;

ρ is the density of the test fluid in grams per cubic centimetre.

NOTE This equation is derived from the Bernoulli Equation. The constant (51,6) is not dimensionless, thus this equation is only valid with the units shown.

Figure 4.21: Minimum performance requirements given by the normative for the in vitro test;

In our case we refer to the aortic valve, characterized by a diameter of 23 millimeters.

The first important parameter to control is thus the effective orifice area (EOA or AEO), why is it so important? The aortic valve is fundamental for the functioning of the heart and the systemic circulation, and its malfunctioning always affects the wellness of the organism. One of the most common consequences of the pathologies concerning the heart valves is the stenosis, in which the valve, in its maximum opening, has an orifice through which blood flows in a lower amount respect to the physiological one. The flow pattern across an aortic stenosis can be compared to the one occurring in a circular pipe of assigned diameter, inside which it flows a one-dimensional current. The latter has to cross the stenotic valve, which hydraulically looks like a contraction of the pipe, passing through a smaller diameter respect to the initial one. In particular as the flows passes through the stenotic valve, a jet is produced. The flow accelerates from some distance upstream from the stenosis in the left ventricular outflow tract (location 1 in figure 4.22) as far downstream as the vena contracta (location 2). The vena contracta corresponds to the location where the cross sectional area of the jet is minimal. The area is named EOA. Beyond the vena contracta, the fluid decelerates as the area occupied by the flow increases to fill the cross-

section of the ascending aorta. The jet is rapidly lost in a region of turbulent mixing which involves significant fluid energy dissipation. In this region, the pressure increases until it reaches a maximum at the location where the reattachment of the flow occurs (location 3). The difference between the ventricular pressure and the aortic one is the so-called transvalvular pressure gradient. (7)

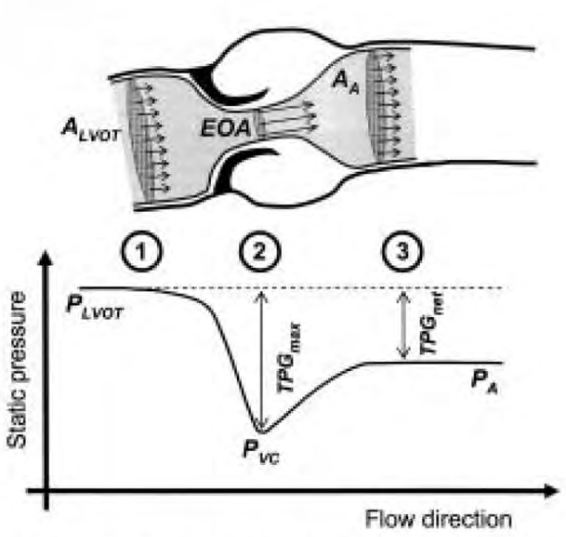

Figure : Schema of the systolic flow through an aortic stenosis. A_A: Aortic cross-sectional area; A_{LVOT}: LVOT cross-sectional area; EOA: Effective orifice area; P_A: Aortic pressure; P_{LVOT}: LVOT pressure; P_{VC}: Pressure at the vena contracta; TPG_{max}: Maximal transvalvular pressure gradient (= P_{LVOT} - P_{VC}); TPG_{net}: Net transvalvular pressure gradient (= P_{LVOT} - P_A).

4.22: Schema of a systolic flow through an aortic stenosis

As I can see in the previous figure the value of EOA is linked to other parameters that it is important to analyze. To describe their meaning I refer to one of the previous pressure-graph, highlighting the points of interest.

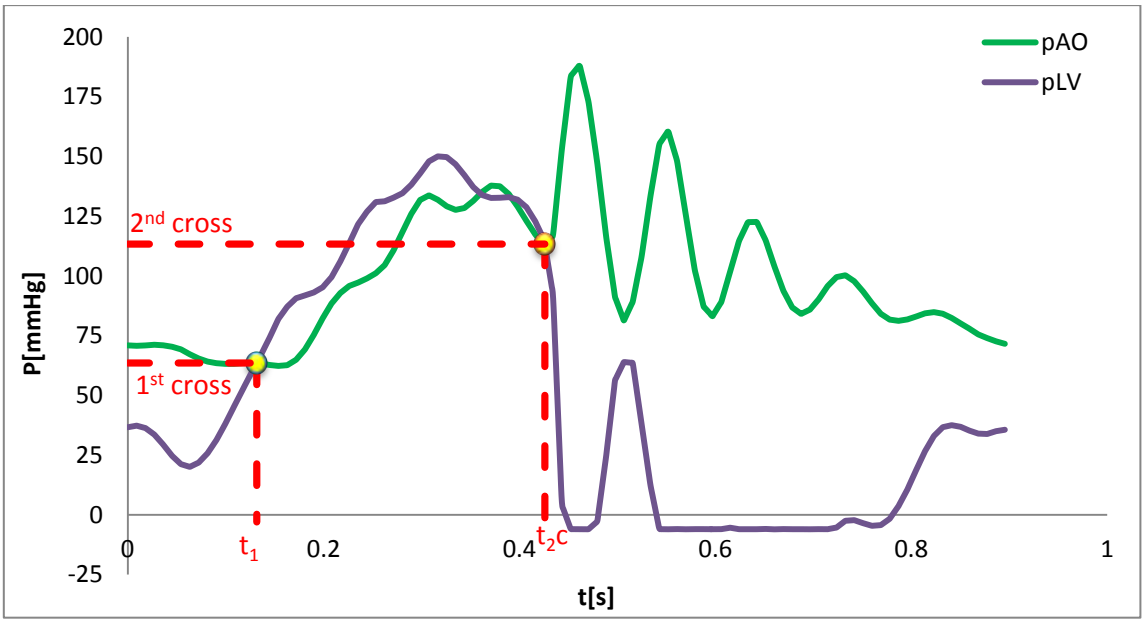

4.23: Aortic pressure (pAO) and ventricular pressure (pLV) crossing;

The main parameters of interest are:

- Pressure 1 and 2 cross: they represents the two moments at which the curve of the ventricular pressure crosses the one of the aortic.
  In particular the first cross correspond to the instant at which the valve opens, while the second correspond to that of its closure;
- Time crossing: it is the period of time in which the valve stay open, that is the time between the two crosses;
- Time Crossing percent: it is the percentage of the time crossing in the total period of a cycle;
- TransAortic Max Pressure: it is the maximum difference in terms of pressure between the two curves;
- TransAortic Mean Pressure [CT]: it is the mean value of the pressure between the two pressure curves (aortic and ventricular one);
- TransAortic Mean Pressure [CP]: it is the mean value between the aortic and ventricular pressures, by just considering their positive value respect to the total mean;

Taking everything into account let's go back to the analysis of the results in our tests. We will compare, the operative conditions being equal, the differences involving these parameters between the two upstream sections 1D and 2D for different flow rates (20, 25, 30 and 35 l/min).

All the test are carried out with a physiological heart rate of 67 bpm (beats per minute).

❖ Reference flow rate = 20 l/min

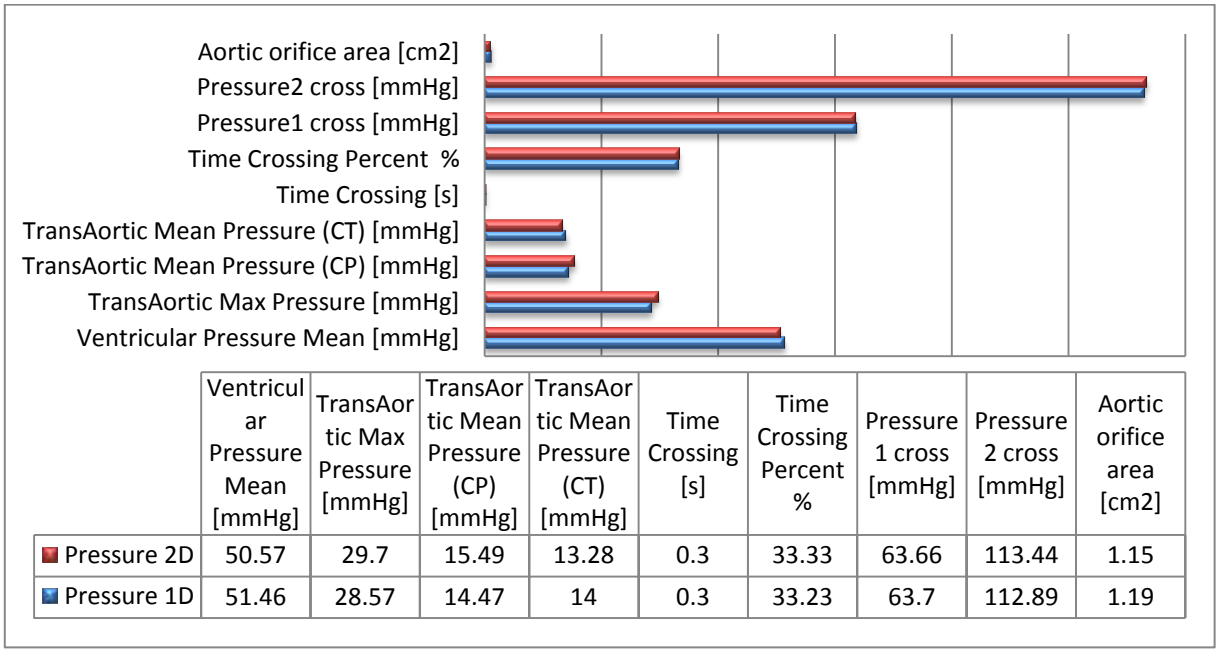

	Ventricular Pressure Mean [mmHg]	TransAortic Max Pressure [mmHg]	TransAortic Mean Pressure (CP) [mmHg]	TransAortic Mean Pressure (CT) [mmHg]	Time Crossing [s]	Time Crossing Percent %	Pressure 1 cross [mmHg]	Pressure 2 cross [mmHg]	Aortic orifice area [cm2]
Pressure 2D	50.57	29.7	15.49	13.28	0.3	33.33	63.66	113.44	1.15
Pressure 1D	51.46	28.57	14.47	14	0.3	33.23	63.7	112.89	1.19

Figure 4.24: differences in hydrodynamics valve performance between the sections 1D and 2D for the pulsatile flow of 20 l/min;

❖ Reference flow rate = 25 l/min

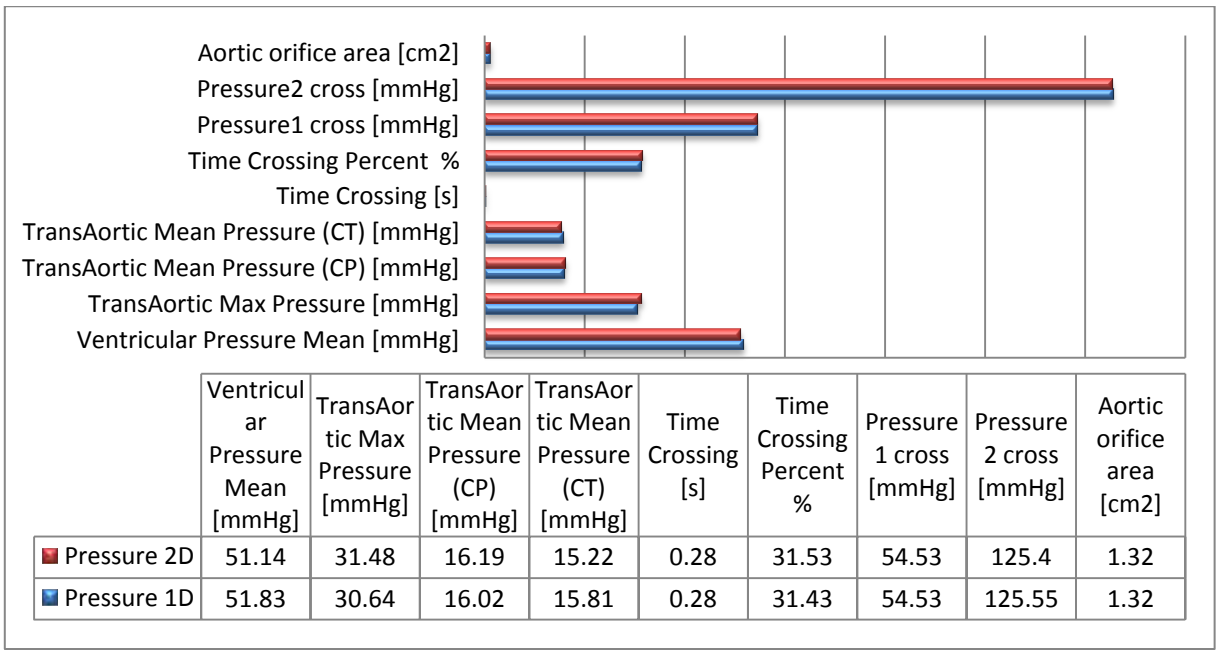

	Ventricular Pressure Mean [mmHg]	TransAortic Max Pressure [mmHg]	TransAortic Mean Pressure (CP) [mmHg]	TransAortic Mean Pressure (CT) [mmHg]	Time Crossing [s]	Time Crossing Percent %	Pressure 1 cross [mmHg]	Pressure 2 cross [mmHg]	Aortic orifice area [cm2]
Pressure 2D	51.14	31.48	16.19	15.22	0.28	31.53	54.53	125.4	1.32
Pressure 1D	51.83	30.64	16.02	15.81	0.28	31.43	54.53	125.55	1.32

Figure 4.25: differences in hydrodynamics valve performance between the sections 1D and 2D for the pulsatile flow of 25 l/min;

❖ Reference flow rate = 30 l/min

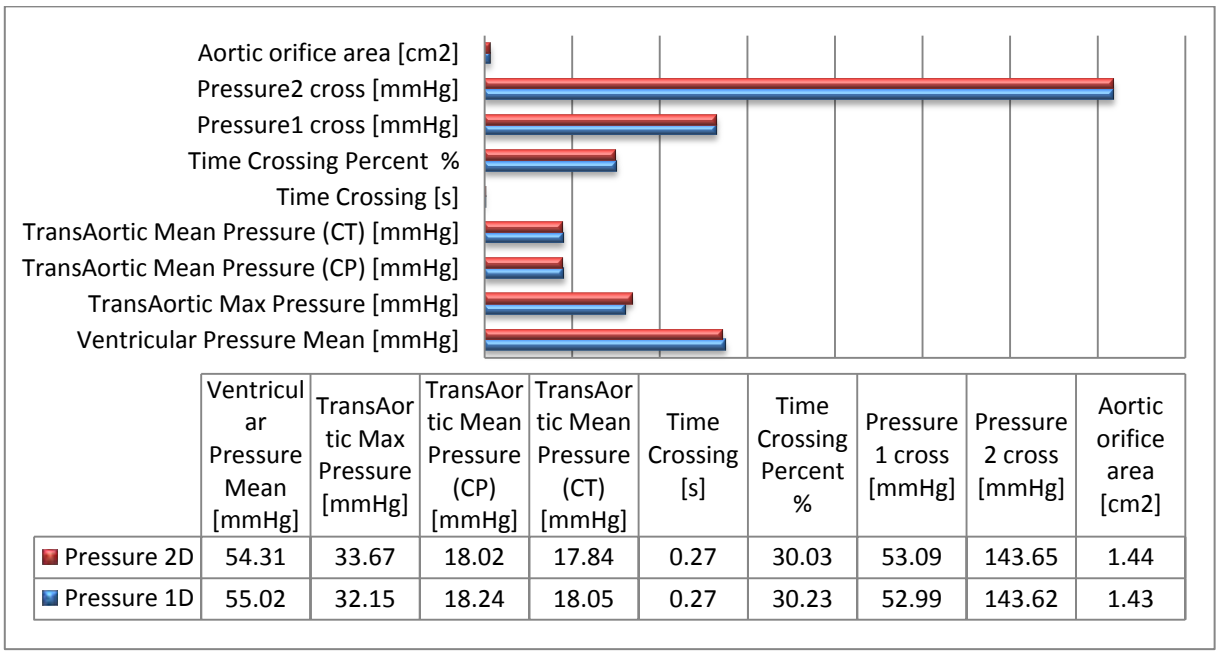

	Ventricular Pressure Mean [mmHg]	TransAortic Max Pressure [mmHg]	TransAortic Mean Pressure (CP) [mmHg]	TransAortic Mean Pressure (CT) [mmHg]	Time Crossing [s]	Time Crossing Percent %	Pressure 1 cross [mmHg]	Pressure 2 cross [mmHg]	Aortic orifice area [cm2]
Pressure 2D	54.31	33.67	18.02	17.84	0.27	30.03	53.09	143.65	1.44
Pressure 1D	55.02	32.15	18.24	18.05	0.27	30.23	52.99	143.62	1.43

Figure 4.26: differences in hydrodynamics valve performance between the sections 1D and 2D for the pulsatile flow of 30 l/min;

❖ Reference flow rate = 35 l/min

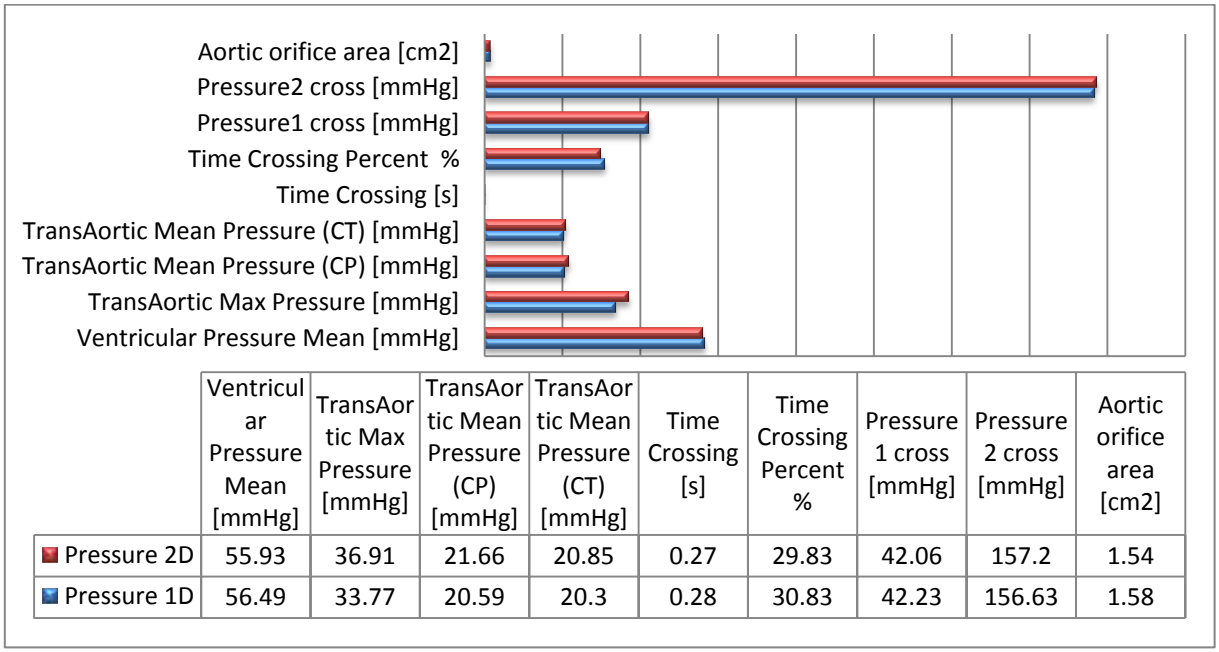

	Ventricular Pressure Mean [mmHg]	TransAortic Max Pressure [mmHg]	TransAortic Mean Pressure (CP) [mmHg]	TransAortic Mean Pressure (CT) [mmHg]	Time Crossing [s]	Time Crossing Percent %	Pressure 1 cross [mmHg]	Pressure 2 cross [mmHg]	Aortic orifice area [cm2]
Pressure 2D	55.93	36.91	21.66	20.85	0.27	29.83	42.06	157.2	1.54
Pressure 1D	56.49	33.77	20.59	20.3	0.28	30.83	42.23	156.63	1.58

Figure 4.27: differences in hydrodynamics valve performance between the sections 1D and 2D for the pulsatile flow of 35 l/min;

Analysing the results in terms of the parameters correlated to the hydrodynamics valve performance we can say that we recorded fast the same values in the two sections of 1 and 2 diameters upstream of the valve. The most important factor we wanted to verify was the EOA, that for all the tests we carried on, verified the demand of the normative of being higher than 1.

4.3 Pressure trend downstream of the aortic valve

By working in physiological conditions of pulsatile motion, the response in terms of pressure downstream of the valve shows values that are not properly physiological. As it was already highlighted in the charts 4.3-4.6, a problem involving the birth of high pressure peaks had arisen. If we refer to the physiological chart we are expected to obtain (figure 4.2), it is evident that the results recorded are far from the reality. Hence, we diverted the analysis from which we began, to study a solution to fix it.

We decided to act on the system by inserting a damper represented by an aortic compliance. The following photos show the original configuration, without the compliance chamber, and the second one represents the situation after its installation:

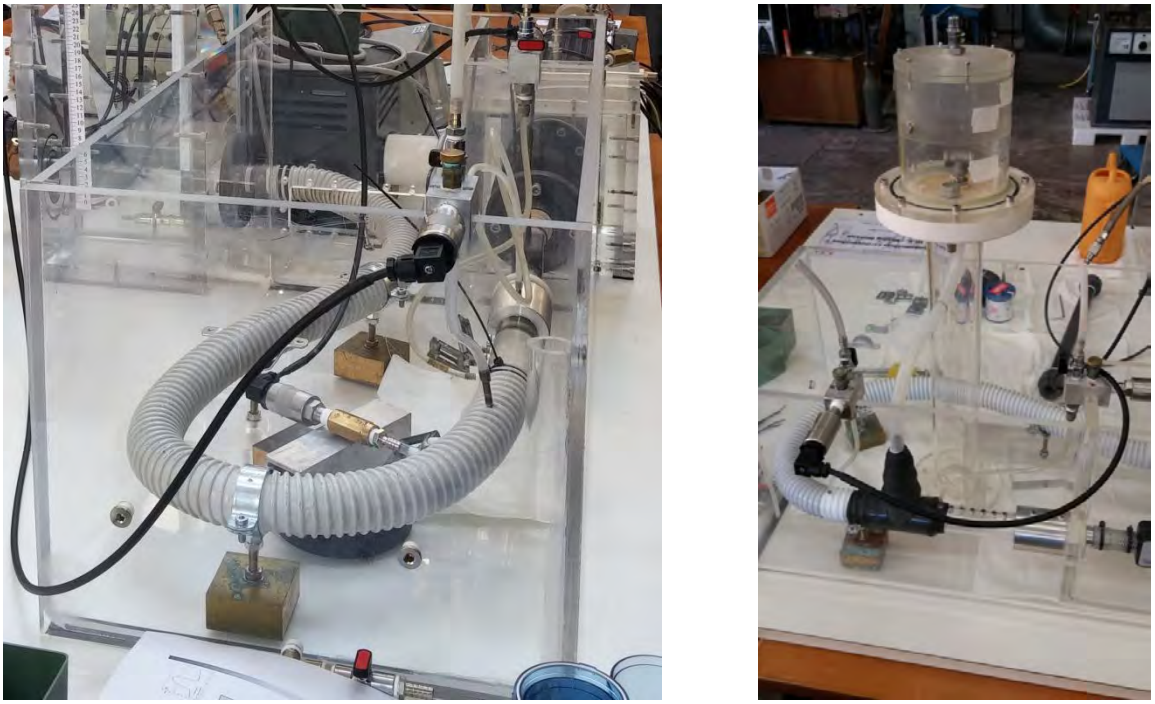

Figure 4.28: Pulse duplicator with the aortic compliance (right), and before its installation (left)

The function of this tank is to simulate the capability of the blood vessel volume to increase as the blood pressure increases. In the human body, in effect, following closure of the aortic valve, tension forms in the dilated aorta because of the sudden force increase against the aortic wall due to the abrupt change in blood volume and pressure. This tension of the elastic vessel wall propels blood through the circulatory system after it is pumped from the heart. A similar effect is obtained by using a trapped volume of air above the circulatory fluid. When the pulsatile pump delivers water to the chamber, during systole, the fluid is temporarily stored inside the chamber until the valve closes to allow the pump to fill, during diastole. The stored energy then pushes the fluid through the loop. Therefore the compliance chamber we added to the system emulates the elasticity of all blood vessels.

The Normative (3) suggests the use of a compliance chamber and gives us a formula to indicate how to proceed with its dimensions.
The recommended definition of compliance, over the pulse pressure, to be used in testing and reporting values is:

$$C = 100\% \cdot \frac{(d_2 - d_1)}{d_1 \cdot (p_2 - p_1)}$$

where:

- C is the compliance, $\frac{\%}{mmHg}$, that is the relation between the variation in volume and the variation in pressure. The normative suggests some values, equal to $0.32\,\frac{\%}{mmHg}$. It means that for every change in pressure of 1 mmHg, it changes its volume by 0.32 per cent;
- p_1 is the diastolic pressure, in mmHg. Physiologically it corresponds to a value of around 80 mmHg (figure 4.2);
- p_2 is the systolic pressure, in mmHg. Physiologically it corresponds to a value of around 120 mmHg (figure 4.2);
- d_1 is the outside diameter at p_1, in millimetres
- d_2 is the outside diameter at p_2, in millimetres

Fixed the diameter d_1 of the aortic arch in diastolic pressure, we can find out the value of d_2 from the formula as:

$$d_2 = d_1 + C \cdot d_1 \cdot (p_2 - p_1)$$

This number gives us the diameter of the vessels when they expand to contain the increase of pressures. The difference between the two areas considering the length of the portion of the arch considered, gives us the volumetric gradient of the flow that the aortic compliance needs to be able to contain.

$$\Delta V = (A_2 - A_1) \cdot L = \frac{\pi}{4} \cdot (d_2^2 - d_1^2) \cdot L$$

The goal of the compliance will thus be that of absorbing all the expansion we need in order to maintain the flow constant, as much as possible.

In the follow I report the test we made for the aortic pressure before (figure 4.22) and after the installation of the compliance (figure 4.23):

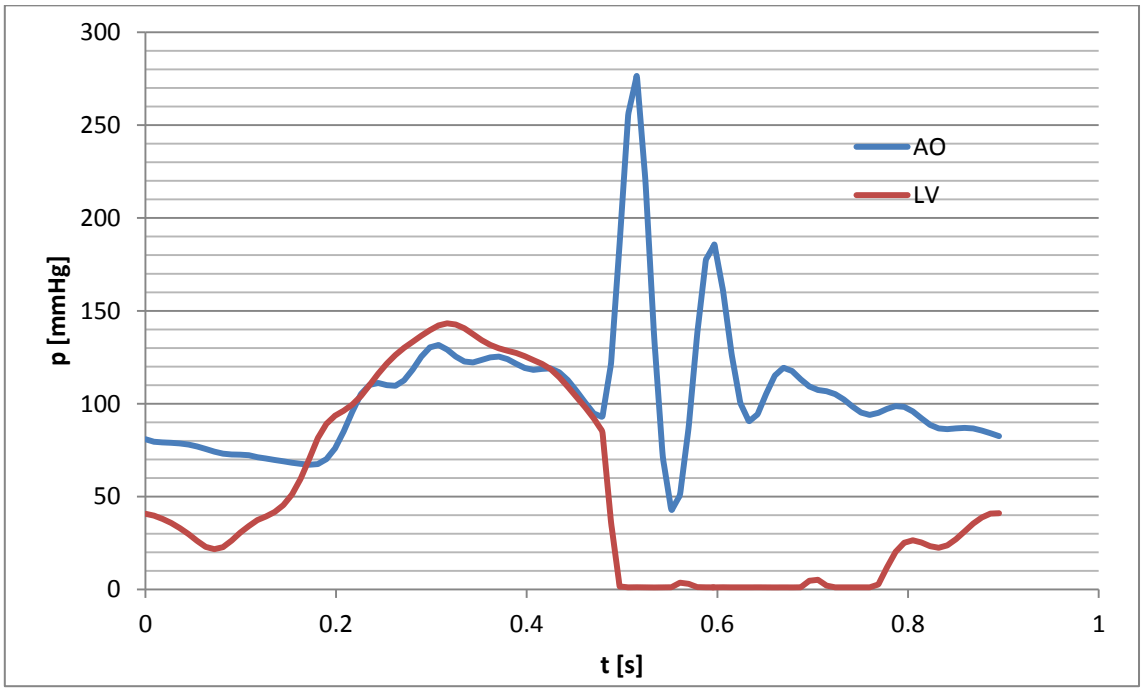

Figure 4.29: Aortic pressure without the compliance;

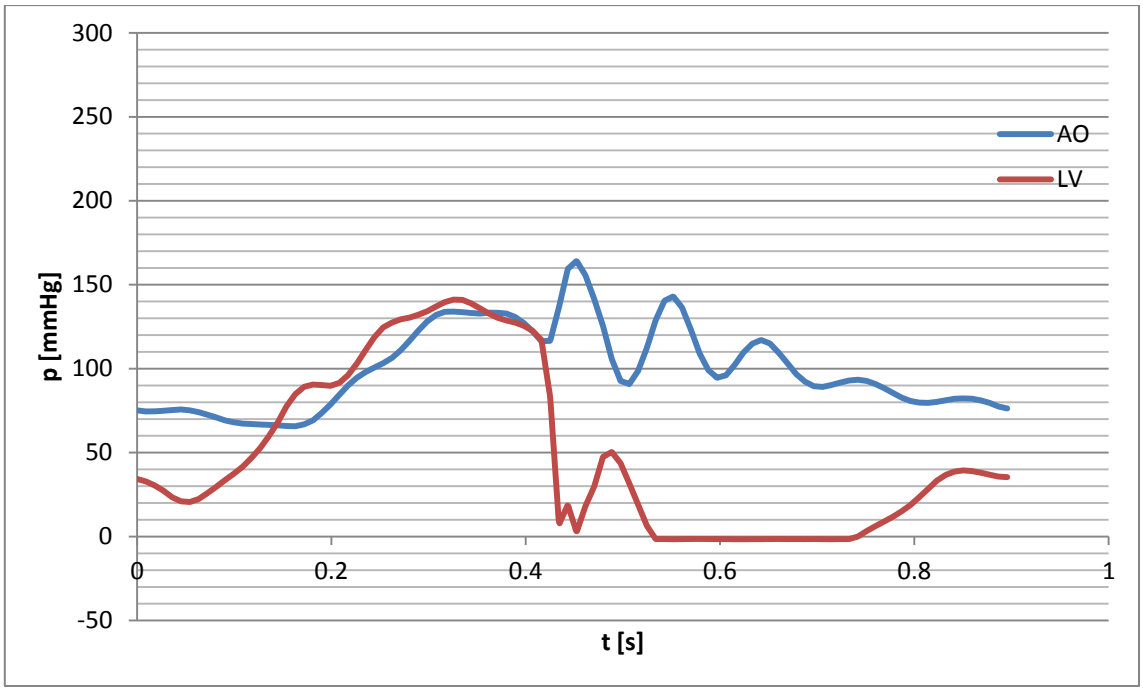

Figure 4.30: Aortic Pressure after the addition of the compliance;

Comparing the situation in terms of pressures, we verified that the adoption of the solution of the compliance was useful to improve the reliability of the device. As a matter of fact the peak of the aortic pressure decreases of fast 120 mmHg after the installation of the compliance, which means that the solution was correct. However we still record a value which is too high respect to what it is expected from the physiological pressure, so that we need to work to completely remove the problem.

4.4 Conclusion of the work

Retracing the steps of my work I can make the following considerations.

As regards the first part of the study, focused on the analysis of the performance of the flow meter, the obtained data confirmed the extreme sensitivity and accuracy of the instrument, which then responds perfectly to our needs. Its introduction obliged us to create a component to link up its tube, characterized by a diameter of 19 mm, to the one of the rest of the aortic arch, having a diameter of 30 mm. Therefore we need to study the effect of this change in geometry in order to understand its effect on the behavior of the pressures. The test confirmed that in the area we use to take the measurement of the pressures, the vein of the flow already attached so the idea of

linking the two parts with the diffuser resulted being a good solution. After the analysis of the pressures in conditions of constant flow, we passed to study their behavior in pulsatile flow; this situation is important because it finally replicates the function of the heart's ventricle which generates pulsatile flow through a heart valve in the left Heart. In particular we investigate the trend of pressures up upstream and downstream of the aortic valve. First of all, fixed the aortic pressure, we took the measurements in two sections at one diameter and two diameters before the valve. The test highlighted that the differences in terms of hydraulic parameters such as the transAortic mean pressure and the effective orifice area between the two sections are negligible, so that it does not matter whenever we choose the first or the second point as reference for the value of the pressure upstream of the valve. Moreover we analysed the relation between these pressures and the acceleration of the flow, in particular they decreases with the increasing of the acceleration. It will be a theme to examine more in detail in the next future.

Talking about the study of the pressure downstream of the aortic valve, a problem involving the birth of high pressure not physiological peaks had arisen. Hence, we diverted the analysis from which we began, to study a solution to fix it. To solve the problem we inserted a damper represented by an aortic compliance, with which the peak of the aortic pressure decreases consistently. Even if we still need to work to completely remove the problem, it resulted being a good idea to follow.

Taking everything into account I can be satisfactory of the work done on the pulse duplicator, which confirmed to be an excellent device with great possibility for improvement.

BIBLIOGRAPHY

1. Bellio, Silvia. Messa a punto di un dispositivo Pulse Duplicator per l'analisi sperimentale di protesi cardiovascolari. aa. 2014-2015. Tesi di laurea in bioingegneria, Università degli studi di Padova.

2. Di Micco, Luigi. Messa a punto di un circuito idraulico che simula la circolazione cardiovascolare sistemica umana. aa. 2013.2014. Tesi di laurea in ingegneria civilie, Università degli Studi di Padova.

3. CEN, European Committee for Standardization. European Standard for Cardiovascular Implants - Cardiac valve protheses. Brussels 2009 : s.n.

4. Ghetti, A. *Idraulica.* s.l. : edizioni libreria cortina, 2006.

5. Donald C. Rennels, Hobart M. Hudson. *Pipe Flow: A Practical and Comprehensive Guide.*

6. Rushmer, Robert F. Structure and Function of the Cardiovascular System. *Handbook of Research Methods in Cardiovascular Behavioral Medicine.*

7. Damien Garcia, Philippe Pibarot, Louis-Gilles Durand. Analytical modeling of the instantaneous pressure gradient across the aortic valve. *Journal of Biomechanics.*

8. [Online] http://www.transonic.com/resources/research/ts410-tubing-flow-module-specifications/.

LIST OF FIGURES